マイクロ波照射 NMR 分光法による液晶分子のマイクロ波加熱現象の解明

Microwave heating effects of liquid crystalline molecules as revealed by microwave irradiation NMR spectroscopy

横浜国立大学大学院工学府
機能発現工学専攻　博士課程後期
内藤・川村研究室

田制　侑悟

目次

公表論文

1. Mechanism for microwave heating of 1-(4'-cyanophenyl)-4-propylcyclohexane characterized by *in situ* microwave irradiation NMR spectroscopy (Journal of Magnetic Resonance 2015)

2. The microwave heating mechanism of N-(4-methoxybenzyliden)-4-butylaniline in liquid crystalline and isotropic phases as determined by *in situ* microwave irradiation NMR spectroscopy (Physical Chemistry Chemical Physics 2015)

3. Separation of Local Fields of Individual Protons in Nematic Phase of 4'-Ethoxybenzylidene-4-n-Butylaniline by Microwave Heating 2D NMR Spectroscopy (MS&T 2010)

１序論[1-4]

1.1 マイクロ波

マイクロ波は可視光や近赤外光よりもかなり長い波長が 1 mm から 1 m の電磁波であり（Figure 1.1）、多くの物質はマイクロ波を照射することで容易に加熱することができる。通常は電子レンジで用いられている波長 12.2 cm の 2.45 GHz 帯が使われている。誘電損失によって加熱される波長域であるマイクロ波やラジオ波は NMR における強磁場下でのスピンの異なる準位間を遷移させる程度のわずかなエネルギーである。

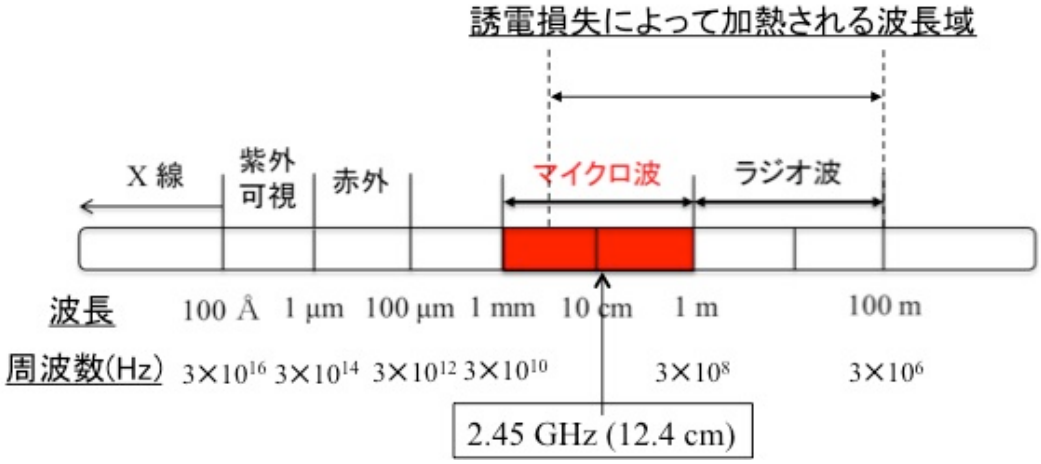

Figure 1.1 電磁波の波長・周波数領域

1.2 なぜ 2.45 GHz なのか

マイクロ波研究で使われる周波数でも 2.45 GHz が多いのだが、そもそも電子レンジで用いられている周波数がなぜ 2.45 GHz なのか。それは,もともとマイクロ波はレーダーや通信機器に用いられてきたことに起因する。現在、日本では電波法という法律によって ISM（Industrial, Scientific, Medical）バンドと呼ばれる３つの周波数帯（2.45 GHz、5.8 GHz、24 GHz）だけが工業や医療などに使えることになっている。それ以外の波長を使用すると通信をはじめとした領域と重なるので大きな問題になる。2.45 GHz はマイクロ波の遮蔽のレベルが低くてよい周波数帯であるため使用が楽である。また電子レンジの普及したことにより、メーカーではマイクロ波の振源であるマグネトロンは外国で作ったものを買っていることがほとんどである。このように発信機が手に入りやすいことからも 2.45 GHz が使用されることが多い原因である。

1.3 マイクロ波加熱

先述したがマイクロ波は当初、レーダーや通信機器に用いられていた。それがマイクロ波加熱の方に注目が集まっているここでマイクロ波加熱の発見の有名なエピソードがあるので一つ紹介する。1945 年頃、レーダーの研究をしてい

たレイセオン社のパーシー・スペンサー博士が研究室の作動中のマグネトロン（マイクロ波発信機）の前に立っているとポケットの中のチョコレートが溶けているのに気づいた。そこでポップコーンをマグネトロンの前に置くとポップコーンを弾けた。これが電子レンジの開発のきっかけであり、ここからレイセオン社から販売されることになった。これがマイクロ波加熱の注目した最初といわれている。

マイクロ波加熱は電磁波がキャビティ内で分布することで加熱される。いくつかに定在波がランダムに立っている状態をマルチモードといい、一つの定在波だけを立たせた状態をシングルモードという。マイクロ波加熱は熱伝導による加熱方法とは異なる特徴を多くもつ。特に重要だと思われるものをいくつか挙げてみたい。

1) 内部加熱
熱伝導を必要しないので複雑な形状のものでも均一に加熱できる。目的物を直接加熱することができる。通常の加熱では熱伝導と対流が起こり、化学反応容器を加熱するときには壁際で反応が起こって不均一性が発生する。しかし、マイクロ波加熱では内部加熱によりこうした問題が解消できる。

2) 選択加熱
物質によって誘電損失係数に差が生じるため加熱効率が異なる。そのため目的物を選択的に加熱することができる。例えば、水とガラスでは 2.45 GHz のマイクロ波吸収効率が 200 倍以上の差があるのでほとんど水にマイクロ波が吸収して加熱される。

3) 局所加熱
マイクロ波加熱を用いることで溶媒の温度が沸点以上になる現象（スーパーヒーティング）が起こる。これは溶液内部が集中的に加熱されるためである。この加熱現象は様々な方法で観測されており、後述するマイクロ波効果の原因としている研究者も多い。

4) 均一加熱
電子レンジでも真ん中が暖まらずに周りだけが熱くなることもよくあるが電磁波が不均一に分布するからである。不均一性を解消するためには定在波を非定常にするか、定在波の真ん中に対象物を置くことが考えられる。加熱の均一性は難しいが工夫すれば可能であるともいえる。

5) 省エネルギー
熱伝導による加熱方法に比べて劇的に加熱効率が良く、短時間で加熱できる上にエネルギー消費が低い。また排ガスが生じないため環境負荷が少ない。

このような特徴からグリーンケミストリーの観点から非常に優秀な加熱方法として大きく注目されている。

1.4 マイクロ波加熱の原理

溶液系におけるマイクロ波加熱の原理は交流電場を加えたときにエネルギーの一部が熱になる誘電損失という現象から起こる[5-8]。電磁波は電場と磁場の合成波であり、照射された分子が極性をもつ場合は電場の動きに追従しようとする。波長が長い場合は電場の変化が十分に長いので分子は滞りなく追従する。逆に波長が短い場合は電場の変化が速すぎるために追従することができない。しかしながら、適当な波長では電場の変化に対して一致しなくなり、結果として時間的に遅れて追従することで、分子同士で摩擦が起こり加熱される。この適当な波長というのがマイクロ波やラジオ波の波長域にあたり、誘電損失の大きい物質に吸収されると迅速に加熱される。

Table 1 にマイクロ波照射によるさまざまな溶媒の温度上昇を調べたものである。水をはじめとするほとんどの極性溶媒はマイクロ波照射で温度が急上昇するが、トルエンやヘキサンは上昇しないことがわかる。

（10ml, 500 W, *200 W）

溶媒	温度（℃）		誘電率	誘電損失
	30秒	60秒	ε	tan δ
水	62	104	80.4	0.123
アセトニトリル	91*	113*	38	0.659
ジメチルホルムアミド	139	151	37	0.062
エタノール	81	85	25	0.054
酢酸エチル	37	60	6	0.174
トルエン	32	34	2	
ヘキサン	20	23	2	

Table 1　マイクロ波照射（2.45 GHz）による溶媒の昇温

マイクロ波による単位体積当たりの出力の算出式は以下の様になる。

$$P=\frac{1}{2}\sigma|E|^2+\pi f\varepsilon_0\varepsilon_r''|E|^2+\pi f\mu_0\mu_r''|H|^2$$

P [W/m^3]: power dissipation par unit volume
|E| [V/m]: electric
|H| [A/m]: magnetic field
σ [S/m]: conductivity
f [1/sec]: frequency
ε_0[F/m]: permittivity in vacuum
ε_r''[F/m]: dielectric loss factor
μ_0[H/m]: permeability in vacuum
μ_r''[H/m]: magnetic loss factor

この式から電場が一定であれば物質の誘電損失(ε_r'')が大きいほど熱出力が大きく、溶媒の温度は大きく上昇することがわかる。つまり誘電率を下げるような変化が大きいほど発熱量が大きくなる。

そして注意しなければならないのは物質の状態で周波数依存性が変わるという点である。例えば氷は電子レンジを使ってもマイクロ波を吸収せず加熱されないのは有名な話であるが、900 MHz 程度の低周波数では吸収する。このマイクロ波を利用して冷凍肉の解凍に実際に用いられている。また温度が変わることで誘電率は大きく変わらないが誘電損失は大きく変わる。例えば、エタノールでは 10 °C と 70 °C で比べると 70°C の方が 2.45 GHz のマイクロ波を吸収する。つまり 10 °C のエタノールに 2.45 GHz のマイクロ波を照射すると照射時間と共に温度と誘電損失が増大する。その結果、温度上昇によって加速的にマイクロ波加熱が進む場合があるといえる。また、固体物質にマイクロ波照射を行った場合に固体部分が熱発生で少し液化した途端、その部分の誘電損失が大きいと急激な温度上昇が起こる場合があるといえる。

1.5 マイクロ波効果

化学分野におけるマイクロ波照射の利用は無機化学では 1970 年後半、有機化学では 1980 年半ばから発表されている。しかしそれ以前でも当たり前のように加熱方法としてマイクロ波は使われているようである。注目されるようになったのは様々な反応系に対して既存の加熱方法と比べて、マイクロ波によって有機反応の反応時間が大幅に向上する[5,6,9-17]、重合時間が減る[18-21]、酵素の活性化[22-25]といったものが数多く発表されたからである。これらは熱的効果だけでは説明できないものばかりであった。そのため、マイクロ波特有の非熱的効果の存在が示唆されてきた[26]。例えば、ケトンの還元反応(Figure 1.2)では同じ温度にも関わらず通常加熱より反応が迅速に終了し収率が劇的に上昇した。また 1, 2, 4-トリアゾールの反応で（Figure 1.3）は通常加熱では 3 つ（N_1, N_4, $N_{1,4}$）の化合物が生成されるが、マイクロ波加熱では 1 つ（N_1）のみが生成されて選択性を与える。

この非熱的効果の有無については様々な議論がされてきたが、2008 年にマイクロ波照射による非熱的効果があるとされていた 4 つの有機反応を精査したところ非熱的効果が認められなかったという論文[17,27]が発表されていて支持を得ておりマイクロ波による反応性の向上は熱的効果によるものだと考えられている[6]。一方では 2010 年にコバルト(Co)粒子が混入してある DMSO でラマン分光法によって非熱的効果を検証されている[13]。Co 粒子はマイクロ波照射のよる加熱効率が非常に良い。マイクロ波照射中の DMSO のラマンスペクトルによって算出された温度が溶媒の温度(450 K)よりもかなり高いスポット(500 K)が見られた。これはマイクロ波によって加熱された Co 粒子に影響を受け近接した DMSO 分子が超高温になっているとし、結論として Co 粒子に近接した DMSO

分子の非平衡局所加熱状態(Non-equilibrium local heating state)を観測したとしている。また、2014 年にはマイクロ波を用いることで今までの加熱方法ではできなかったポリ乳酸の短時間合成に成功しており、特に電場による非熱的効果が強いことが報告されている[21]。このように化学分野においてもマイクロ波加熱現象は注視されている状況である。

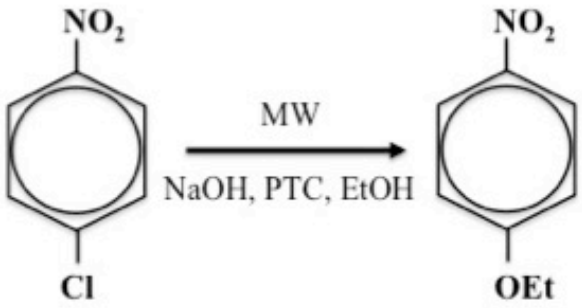

	Time	Yield
Δ-heating	4 h	99 %
MW-heating	2 min	99 %

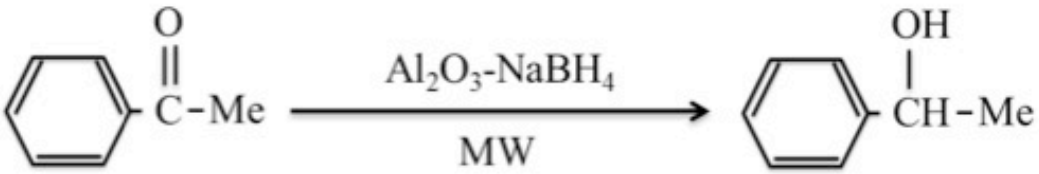

	Temp.	Time	Yield
Δ-heating	130 ^{0}C	4 h	40%
MW-heating	130 ^{0}C	2 min	90%

Figure 1.2 マイクロ波加熱を用いることで反応促進を示すケトンの還元反応例

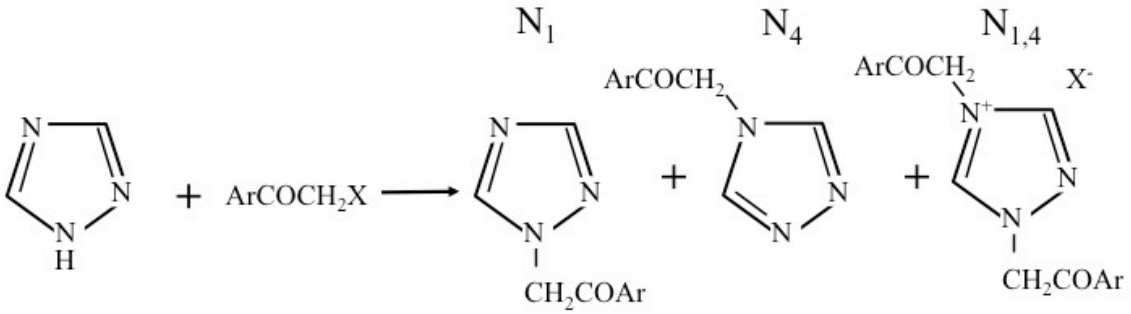

Ar	X	時間[分]	温度[°C]	加熱方法	収率(%)	N_1	N_4	$N_{1,4}$
	Cl	25	140	MW	90	**100**	-	-
				Δ	98	38	29	38
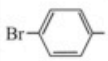	Cl	20	140	MW	95	**100**	-	-
				Δ	98	38	22	37
	Br	24	170	MW	90	**100**	-	-
				Δ	98	38	28	34

Figure 1.3 マイクロ波加熱を用いた 1, 2, 4-トリアゾールの反応による選択性の変化

1.6 まとめ

今後、化学分野において非常に有用であるマイクロ波加熱を用いた応用が増えることが予想される中でマイクロ波加熱現象の理解が非常に重要になってくる。これまでマイクロ波照射状態を分子レベルで観測する実験法はまだ確立されていないことと熱的効果との区別が難しいことから、マイクロ波加熱機構が未だによく分かっていないのが現状である。

そこで、本研究ではマイクロ波照射状態を分子レベルで観測する実験法として既存のプローブにマイクロ波回路を組み込んだマイクロ波照射 NMR を開発し、マイクロ波加熱中の試料を NMR 測定することでマイクロ波加熱現象を分子論的に理解することを目指した。局所加熱 NMR、高温 NMR、温度ジャンプ NMR のマイクロ波加熱を用いた測定を行い、熱的効果との区別はスペクトルの線幅や化学シフトで温度を換算することで行った。研究対象にした液晶分子は大きな双極子モーメントを有しており、誘電損失による加熱効率が高い物質である。その液晶分子を用いてマイクロ波加熱現象を明らかにすることを目的とした。

本稿では第２章ではマイクロ波照射 NMR 装置の開発とし装置開発と実際の測定を述べる。特にプローブ開発ではさまざまな工夫を凝らしたので注目していただきたい。第３章ではマイクロ波照射 NMR による液晶分子(PCH3)の解析とし液晶分子である 1-cyano-4-(trans-4-propylcyclohexyl) benzene (PCH3) の相転移温度付近における局所加熱 NMR と相転移温度以上の高温 NMR 測定結

果について述べる。局所加熱 NMR ではスペクトルの線幅から温度を算出することでマイクロ波加熱の実態を調べた。高温 NMR では各プロトンの ^{1}H NMR 化学シフトの変化に注目し、分子内におけるマイクロ波加熱による変化を調べた。第 4 章ではマイクロ波照射 NMR による液晶分子(MBBA)の解析とし液晶分子である N-(4-methoxybenzyliden)-4-butylaniline (MBBA) の高温 NMR 結果について述べる。第 3 章で述べる PCH3 よりもマイクロ波照射により変化が大きくが非常に興味深い結果が得られた。第 5 章では液晶―等方相状態相関二次元 NMR 分光法の開発とし開発したマイクロ波加熱 NMR 装置で高速温度ジャンプの実験を行った。4'-ethoxybenzylidene-4-n-butylaniline (EBBA)試料において、高速での相転移が可能になったのを利用して、液晶相―等方相の状態相関二次元 NMR スペクトルの観測結果を述べる。

第 2 章　マイクロ波照射 NMR 装置の開発

2.1　マイクロ波照射 NMR プローブの開発

マイクロ波照射 NMR 分光器の模式図を Figure 2 A に示す。既存の固体 NMR 分光器(Chemmagnetics CMX-400 infinity)にマイクロ波共振回路(Figure 2 B,C 次ページ)が備えてあるプローブを組み込んでいる。このプローブはマグネトロン（東京電子 2.45 GHz, 1.3 kW）と同軸ケーブルで接続している。またマグネトロンと NMR 分光器とも接続することでパルスプログラムの中でマイクロ波照射を可能にした。

マイクロ波共振回路はラジオ波回路の分離を良くし、さらにマイクロ波加熱を防ぐために NMR 信号強度が下がってしまうが、ラジオ波共振回路の中に組み込んだ。幅 4 mm、長さが 38 mm の銅泊を 6φ のガラス管（シゲミ）で挟むことでコンデンサーの役割を果たし、端の部分で 180° 銅泊を覆ったものをコイルとしてマイクロ波共振回路として使用した(Figure 2 B,C)。ラジオ波の共振回路ではコイルに試料を挿入してコンデンサーで同調をとっていて、マイクロ波の共振回路では試料をコンデンサーに挿入してコンデンサーのキャパスタンスを変化させて同調をとることで双方の回路の分離をよくした二重同調回路になっている(Figure 2 B 次ページ)。

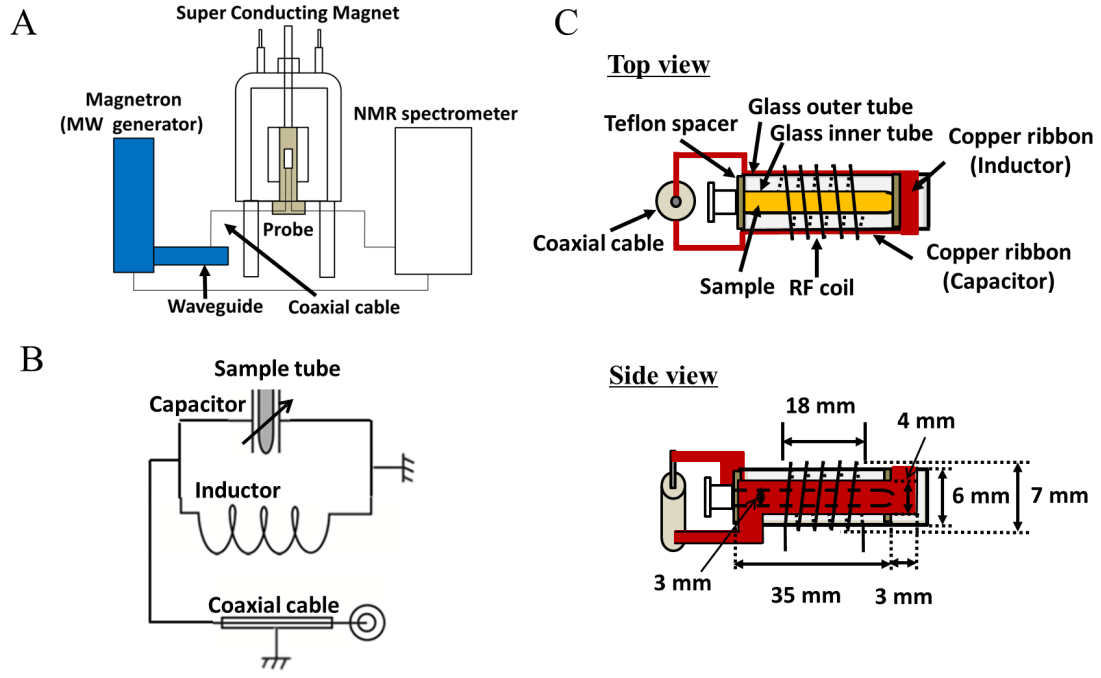

Figure 2 (A) *in-situ* マイクロ照射 NMR 分光器 (CMX Infinity 400, Chemagnetics)の模式図 (B) マイクロ波回路　(C) サンプル管、マイクロ波回路およびラジオ波回路の模式図　上：上面図　下：側面図

NMR プローブに接続されたマグネトロンは最大 1.3 kW のパルスおよび連続波照射が可能である。マグネトロンから発生したマイクロ波は導波管から同軸ケーブルに変換して NMR プローブに導入している。また、高温実験にするにあたって本来使用する系である 5φ の試料管ではなく、径の小さい 3φ 試料管を用いて Figure 2 C（前ページ）のようにマイクロ波回路と接触しないようにし、空気で断熱することで試料のみが加熱されるようにした。

この装置の開発によってマイクロ波照射中の分子を解析できる実験方法として利用できるようになり、さらに後述する局所加熱 NMR、高温 NMR、温度ジャンプ NMR 測定が可能になった。

2.2 マイクロ波照射装置

マイクロ波発信機（東京電子 2.45 GHz, 1.3 kW）は東芝製のマグネトロン２M１６４の発信管が搭載されている。この装置は以下の手順でマイクロ波照射を行う。

①入力端子台に３相交流及びアースに接続する。
②AC200V 3 ϕ を配電盤から供給し、ブレーカーを ON にする。
③STANDO BY「OFF」ランプが点灯するので STANDO BY「ON」を押す。
④STANDO BY「ON」が点灯し、約１分後に OPERATE「OFF」ランプが点灯するので「OUTPUT CONTROL」が０になっていることを確認して OPERATE「ON」を押す。

＜CW（連続波）の場合＞
CW-PULUS 切り替えスイッチを CW にし、「OUTPUT CONTROL」によって出力調整する。

＜PULSE（パルス）の場合＞
CW-PULUS 切り替えスイッチを PULSE にし「EXT. PULSE IN」コネクターにトリガー回路を接続し「OUTPUT CONTROL」によって出力調整する。

停止する場合は「OUTPUT CONTROL」を０にし、OPERATE「OFF」、STANDO BY「OFF」の順番に押す。そして３分以上待ち、十分冷めてからブレーカーを OFF にする。

2.3 NMR 測定

NMR 測定は Chemmagnetics CMX-400 infinity で行った。まず、水を標準試料とし温度を 20°C に設定し、シム調整を行った。磁場勾配を変えながら水の ^{1}H NMR スペクトルを見て、ピークの形が対称で線幅が狭いものにすることで試料中の磁場の均一化をした。実際、銅泊など通常の測定ではない材料が組み込まれているためにシム調整が非常に難しいので注意が必要である。例えばサンプル管の長さもよってもシムが変わるので標準試料と実際に測定する液晶試料の

サンプル管は同一の長さが望ましい。また、用いた液晶試料でもシム調整の確認を行うことでこの後、行った化学シフトによる温度測定を正確なものにした

次に試料を水（20°C）にして、^{1}H NMR 測定によってでてくるピークを 0 ppm に設定した。これからの ^{1}H NMR スペクトル結果は全てこのリファレンスで表示している。ここで注意しなければならないのが温度による化学シフト変化である。水素結合を含む水は特に温度による化学シフト変化が激しいので、温度設定をしっかり行うことが肝心である。

リファレンスを決めた後、90°パルスの長さの決定を行った。パルス幅を任意で ^{1}H NMR 測定を行い、信号が無くなったところを 180°パルスの幅とし半分の値を 90°パルスの長さとした。この後、固体 NMR で標準的な手法である MAS 法の角度調整があるが、今回の測定では用いらなかったため行わなかった。

第 3 章　マイクロ波照射 NMR による液晶分子(PCH3)の解析

3.1 PCH3 (1-cyano-4-(trans-4-propylcyclohexyl)benzene)

PCH3 は Figure 3.1 A で示される構造をもつ、液晶ゲル相転移温度(Tc)が 45°C の液晶分子である。Figure 3.1 B, C で示すように Tc より低い温度である 35°C に設定して ^{1}H NMR スペクトルを測定したところ、20 kHz の広幅の液晶特有のスペクトルであり、Tc より高い温度である 50°C では等方相の先鋭な信号が現れ、個々のプロトンで帰属ができるようになった[26]。この試料を用いてマイクロ波照射を用いた局所加熱および高温 NMR 測定を行った。

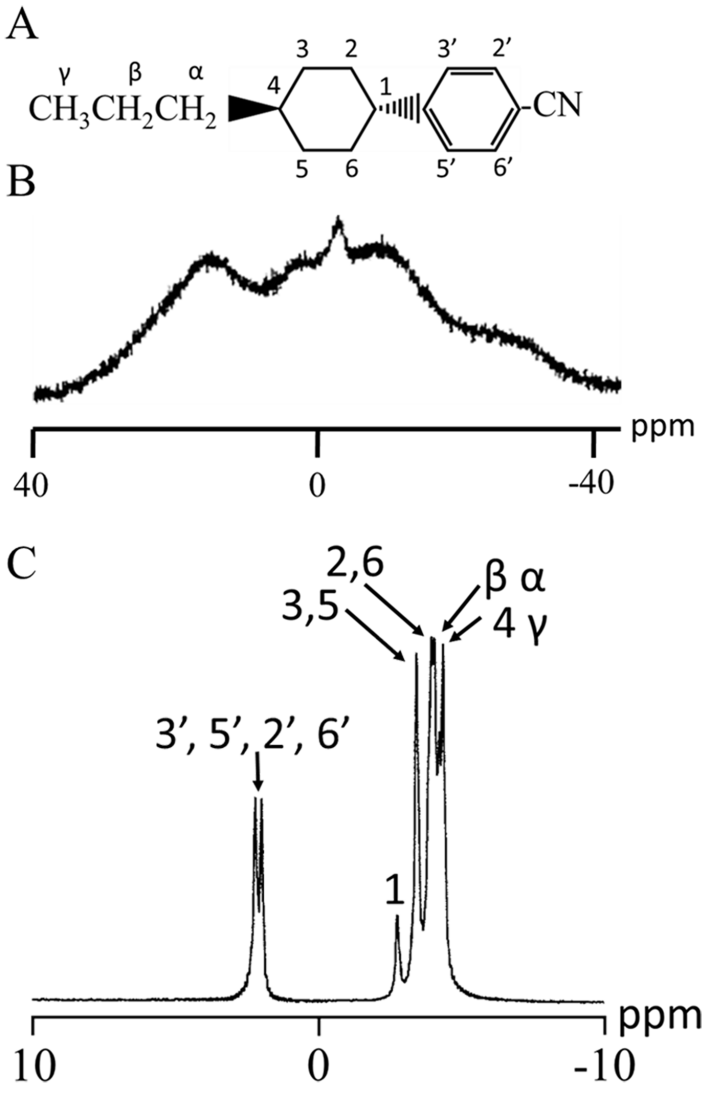

Figure 3.1 PCH3(A) 分子構造　(B) 40 °C（液晶相）の ^{1}H NMR スペクトル　(C) 50 °C（等方相）の ^{1}H NMR スペクトル.

3.1.2　液晶分子の ^{1}H NMR

液晶分子は高い双極子モーメントをもち、磁場中では配向する性質がある。つまり強磁場下である NMR では配向した状態で観測していることになる。液晶相では ^{1}H NMR では双極子-双極子相互作用が存在する。ここで Figure 3.2 に示した太枠で囲われているプロトン間のみに注目してみる。ここの間の双極子-双極子相互作用は NMR スペクトルと依存しており、分裂幅を $\Delta\nu$ とすると以下の式に表すことができる。

$$\Delta\nu = \frac{3\gamma^2\hbar}{4\pi r^3}(3\cos^2\theta - 1)\cdot S$$

S は配向因子と呼ばれるもので以下の式表すことができる。

$$S = \frac{1}{N}\sum_{i=1}^{N}\frac{1}{2}(3\cos^2\zeta - 1)$$

この式には配向角である ζ が含まれているため液晶分子の物性を知ることが ^{1}H NMR から知ることができる。しかしながら実際にはプロトンの数は多いため分裂した双極子パターンの重なりになり、結果として広幅なスペクトルが得られる。

等方相の ^{1}H NMR は ^{1}H 同士の双極子－双極子相互作用が分子の等方運動で平均化されるため先鋭な信号が得られる。ここで得られる ^{1}H の等方化学シフトは反磁性しゃへい定数に依存する。これは電子密度に依存することと対応していて、^{1}H が 1 s 電子のため球対称性が高いことに起因している。

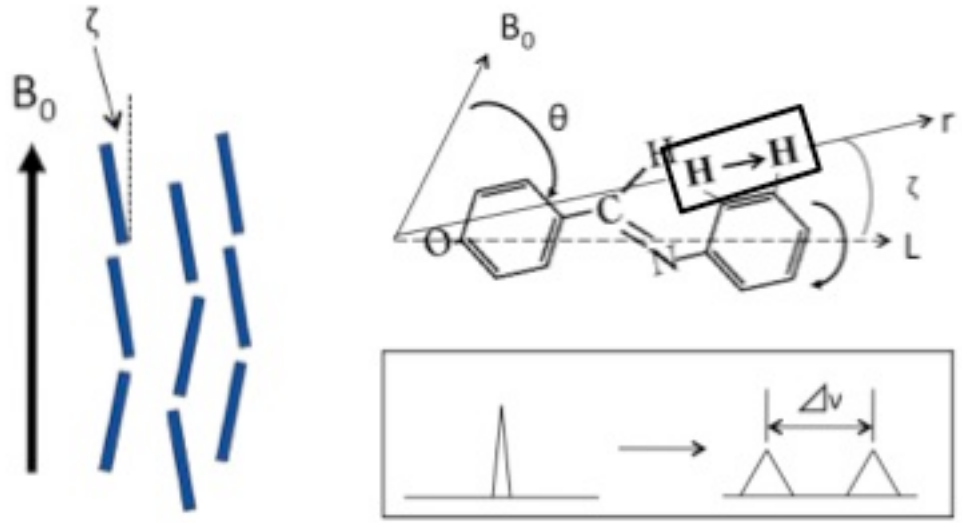

Figure 3.2 液晶分子の磁場配向の様子（左）と双極子パターンの分裂幅（右）の関係

3.3 実験方法

3.3.1 局所加熱 NMR（相転移温度付近）

第 2 章で開発した装置を用いて、相転移温度付近における熱伝導加熱(Thermal heating)とマイクロ波加熱(MW heating)で ^{1}H NMR スペクトルの比較を行った。熱伝導加熱では NMR 装置に付属されている温度コントロール装置で任意の温度設定を行った。この装置は空気をプローブに流入しつづけることで温度コントロールを行っている。マイクロ波加熱では初期温度として 20℃に設定して空気を流入しつつ、連続波(Continue Wave)によるマイクロ波照射を相転移温度付近になるようにパワー調節を行い 30 分後に ^{1}H NMR 測定を行った。^{1}H NMR 測定は 400 MHz の共鳴周波数で 90°パルスは 2.0 μ 秒で行った。

3.3.2 高温 NMR

50°Cに温度設定を行い、試料を完全に等方相にした後に30分放置したものを初期条件とした。そこから任意の外部出力(65 W, 130 W, 195 W)のマイクロ波を連続波として照射しながら1分ごとに繰り返し時間を1.0秒で4回の積算で^{1}H NMR測定を行い、マイクロ波加熱過程を追った。また、50°C から95°Cの間 を5°C おきに^{1}H NMR測定を行い、それぞれのプロトンに対応する化学シフト値のプロットを行った。これは化学シフトの温度依存性から試料の温度測定するためである。^{1}H NMR測定は前節と同様に400 MHzの共鳴周波数で90°パルスは2.0 μ秒で行った。

3.4 結果と考察

3.4.1 局所加熱 NMR（相転移温度付近）

それぞれの加熱過程における ^{1}H NMR スペクトルを Figure 3.2 に示す。熱伝導加熱では 45℃(Figure 3.3 C)と 46℃(Figure 3.3 D)の境目に一斉に等方相になった。マイクロ波加熱で特徴的なスペクトルは 54.6 W(Figure 3.3 G J)であり、ほとんどが液晶相の中にわずかの等方相が観測された。これは温度変化では観測されなかったスペクトルである。Figure 3.4 A のグラフは温度変化によるスペクトルから横軸を温度、縦軸は液晶相の線幅をプロットしたものである。その結果、相転移温度に近づくにつれて線幅が狭まることがわかった。その関係を用いてマイクロ波加熱によって相転移が起きた 54.6 W の液晶相の線幅から温度を算出したところ 38.1℃だった(Figure 3.4 B)。つまり相転移温度より低い温度で等方相が観測されたことからマイクロ波局所加熱状態が起こり、空間的温度分布が生じたと考えられる。これらの結果を考慮に入れたマイクロ波加熱と熱伝導加熱の違いを Figure 3.5 に示す。単なる熱伝導加熱(E,F,G)では表面から加熱され、相転移温度になると全体に熱伝導し等方相に転移するが、マイクロ波加熱(A,B,C,D)では一部が局所加熱状態になりそれが周り熱伝導して加熱されることで等方相と液晶相の温度に差が生まれると考えられる。この局所加熱状態を捕らえているのが Figure 3.2 G J のスペクトルだと考えられる。

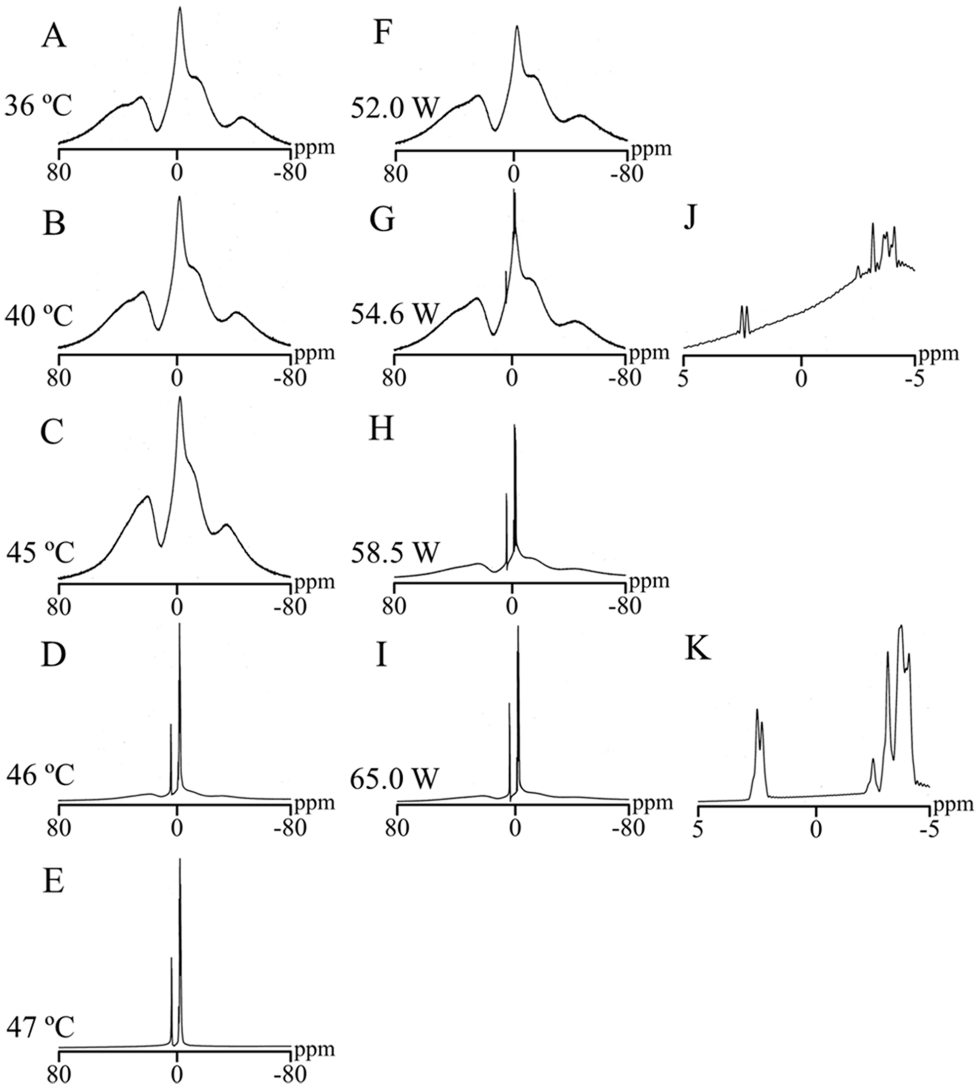

Figure 3.3　PCH3 の ^{1}H NMR スペクトル
温度変化 (A)36°C(B)40°C (C)45°C (D) 46°C (E) 47°C および連続波照射（マイクロ波）による マイクロ波照射パワー変化(F)52.0 W (G,J)54.6 W (H)58.5 W (I,K) 65.0 W

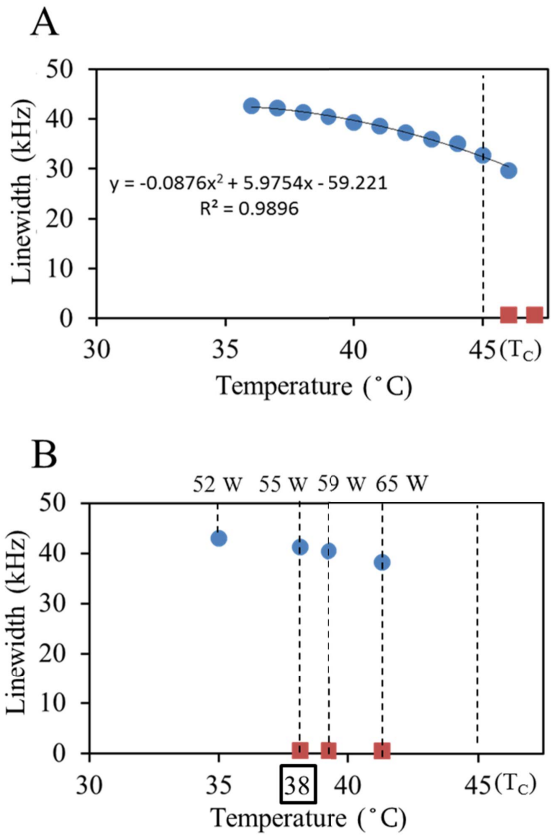

Figure 3.4　PCH3 の ^{1}H NMR スペクトルの線幅と温度の関係
(A)温度コントロール（熱伝導加熱）　(B) マイクロ波加熱

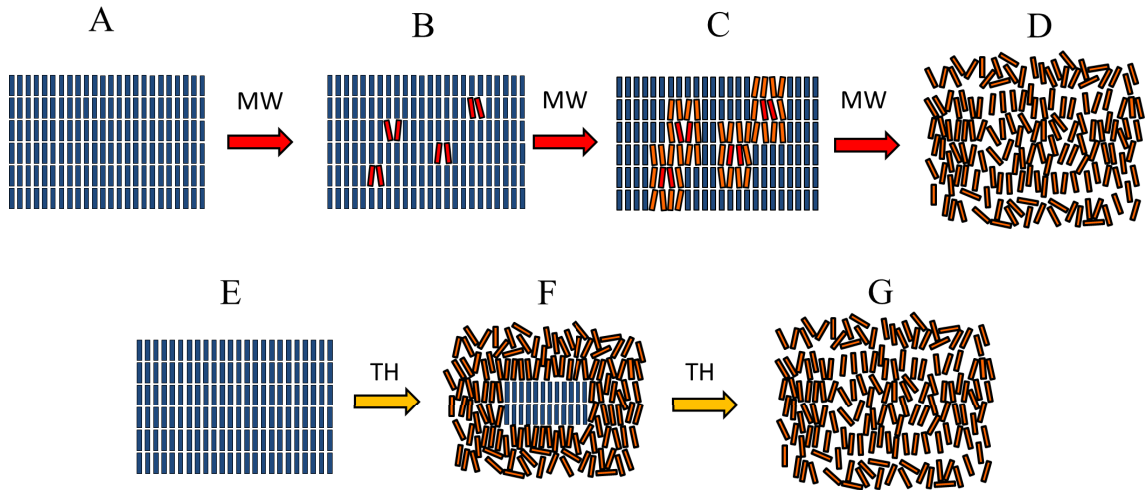

Figure 3.5 液晶分子のマイクロ波加熱と通常加熱の違い
上： マイクロ波加熱　下：通常加熱

3.4.2 高温 NMR

それぞれのマイクロ波出力における照射開始から 10 分後の ^{1}H NMR スペクトルを Figure 3.6 に示す。その結果、マイクロ波出力の増加に伴い、高磁場シフトと線幅の広がりが観測された。この高磁場シフトや広幅化を詳細に解析するために温度変化による化学シフトの変化をすべてのプロトンで調べた結果が Figure 3.7 である。縦軸が化学シフトの変化、横軸は温度で温度によってどれだけ高磁場シフトしているか示したものである。この結果から温度上昇でそれぞれのプロトンによって異なった値でリニアに高磁場シフトすることがわかった。化学シフトには温度依存性がありリニアに変化することが様々な核種で報告されており、それと合致する結果となった[27-30]。

高磁場シフトと広幅化はそれぞれ高温化と空間的温度分布に対応していると考えられる。次にこの化学シフトと温度の関係を用いて各時間におけるプロトン温度を求めてみた。Figure 3.8 はマイクロ波による高磁場シフトから求めたプロトン温度の径時変化である。特に高温では各プロトンの温度にある程度のばらつきがあり空間だけではなく分子内でも温度分布が生じていることもわかった。また一番強いパワーである 195 W においては 200 ºC 以上の化学シフトを示しマイクロ波加熱による高温 NMR を達成することもできた。

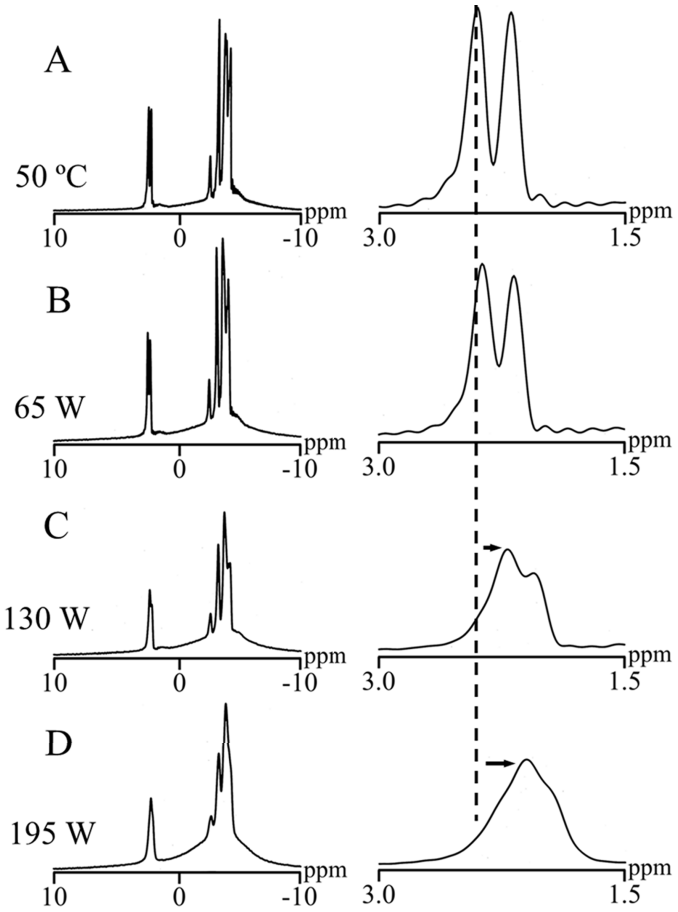

Figure 3.6

PCH3 の ^{1}H NMR スペクトル　(A) 50 ^{o}C （初期条件）

10 分間のマイクロ波照射　(B) 65 W　(C) 130 W　(D) 195 W

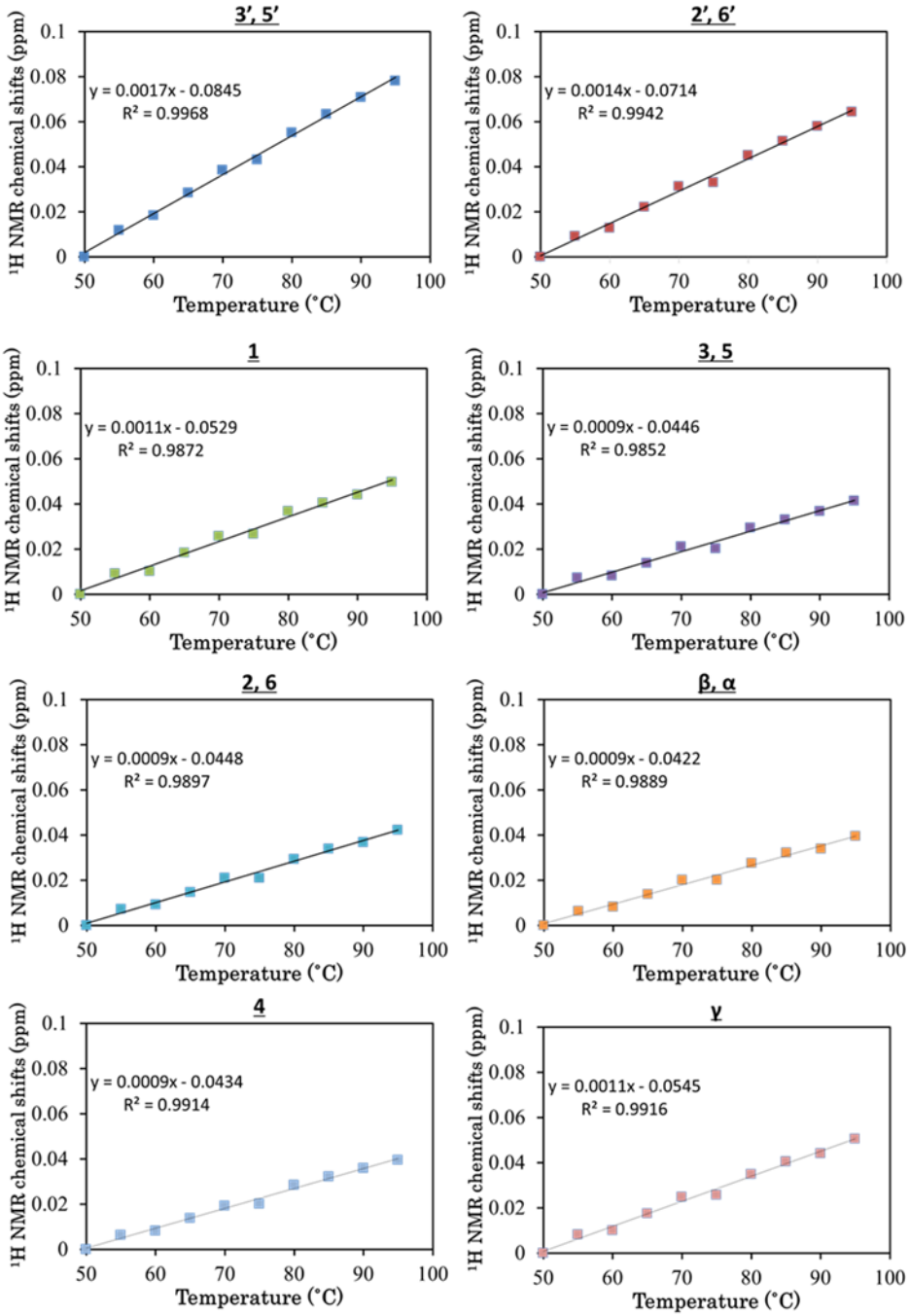

Figure 3.7　PCH3 における ^{1}H 化学シフト値と温度の関係

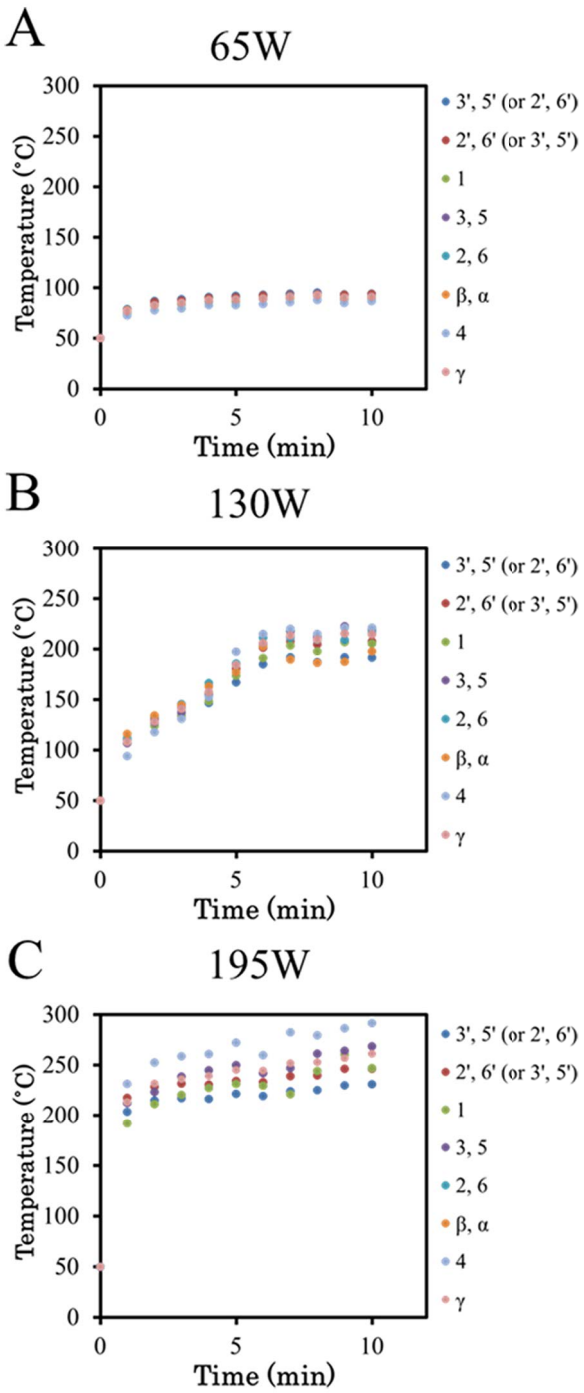

Figure 3.8 PCH3 におけるマイクロ波照射時間による温度プロット **(A) 65 W, (B) 130 W (C) 195 W**

第４章　マイクロ波照射 NMR による液晶分子(MBBA)の解析。

4.1 MBBA

MBBA は Figure 4.1 A で示される構造をもつ、液晶ゲル相転移温度(Tc)が 40°C の液晶分子である。Figure 4.1 B, C で示すように Tc より低い温度である 35°C に設定して ^{1}H NMR スペクトルを測定したところ、広幅の液晶特有のスペクトルであり、Tc より高い温度である 50°C では等方相の先鋭な信号が現れて、個々のプロトンで帰属ができるようになった[31]。この試料を用いてマイクロ波照射 NMR 測定を行った。

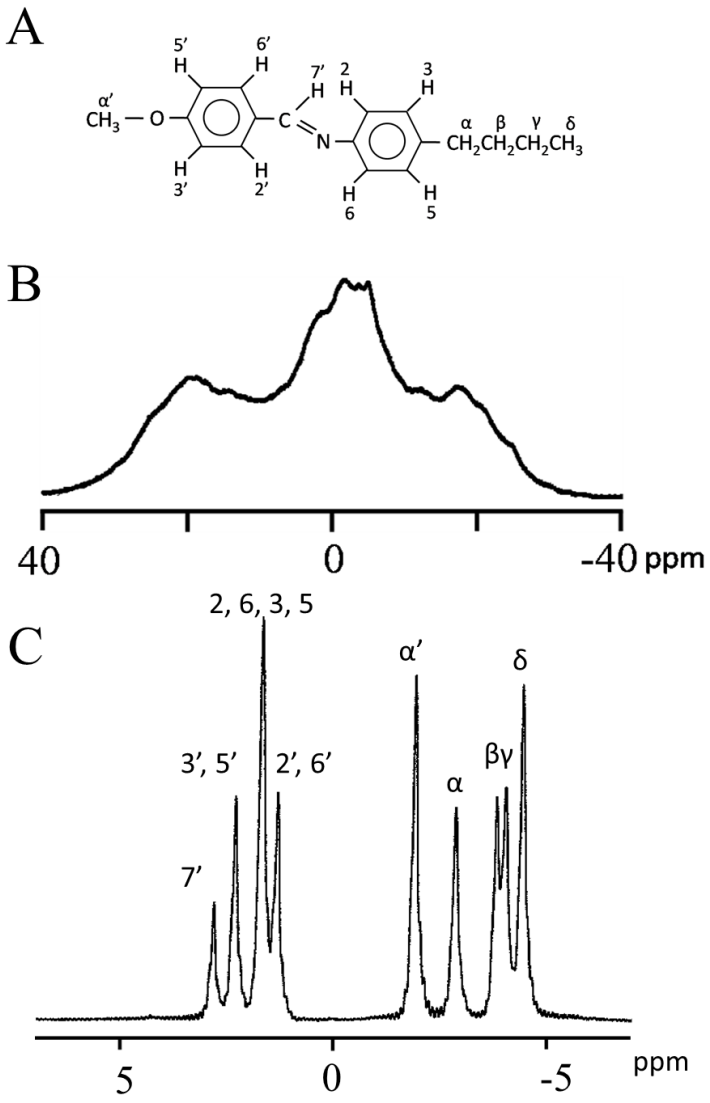

Figure 4.1 MBBA の(A) 分子構造　(B) 35 °C（液晶相）の ^{1}H NMR スペクトル　(C) 50 °C（等方相）の ^{1}H NMR スペクトル.

4.2 実験方法

50°C に温度設定を行い、試料を完全に等方相にした後に 30 分放置したものを初期条件とした。そこから任意の外部出力(65 W, 130 W, 195 W)のマイクロ波を連続波として照射しながら 1 分ごとに繰り返し時間を 1.0 秒で 4 回の積算で ^{1}H NMR 測定を行い、マイクロ波加熱過程を追った。また、50°C から 90°C の間 を 5°C おきに ^{1}H NMR 測定を行い、それぞれのプロトンに対応する化学シフト値のプロットを行った。^{1}H NMR 測定は 400 MHz の共鳴周波数で 90°パルスは 2.0 μ 秒で行った。

4.3 結果と考察

それぞれのマイクロ波出力における照射開始から 10 分後の ^{1}H NMR スペクトルを Figure 4.2 に示す。PCH3 と同様にマイクロ波出力の増加に伴い、高磁場シフトと線幅の広がりが観測された。この高磁場シフトや広幅化を詳細に解析するために温度変化による化学シフトの変化をすべてのプロトンで調べた結果が Figure 4.3 である。こちらも PCH3 と同様に温度上昇でそれぞれのプロトンによって異なった値でリニアに高磁場シフトすることがわかった。この化学シフトと温度の関係を用いて各時間におけるプロトン温度を求めてみた。Figure 4.4 はマイクロ波による高磁場シフトから求めたプロトン温度の径時変化である。高温では各プロトンの温度にある程度のばらつきがあり分子内でも温度分布が生じているが PCH3 と大きく違い、特定のプロトンが大きな温度上昇を示し、より大きい温度分布を示した。Figure 4.5 では温度上昇を示すプロトンとそうでないもので分けたものだが、温度上昇を示すのは 7'と α'であり極性基近傍のプロトンであり、それ以外のプロトンでは温度分布が見られなかった。さらに、これは温度校正されている温度内でも起こっていることである。

この結果はマイクロ波の電場の効果により、このグループの分極が変化して、プロトンの電子密度が変化したため、大きく化学シフト値が変化したことが示唆された。このマイクロ波照射による分極変化は温度上昇で起こる分極変化より格段に大きいものであり、マイクロ波特有の現象であると考えられる。さらに分子の極性部位の分極が変化することは、分子の反応性にも大きな効果があることを意味しており、マイクロ波による有機化学の反応性の促進と関係していることを示唆している。

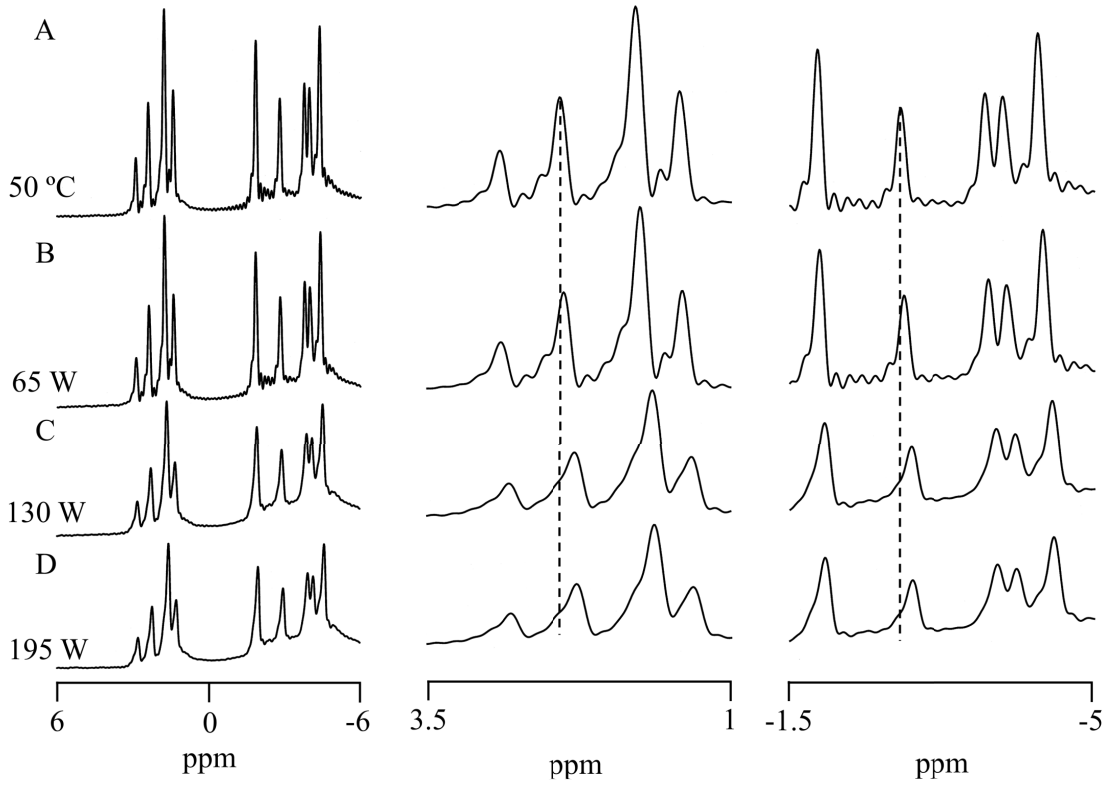

Figure 4.2

MBBA の ^{1}**H NMR** スペクトル　**(A) 50** ^{o}**C**（初期条件）および **10** 分間のマイクロ波照射 **(B) 65 W　(C) 130 W　(D) 195 W**

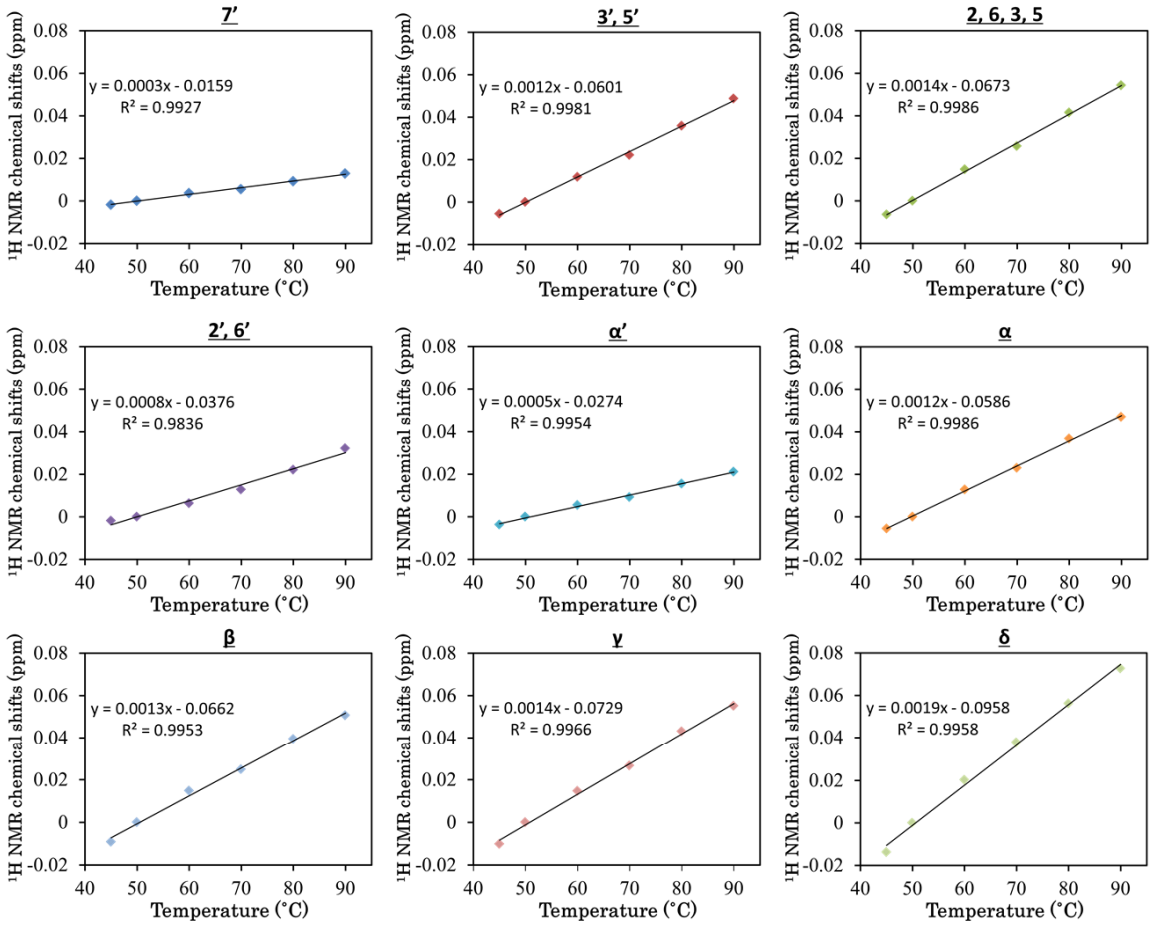

Figure 4.3　MBBA における ^{1}H 化学シフト値と温度の関係

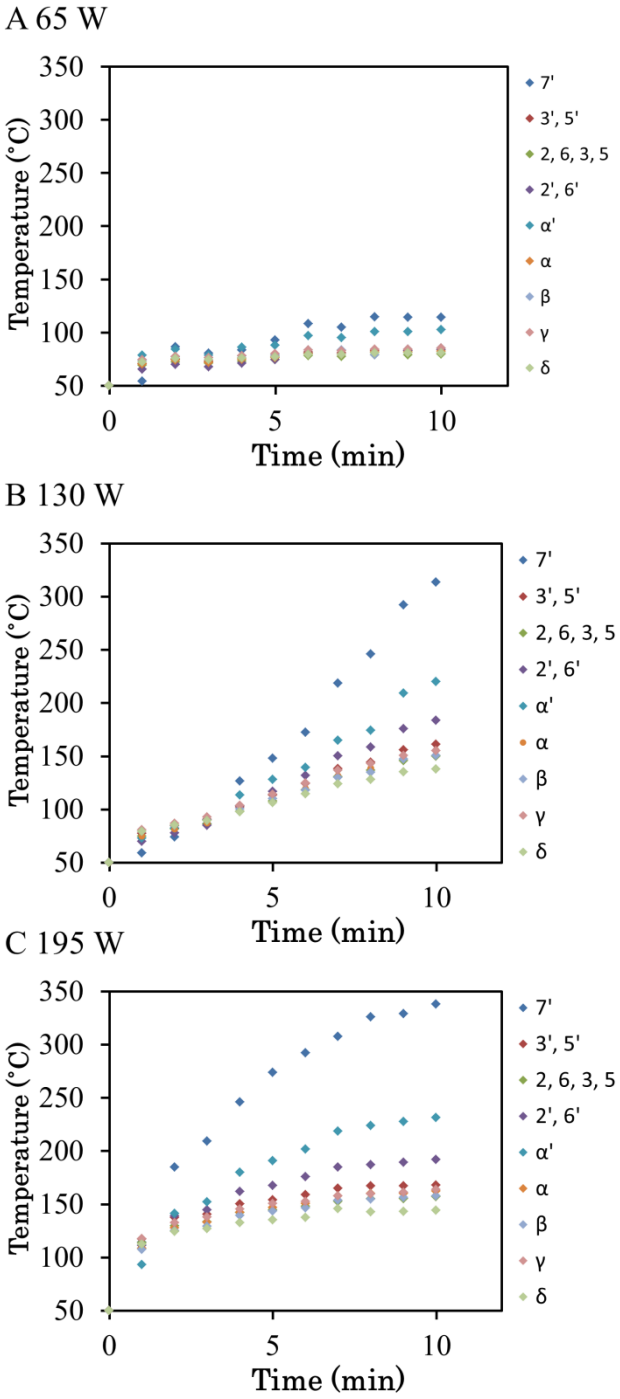

Figure 4.4 MBBA におけるマイクロ波照射時間による温度プロット **(A) 65 W, (B) 130 W (C) 195 W**

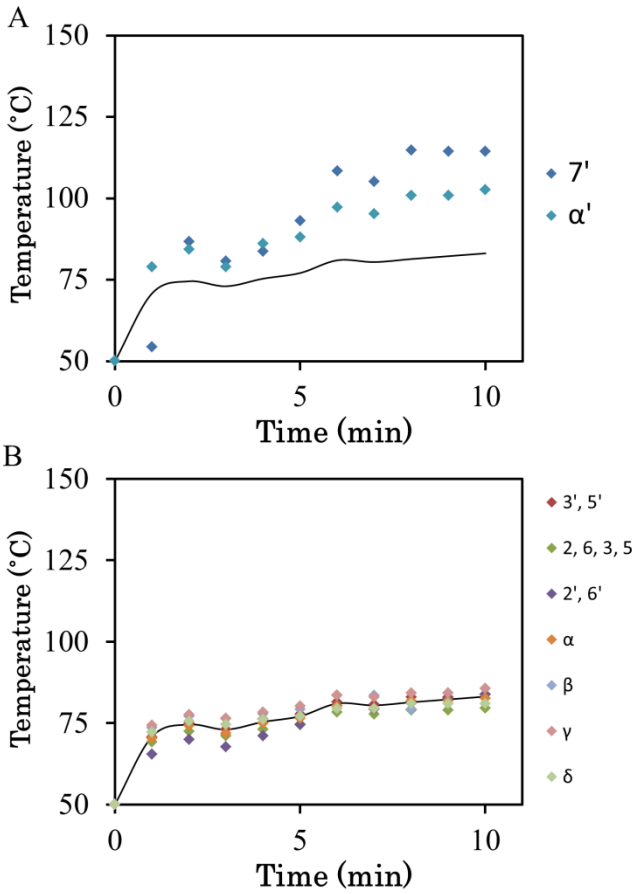

Figure 4.5 Figure4.4(A)におけるマイクロ波照射時間による温度プロット**(A:7',α' B:**それ以外**)** グラフ中の線は **B** の平均値を示している。

第 5 章　液晶―等方相状態相関二次元 NMR 分光法の開発

5.1 EBBA

EBBA の構造ならびに ^{1}H NMR スペクトルを Figure. 5.1 に示す。EBBA は液晶ゲル相転移温度(Tc)が 80°C の液晶分子である。Figure 5.1 B, C で示すように Tc より低い温度である 78°C に設定して ^{1}H NMR スペクトルを測定したところ、広幅の液晶特有のスペクトルであり、82 °C では等方相の先鋭な信号が現れた。この液晶試料を用いて、マイクロ波を照射して温度を上昇させ温度ジャンプ実験および状態相関二次元 NMR 測定[32-35]を行った。

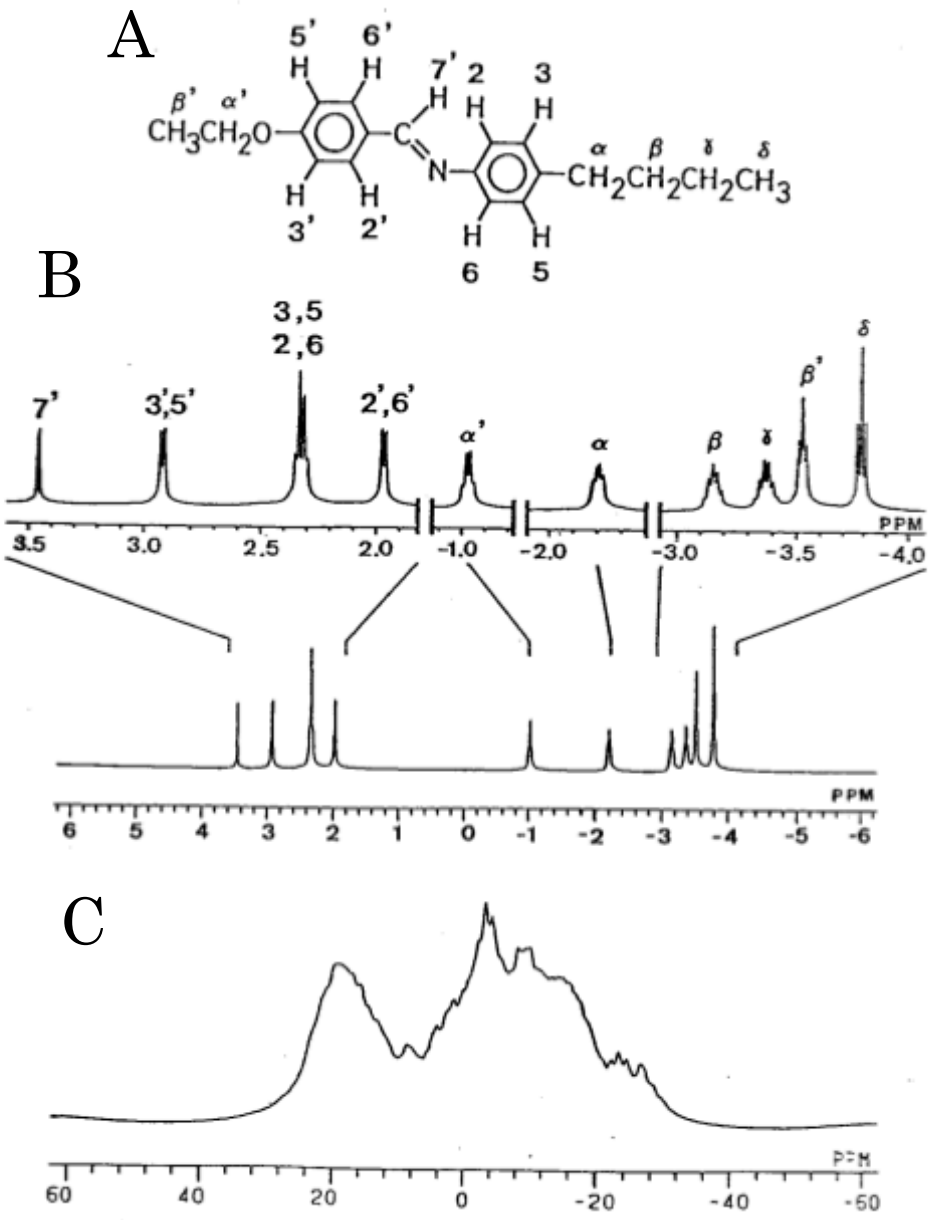

Figure 5.1 EBBA の(A) 分子構造　(B) 78 °C（液晶相）の ^{1}H NMR スペクトル　(C) 82 °C（等方相）の ^{1}H NMR スペクトル.

5.2 実験方法

5.2.1 温度ジャンプ実験

本研究では状態相関二次元 NMR を行う前に、まずパルスマイクロ波を用いて温度ジャンプ実験を行った。これは液晶分子の高速加熱現象を観測すると同時に状態相関二次元 NMR 測定における繰り返し時間を決定するために行った。また、状態相関二次元 NMR を行うにあたってスピン-格子緩和時間より液晶相から等方相へ速く転移することが必要である。EBBA の ^{1}H のスピン-格子緩和時間を測定したところ、液晶相(78℃)では 1.4 秒、等方相(82℃)では 0.9 から 1.9 秒の間であった。そのため、マイクロ波のパルス幅は十分に短い 10 ms で行い、液晶相から等方相の相転移が起こるか実際ことを ^{1}H NMR 測定で確認した。

5.2.2 状態相関二次元 NMR 測定

状態相関二次元 NMR に用いるパルス系列は２D 交換または NOE 実験(NOESY)と同じものである（Figure 5.3)。最初の 90 度パルスによって横磁化を作り出し、展開期間においてサンプルの温度は ^{1}H スピンがプロトン間による強い双極子相互作用下で歳差運動を示すように液晶相を維持する。t_1 時間で 2 回目の 90 度パルスを行い、磁化ベクトルを z 軸方向にそろえる。混合期間では、マイクロ波パルス照射を行い液晶相から等方相へ転移するまで短時間で温度を上げる。残った横磁化は液晶相の強い双極子相互作用下で、混合期間の間に 2-3 ミリ秒内で消えることが期待できる。ここでスピン拡散過程を研究するために混合期間の始めに混合時間(τ_m)を入れる。検出期間では３回目の 90 度パルスで t_2 時間で等方相の FID(Free Induction Decay)を取り込む。t_1 および t_2 の関数として記録された FID 信号は液晶相と等方相間における状態相関二次元 NMR スペクトルを得るため二重フーリエ変換を行う。

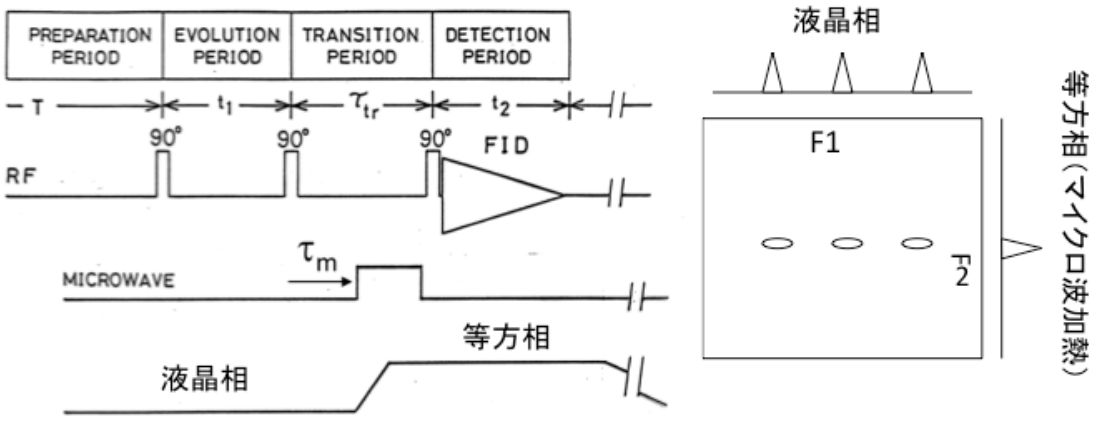

Figure 5.2 状態相関2次元NMRのパルス系列

5.3 結果と考察

5.3.1 温度ジャンプ実験

マイクロ波パルス実験の ^{1}H NMR スペクトルを Figure 5.3 に示す。試料管の径の大きさに関わらずにマイクロ波パルス照射直後の ^{1}H NMR スペクトル(Figure 5.3 B)は等方相であった。この結果から液晶相から等方相への相転移がマイクロ波照射によってスピン-格子緩和時間内である 10 ミリ秒で完了したといえる。また等方相から 78 度の液晶相へ戻るのは 5 φ の試料管では 60 秒後(Figure 5.3 D)であった。このことから状態相関二次元 NMR 実験の繰り返し時間は 120 秒に設定して行った。

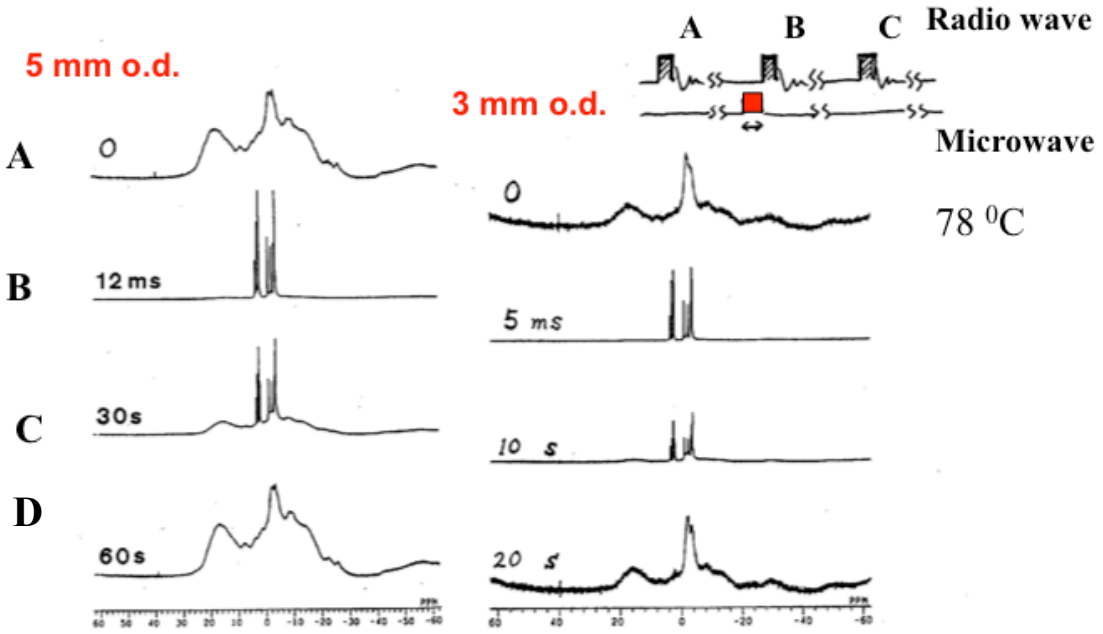

Figure 5.3 EBBA の ^{1}H NMR スペクトル　（サンプル管の径 左：5 mm 右：3 mm）

(A) 0 s (78°C、液晶相), マイクロ波パルス照射後　(B) 12 ms と 5 ms　(C) 30 s と 10 s　(D) 60s と 20s

5.3.2 状態相関二次元 NMR 測定

Figure 5.2 のパルス系列を用いた EBBA の状態相関２次元 NMR スペクトルを Figure 5.4（次ページ）に示す。このスペクトルは EBBA を用いて状態相関二次元 NMR 測定に成功していることはっきり示している。プロトンの双極子スペクトルは F2 軸の分解能、つまり等方相の分解能で F1 軸に現れていることがわかる。

Figure 5.4 の左に示しているのは EBBA の等方相と液晶相間の状態相関二次元 NMR スペクトルの等高線である。右に示しているのは F1 軸上におけるプロト

ンの断面である。実際には局所双極子磁場のプロトンは９つの種類に分けられるが、2,6 と 3,5 位のプロトンは化学シフト値がとても近いために重なってしまう。エトキシ基(β'位)のメチルプロトンの局所双極子磁場は 9.6kHz の分裂幅で 1:2:1 の強度比のトリプレットパターンであった。さらに三重線はα'位のプロトンからのカップリングに起因してさらに分かれる。一方、δ位のメチルプロトンは分離定数が非常に小さいことを表すシングレットパターンを示す。芳香環のプロトン(3, 5/3', 5'と 2,6/2',6')は主に分裂幅が 12.8 kHz のダブレットパターンを与える。メチレンおよびメチルプロトン(α, β, γ, δ)のスペクトルの特徴はそのグループの運動性を反映していることである。特に最も運動性が高いδ位のメチルプロトンはδからαプロトンへの広がりに相当する分裂幅が 8〜15 kHz を含むコアグループに近いプロトンとして線幅が広がりながらシングレットパターンを示す。メチレンプロトンにおけるダブレットパターンの分裂は芳香環のプロトンよりも少し小さいプロトンとして観測された。7'のプロトンはダブレットとシングレットパターンが混ざり合っていることものを示している。

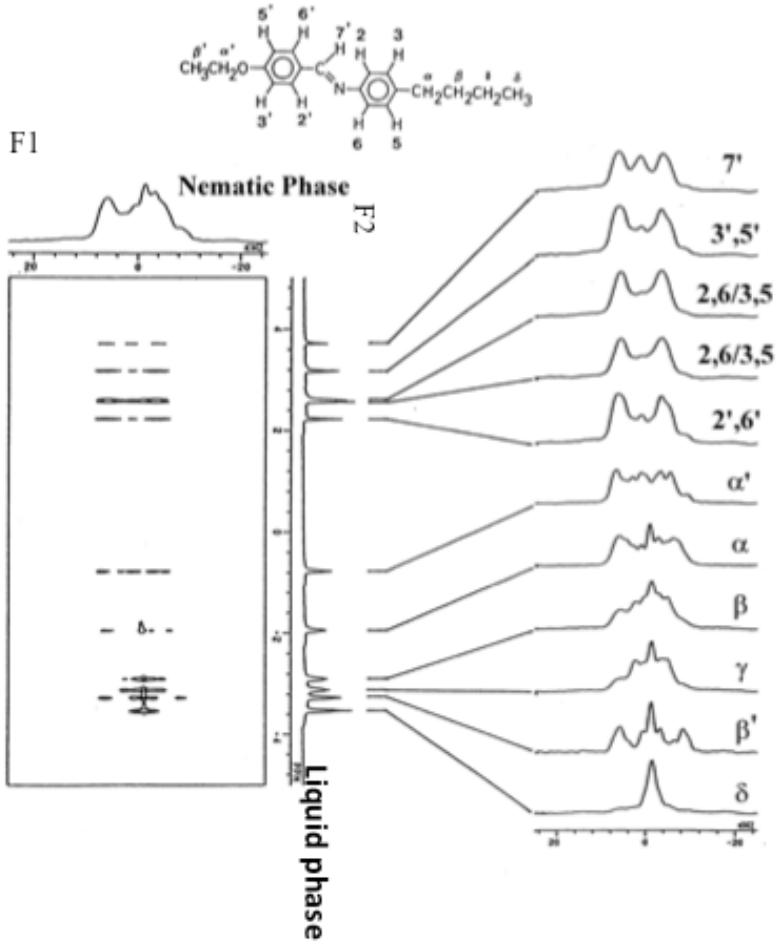

Figure 5.4 EBBA の液晶-等方相相関 2 次元 NMR

τ_m＝0 ms ではトリプレットとシングレットパターンはβ’およびδメチルプロトンのそれぞれで観測されたが、τ_m＝200 ms にすると他のプロトンのダブレットパターンがβ’とδの両方の線形と混ざり合った(Figure 5.5)。これは双極子相互作用によってメチルプロトンと他のプロトンでスピン交換が起こっていることを示している。この現象は分子内における相互作用の強さと領域に関係性が強いことから液晶相の構造解析に期待できる。なぜなら分子内双極子相互作用はより分子の速い分子の再配列によって効率的に平均化するため、等方相のプロトン間の混合速度は液晶相のプロトンよりも遅い。したがってスペクトルの混合はスピン拡散の経路を表している。実際に Figure 5.5 では芳香環のプロトンではもっとも効率的に混合して、メチルプロトンおよびメチレンプロトンは効率的に混合しない。特にエトキシ基のメチルプロトンのトリプレットパターンは明らかであり、なぜなら芳香環とブチルプロトンでは拡散が遅いためパターンは分離されるからである。一方、δプロトンは他のプロトンと速く混合してダブレットパターンに成長する。対照的にβ’プロトンはトリプレットパターンの特徴が長い混合時間後も残っている。τ_m＝600 ms の時は全てのプロトンが平衡になるには十分な長さなので、ほとんどのプロトンが同一の線形を示した。

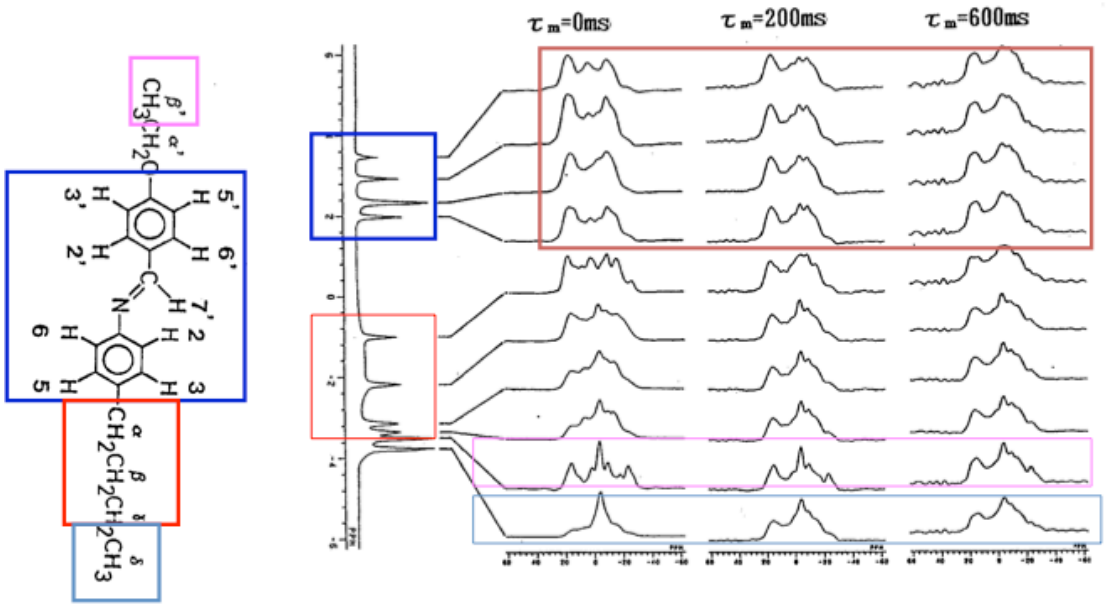

Figure 5.5　EBBAの状態相関2次元NMRの交差ピークによる混合時間(0, 200, 600 ms)の依存性

第6章　結論

１. *In situ* マイクロ波照射 NMR によってマイクロ波照射下における液晶分子内での空間的な局所加熱状態が観測された。

2. マイクロ波励起効果が分子内で異なり、特に極性基付近ではマイクロ波による分極効果が強いと考えられる。このことは化学反応機構に大きく関わることが示唆された。

3. マイクロ波照射システムを用いることで 200˚C 以上の高温 NMR 測定や温度ジャンプを利用した状態相関二次元 NMR が行うことができる。

これらの結果はマイクロ波照射 NMR 分光法がマイクロ波化学に重要な情報を提供するとともに新たな NMR 法の可能性を示している。

[1] マイクロ波の新しい工業利用技術 エヌ・ティー・エス社発行(2003)

[2] マイクロ波加熱技術集成　エヌ・ティー・エス社発行 (1994)

[3] マイクロ波エネルギーと応用技術　産業技術サービスセンター発行(2014)

[4] 化学を変えるマイクロ波熱触媒　化学同人発行 (2004)

[5] L. Perreux, A. Loupy, *Tetrahedron*, 57 (2001) 9199-9223

[6] C. O. Kappe, *Angew Chem. Int. Ed*., 43 (2004) 6250-6284.

[7]. M. Tanaka, M. Sato, *J. Chem. Phys*., 126 (2007), 034509.

[8] M. Kanno, K. Nakamura, E. Kanai, K. Hoki, H. Kono, M. Tanaka, *J. Phys. Chem*. A, 116 (2012) 2177-2183.

[9] R. Gedye, F. Smith, K. Westaway, H. All, L. Baldisers, L. Laberge and J. Rousell, *Tetrahedron Lett*., 1986, **27**, 279-282.

[10] R. J. Giguere, T.L. Bray, S.M. Duncan and G. Majetcih, *Tetrahedron Lett*., 1986, **29**, 4945-4948.

[11] D. Adam, *Nature,* 2003, **421**, 571-572.

[12] P. lidström, J. Tiemey, B. Nathey and J. Westman, *Tetrahedron*, 2001, **57**, 9235-9283.

[13] D. Bogdal, M. Lukasiewicz, J. Pielichowski, A. Miciak and Sz. Bednarz, *Tetrahedron*, 2003, **59**, 649-653.

[14] Y. Yoshimura, H. Shimizu, H. Hinou and S. -I. Nishimura, *Tetrahedron Lett.*, 2005, **46**, 4701-4705.

[15] M. C. Parker, T. Besson, S. Lamare and M. D. Legoy, *Tetrahedron Lett*., 1996, **46**, 8383-8386.

[16] H. Shimizu, Y. Yoshimura, H. Hinou and S. –I. Hishimura, *Tetrahedron*, 2008, **64**, 10091-10096.

[17] C. O. Kappe, B. Pieber and D. Dallinger, *Angew. Chem. Int. Ed*., 2013, **52**, 1088-1094.

[18] R. Hoogenboom, F. Wiesbroch, H. Huang, M.A.M. Leenen, H. M. L. Thijs, S. F. G. M. van Nispen, M. van der Loop, C. –A. Fustin, A. M. Jonas, J. –F. Goby and U. S. Schubert, *Macromolecules,* 2006, **39**, 4719-4725.

[19] T. Iwamura, K. Ashizawa and M. Sakaguchi, *Macromolecules*, 2009, **42**, 5001-5006.

[20] Y. Kajiwara, A. Nagai and Y. Chujo, *Polymer J*., 2009, **41**, 1080-1084.

[21] S. Yamada, A. Takasu, S. Takayama and K. Kawamura, *Polym. Chem*., 2014, **5**, 5283-5288.

[22] B. N. Pramanik, U. A. Mirza, Y. H. Ing, Y. -H. Liu, P. L. Bartner, P. C. Weber and A.K. Bose, *Protein Science,* 2002, **11**, 2676-2687.

[23] W. Huang, Y. -M. Xia, H. Gao, Y. -J. Fang, Y. Wang and Y. Fang, *J. Mol. Catalysis,* 2005, **35**, 115-116.

[24] S. -S. Lin, C. -H. Wu, M. -C. Sun, C. -M. Sun and Y.-P. Ho, *J. Am. Soc. Mass Spectrom.*, 2005, **16**, 581-588.

[25] M. Antonia Herrero et al. *J. Org. Chem*. ***73***, 36-47 (2008)

[26] K. Akasaka, M. Kimura, A. Naito, H. Kawahara, M. Imanari, *J. Phys. Chem.*, 99 (1995) 9523-9529

[27] A.L. Van Geet, Anal. Chem., 40 (1968) 2227-2229.

[28] A.L. Van Geet, Anal. Chem.,42 (1970) 679-689.

[29] A. Bielecki, D.P. Burum, J. Magn. Reson, Ser. A, 116 (1995) 215-220.

[30] C.S. Zuo, K.R. Metz, Y. Sun, and A.D. Sherry, J. Magn. Reson., 133 (1998) 55-60.

[31] J.S. Prasad, *J. Chem. Phys.*, 1976, **65**, 941-944.

[32] A. Naito, M. Imanari and K. Akasaka, *J. Magn. Reson*., 1991, **92**, 85-93.

[33] A. Naito and M. Ramamoorthy, Structural Studies of Liquid Crystalline Materials Using a Solid State NMR Technique. Thermotropic Liquid Crystal: Recent Advances. Springer, 2007, p85-116.

[34] A. Naito, M. Imanari and K. Akasaka, *J. Chem. Phys*., 1996, **105**, 4502-4510.

[35] K. Akasaka, M. Kimura, A. Naito, H. Kawahara and M. Imanari, *J. Phys. Chem*., 1995, **99**, 9523-9529.

謝辞

本研究を行うにあたり、多岐にわたりご指導、ご鞭撻して頂きました内藤 晶先生に心から感謝申し上げます。

マイクロ波照射 NMR プローブ製作に関してご助言ならび製作補助をして頂きました、プローブ工房の藤戸 輝昭さんには深く感謝致します。またマイクロ波照射の基本原理に関して数々のご助言を頂きました佐藤 元泰先生に深く御礼申し上げます。そして NMR 測定ならびに実験操作に関して数々のご助言を頂きました川村 出先生には深く感謝致します。さらにこの研究に携わった谷川文一さん、山上 拓也さんには深く感謝致します。

最後になりましたが内藤・川村研究室の皆様に心から感謝を申し上げるとともに、今後のさらなる発展を願っております。

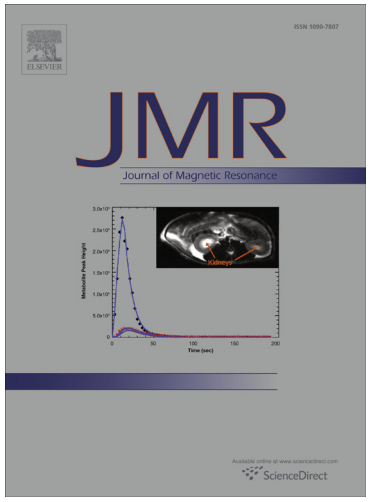

Mechanism for microwave heating of 1-(4'-cyanophenyl)-4-propylcyclohexane characterized by *in situ* microwave irradiation NMR spectroscopy

Yugo Tasei, Takuya Yamakami, Izuru Kawamura, Teruaki Fujito, Kiminori Ushida, Motoyasu Sato, Akira Naito

PII: S1090-7807(15)00029-4
DOI: http://dx.doi.org/10.1016/j.jmr.2015.02.002
Reference: YJMRE 5602

To appear in: *Journal of Magnetic Resonance*

Received Date: 19 December 2014
Revised Date: 4 February 2015

Please cite this article as: Y. Tasei, T. Yamakami, I. Kawamura, T. Fujito, K. Ushida, M. Sato, A. Naito, Mechanism for microwave heating of 1-(4'-cyanophenyl)-4-propylcyclohexane characterized by *in situ* microwave irradiation NMR spectroscopy, *Journal of Magnetic Resonance* (2015), doi: http://dx.doi.org/10.1016/j.jmr.2015.02.002

Mechanism for microwave heating of 1-(4'-cyanophenyl)-4-propylcyclohexane characterized by *in situ* microwave irradiation NMR spectroscopy

Yugo Tasei[1], Takuya Yamakami[2,#], Izuru Kawamura[1], Teruaki Fujito[3], Kiminori Ushida[2], Motoyasu Sato[4], Akira Naito[1,*]

[1]Graduate School of Engineering, Yokohama National University, 79-5 Tokiwadai, Hodogaya-ku, Yokohama 240-8501, Japan

[2]Department of Chemistry, School of Science, Kitazato University, 1-15-1 Kitasato, Minami-ku, Sagamihara 252-0373, Japan

[3]Probe Laboratory Inc.,1-7-17, Kawasaki, Hamura, Tokyo, 205-0021, Japan

[4]Faculty of Engineering, Chubu University, 200 Matsumoto-cho, Kasugai 457-8501, Japan.

[*]Corresponding author. Fax: +81-45-339-4232. E-mail address:naito@ynu.ac.jp

[#]Present address. FUJIYAKUHIN Co., Ltd., 2-292-1 Sakuragi-cho, Omiya-ku, Saitama 330-8581, Japan

Keywords: Microwave irradiation NMR spectroscopy, Microwave heating, Non-equilibrium local heating, High temperature heating, Liquid crystalline phase, Isotropic phase

Abstract

Microwave heating is widely used to accelerate organic reactions and enhance the activity of enzymes. However, the detailed molecular mechanism for the effect of microwave on chemical reactions is not yet fully understood. To investigate the effects of microwave heating on organic compounds, we have developed an *in situ* microwave irradiation NMR spectroscopy. ^{1}H NMR spectra of 1-(4'-cyanophenyl)-4-propylcyclohexane (PCH3) in the liquid crystalline and isotropic phases were observed under microwave irradiation. When the temperature was regulated at slightly higher than the phase transition temperature (Tc = 45 ºC) under a gas flow temperature control system, liquid crystalline phase mostly changed to the isotropic phase. Under microwave irradiation and with the gas flow temperature maintained at 20 ºC, which is 25 ºC below the Tc, the isotropic phase appeared stationary as an approximately 2 % fraction in the liquid crystalline phase. The temperature of the liquid crystalline state was estimated to be 38 ºC according to the line width, which is at least 7 ºC lower than the Tc. The temperature of this isotropic phase should be higher than 45ºC, which is considered to be a non-equilibrium local heating state induced by microwave irradiation. Microwaves at a power of 195 W were irradiated to the isotropic phase of PCH3 at 50 ºC and after 2 min, the temperature reached 220 ºC. The temperature of PCH3 under microwave irradiation was estimated by measurement of the chemical shift changes of individual protons in the molecule. These results demonstrate that microwave heating generates very high temperature within a short time using an *in situ* microwave irradiation NMR spectrometer.

Introduction

Microwave heating is widely used to accelerate organic reactions [1-7] and enhance the activity of enzymes [8-11]. It is considered that microwave effects can be classified as thermal and nonthermal, and it has been reported that microwave thermal effects can be separated from nonthermal effect [12]. It is known that most microwave-assisted organic reactions can be explained by microwave thermal effects [13]. However, it has been recently shown that polymerization reaction rates differ between electric and magnetic field irradiation at the same temperature, which indicates the influence of nonthermal effects on the chemical reaction [14].The microwave thermal effects contribute to a rise in the solvent temperature due to dielectric losses [4,6,15,16]. These effects are characterized as a local heating state that is induced under a microwave irradiation. However, the detailed molecular mechanism for the effects of microwave heating on chemical reaction is not yet fully understood. One of the important heating modes is non-equilibrium local heating, which has been reported for a liquid-solid mixed system under microwave irradiation [17], where non-equilibrium local heating occurred in dimethyl sulfoxide (DMSO) molecules in the proximity of Co particles under microwave irradiation. Non-equilibrium local heating is defined as the phenomenon where microwave irradiation induces domain heating at a much higher temperature than the bulk solution temperature induced by microwave irradiation.

To characterize a non-equilibrium local heating state induced by microwave irradiation, an *in situ* microwave-irradiation solid state NMR spectrometer was developed. A microwave irradiation liquid state NMR spectrometer was first developed by Naito et al. [18,19], where very rapid temperature jump experiments were achieved. Consequently, it was possible to demonstrate state-correlated two-dimensional NMR

spectroscopy to obtain a correlation between liquid crystalline and isotropic phases. This technique was useful to observe ^{1}H-^{1}H dipolar patterns of ^{1}H NMR spectra with high resolution in the liquid state rather than liquid crystalline state. This technique can be used to obtain local dipolar interaction of individual protons in the liquid crystalline state via high resolution resonance peaks in the isotropic phase [20-22], and also to detect the state-correlated two-dimensional NMR spectra of native and denatured states of proteins [23]. It should be stressed that with microwave irradiation NMR spectroscopy, electron dipole moments are excited, which causes heating of samples rather than excitation of electron spins, as in the case of electron spin resonance (ESR) and dynamic nuclear polarization (DNP) experiments.

To measure the microwave heating effects, the microwave irradiation NMR spectrometer was further improved to observe NMR signals under condition of *in situ* microwave irradiation, in contrast to ex-situ NMR spectrometer [24].In this study, it is important to accurately determine the sample temperature under microwave irradiation. It has been reported that chemical shifts change linearly with respect to the temperature [25-28]. Therefore, the relation of the chemical shifts with the temperature is calibrated using the sample itself with respect to the temperature control unit of the NMR spectrometer.

Liquid crystalline samples have high efficiency for microwave absorption, as in the case of liquid crystalline display. In particular, we have previously reported that a liquid crystalline state transferred to the isotropic phase within 10 ms of microwave irradiation [20]. It is therefore expected that a non-equilibrium local heating phenomenon could be observed more clearly under microwave irradiation. The *in situ* microwave irradiation NMR spectrometer was particularly designed to observe NMR

signals under microwave irradiation with good isolation of radio frequency wave for NMR detection from the microwave irradiation for local heating. This makes it possible to observe NMR signals under microwave irradiation condition.

Materials and Methods

A liquid crystalline sample of 1-(4'-cyanophenyl)-4-propylcyclohexane (PCH3; Tokyo Chemical Industry Co., Ltd.) was used as received without further purification. The liquid crystalline to isotropic phase transition temperature (Tc) of PCH3 is 45 °C [21].

It is important to measure the temperature of the sample directly in the NMR probe to observe microwave heating effects. Therefore, the temperature dependence of ^{1}H chemical shifts were observed for PCH3 at various temperatures using the temperature control system of the spectrometer. In the case of liquid state NMR, the difference in chemical shift $\Delta\delta$ between CH_3 and OH protons of methanol and glycol has been commonly used as a thermometer [25,26]. However, $\Delta\delta$ for methanol is not represented as a straight-line over the large temperature range. The coefficient of the quadratic term is small; therefore, the straight line approximation will not cause a large temperature error. Moreover, $\Delta\delta$ for glycol is perfectly linear within the error of 0.3 K over the range 310 – 410K. In the case of solid state NMR, the temperature dependence of the ^{207}Pb chemical shift in magic angle spinning (MAS) spectra is linear over the range of -130 to +150 °C [27]. Paramagnetic lanthanide complexes also show linear dependence on the temperature over a small temperature range [28]. In the present work, $\Delta\delta$ for individual protons in PCH3 was measured in the temperature range from 50 to 95 °C. The temperature of the sample under microwave irradiation were thus evaluated from the slope of this temperature dependence.

The microwave irradiation solid state NMR spectrometer was developed in-house with modification made to a solid state NMR spectrometer (CMX infinity 400, Chemagnetics), as schematically shown in Fig. 1A. A flat 4 mm wide and 38 mm long copper ribbon was used as a capacitor and a half turn of copper ribbon in the edge part was used as an inductor for the microwave resonance circuit (Fig. 1B and Fig. 1C), which is coaxially inserted inside the radio frequency induction coil of 7 mm diameter and 18 mm width (Fig. 1C). The dimensions of the microwave and radio frequency circuits increase the isolation between microwave and radio frequency resonance circuits and allows NMR signals to be observed under microwave irradiation condition. Although the sensitivity of NMR signals is reduced, it is important for the capacitor part of the microwave resonance circuit to be wound inside the radio frequency coil. If the radio frequency coil is located inside of the microwave circuit, strong arcing occurred and the radio frequency coil immediately disrupted. The microwave circuit was appropriately tuned to 2.45 GHz by adjusting the capacitor part of copper ribbon space in the outside of the sample tube and the radio frequency circuit was tuned to 398 MHz by adjusting variable capacitors for matching and tuning using a sweep generator. NMR spectra were recorded at 398 MHz on the CMX infinity 400 NMR spectrometer (Chemagnetics), which was equipped with a microwave generator (IDX, Tokyo Electron Co., Ltd.) capable of transmitting 1.3 kW pulsed and continuous wave (CW) microwave irradiation at a frequency of 2.45 GHz. Microwaves were transmitted from microwave generator to near the magnet through a waveguide, and transformed from the waveguide to coaxial cable. This coaxial cable was guided to the resonance circuit at the probe head. Microwave pulses were controlled by a gating pulse produced by the pulse programmer of the NMR spectrometer. The sample was cooled down to the

temperature of the liquid crystalline phase using a gas flow temperature controller. Samples were filled into a 3 mm OD and 35 mm long inner glass tube (Shigemi) for NMR measurements to insulate thermal contact with a 6 mm OD and 38 mm long outer glass tube (Shigemi) for NMR measurements without the use of any protection apparatus for high temperature experiments (Fig. 1C). As dielectric constant of a glass is much smaller than those of water and polar solvents [29], heating from the glass tube under microwave irradiation can be negligible [30].

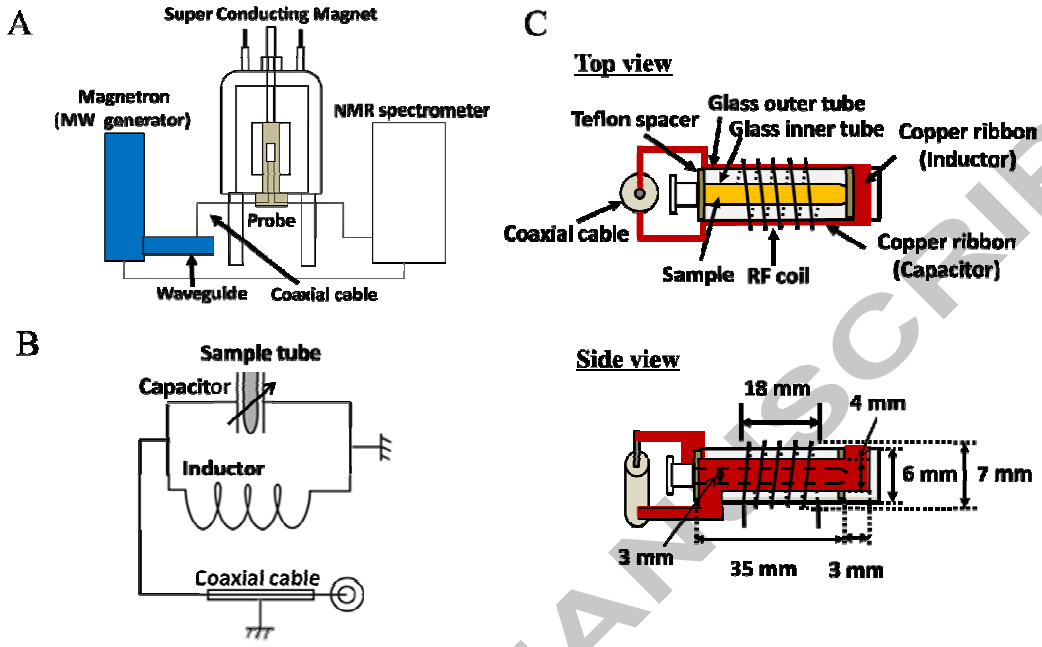

Fig. 1. (A) Schematic diagram of the *in situ* microwave irradiation solid state NMR spectrometer (CMX Infinity 400, Chemagnetics) equipped with a microwave transmitter (IDX, 1.3 kW, Tokyo Electron Co., Ltd.). CW and pulsed microwave are gated by the pulse from the pulse programmer of the NMR spectrometer. Microwaves were transmitted from the microwave transmitter via waveguide and coaxial cable and finally introduced to the microwave resonance circuit in the probe. (B) Equalizing microwave resonance circuit consists of an inductor and capacitor. The sample is inserted into the capacitor in the microwave resonance circuit. (C) Schematic diagrams of sample tube, capacitor and inductor of microwave resonance circuit and inductor of radio frequency. The top view indicates the names of components and the side view indicates the dimensions of components. The inner glass tube (Shigemi) filled with samples is inserted into an outer glass tube, so that the gas flow on the surface of the outer glass tube (Shigemi) is mostly insulated from the inner sample tube. Microwave resonance circuit is attached on the surface of outer glass tube.

Results and Discussion

Phase transition processes of PCH3 induced by microwave heating

Fig. 2A shows the molecular structure of PCH3. Fig. 2B shows ^{1}H NMR spectra for PCH3 at 40 °C, which is 5 °C below the phase transition temperature (Tc = 45 °C). A broad ^{1}H NMR spectrum with a 40 kHz linewidth was obtained for the liquid crystalline sample due to residual ^{1}H-^{1}H dipolar couplings. The ^{1}H NMR spectrum of the isotropic phase was obtained at 50 °C, which is 5 °C higher than the Tc, and many types of proton signals were resolved and assigned to different protons [21] as shown in Fig. 2C.

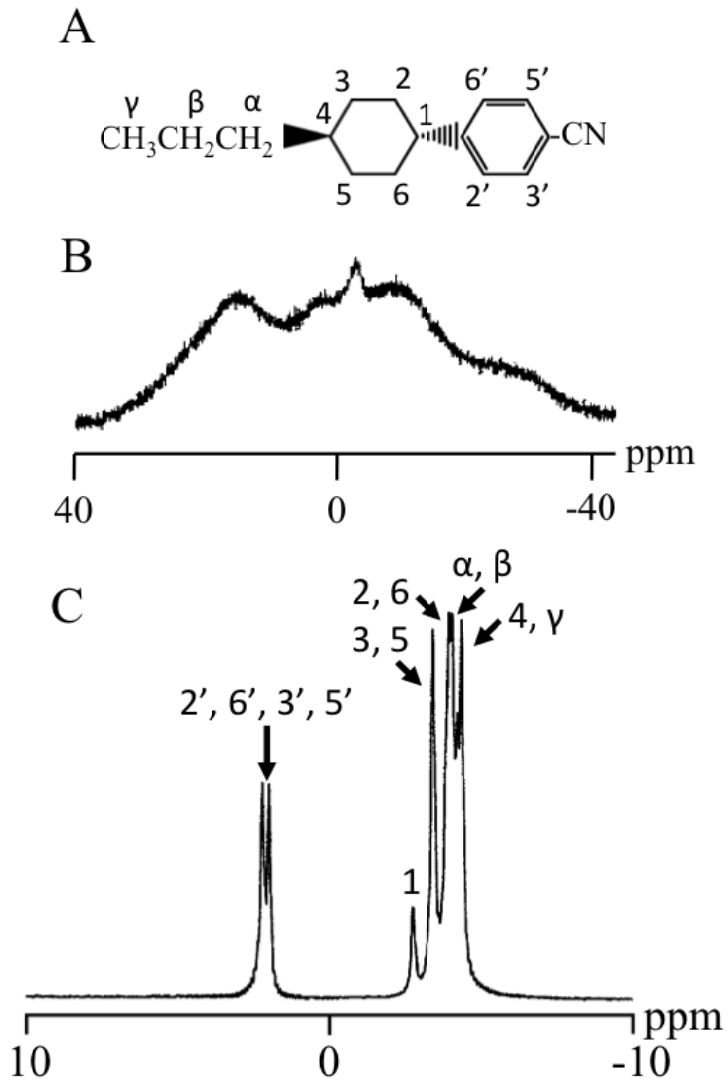

Fig. 2. (A) Molecular structure of PCH3. ^{1}H NMR spectra of PCH3 measured at (B) 40 °C in the liquid crystalline phase and at (C) 50 °C in the isotropic phase. High resolution ^{1}H NMR signals were assigned to individual protons as indicated [21].

The temperature was varied from 36 to 47 °C using the gas flow temperature control system. When the gas flow temperature was set at 46 °C, which is 1 °C higher than Tc, most of the liquid crystalline phase was changed to the isotropic phase (Fig. 3D). The liquid crystalline state could be transferred to the isotropic state with a very small increase in the gas flow temperature, as shown in Fig. 3C and D. The gas flow temperature was then set at 20 °C, which is 25°C below the Tc, and the sample was subjected to CW microwave irradiation. When the CW microwave power was controlled at 54.6 W, a small amount of isotropic signals (ca. 2% fraction) appeared stationary in the majority of signals for the liquid crystalline phase (Fig. 3G and J). The linewidths for the isotropic signals were very narrow as compared with that for the bulk isotropic signals (Fig. 3K). The temperature for the isotropic phase should be higher than the Tc (45 °C), therefore, this result indicates that microwave heat the sample locally to generate isotropic phase with higher temperature than liquid crystalline phase. In this state, temperature of liquid crystalline state was 38 ºC, which was estimated from the temperature dependence of linewidth values (see Fig. 4B).

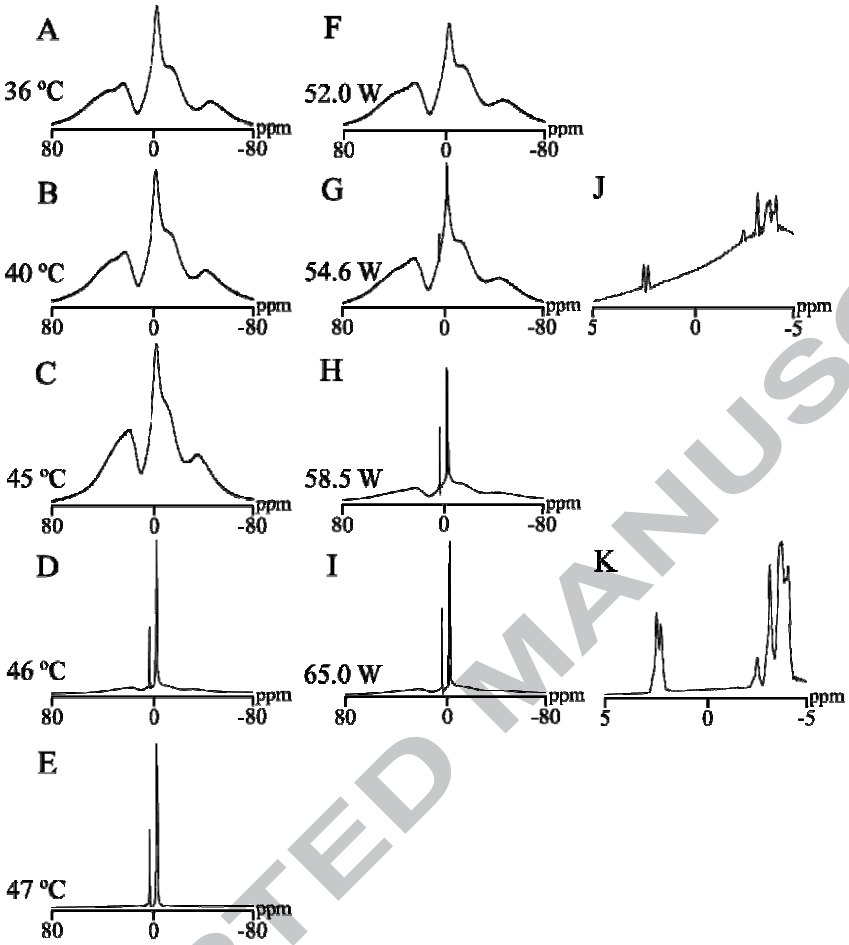

Fig. 3. ^{1}H NMR spectra of PCH3 at (A) 36, (B) 40, (C) 45, (D) 46, and (E) 47 °C, where the temperature was regulated by heated air using a temperature control unit. ^{1}H NMR spectra of PCH3 under CW microwave irradiation at (F) 52.0, (G, J) 54.6, (H) 58.5, and (I, K) 65.0 W, where the gas flow temperature was set at 20 °C using temperature control unit.

The temperature of the local heating state in the liquid crystalline phase has been difficult to evaluate experimentally. Therefore, the temperature characteristics of the liquid crystalline state of PCH3 were correlated with the linewidth, as shown in Fig. 4A. The ^{1}H NMR linewidth gradually decreased with the temperature increase and then suddenly decreased at 46 °C, which is slightly higher than Tc (45 °C). Under microwave irradiation, the isotropic phase appeared at 38 °C, which is 7 °C lower than the Tc of PCH3 (Fig. 4B). Thus, the temperature of the samples under microwave heating was successfully determined by analysis of the linewidth for the liquid crystalline signals from *in situ* microwave irradiated NMR measurements.

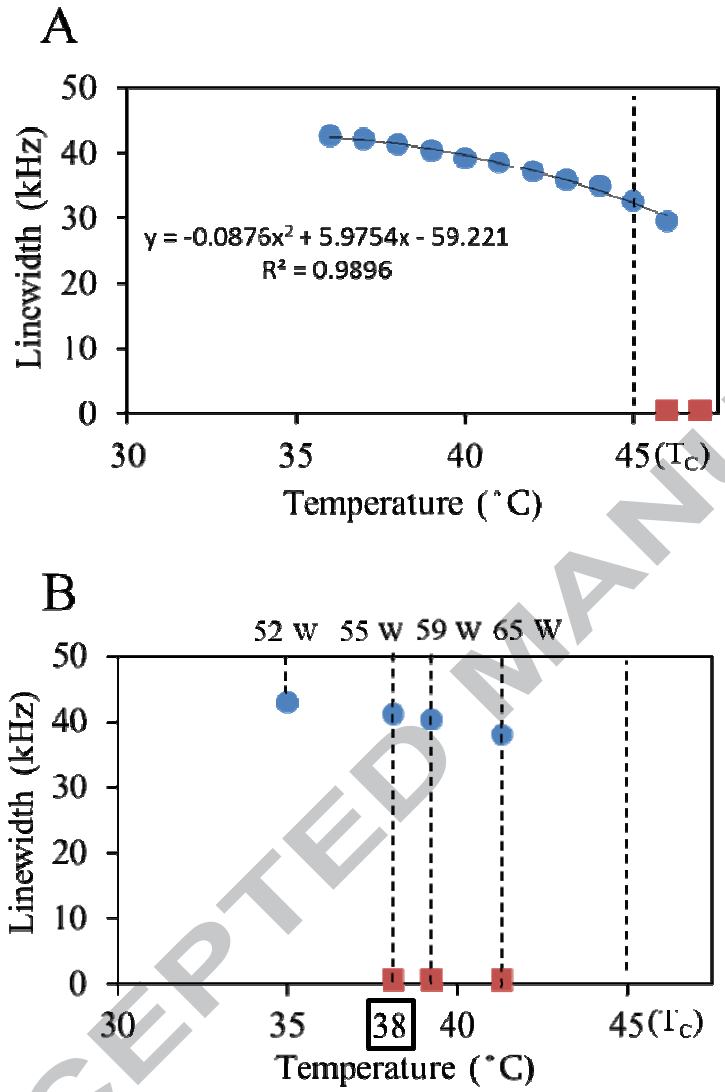

Fig. 4. Plots of ^{1}H NMR spectral linewidths for PCH3 under (A) temperature control with heated air and (B) under microwave irradiation, where the gas flow temperature was set at 20°C using a temperature control unit. Small amount of isotropic phase appeared at 38 °C, which was 7 °C lower than the Tc.

Mechanism for local heating phenomena near the phase transition temperature of PCH3

Fig. 5 gives a schematic illustration for the thermal and microwave local heating phenomena for PCH3 in the liquid crystalline state. When the liquid crystalline phase below the phase transition temperature was heated with microwave irradiation (MW) to reach a temperature near the Tc, a small amount of the isotropic phase appeared at a temperature below Tc (Fig. 5D). The microwave thermal effects are attributed to increase in the solvent temperature due to dielectric loss [4, 6]. The solvent molecule dipoles will align with an applied electric field and in case of microwave irradiation, the applied field will oscillate. As the dipoles attempt to realign itself with this alternating electric field, energy is released in the form of heat by molecular friction and collisions. The amount of heat generated by this process is directly related to the ability of the matrix to align itself with the frequency of the applied field. If the dipole does not have enough time to realign, small amount of heating occurs. In the case where molecule has same dipole moment, a solid state such as ice is not absorb microwave, since molecule will not align to an applied electric field [15]. While liquid state such as water efficiently absorb microwave energy since they have mobility to align to the electric field. Therefore, it is expected that the microwave absorption is higher in the isotropic phase than in the less mobile liquid crystalline phase. This increased the temperature of the sample where the isotropic phase was locally present. This can be considered to be a type of non-equilibrium local heating state. The isotropic phase forms a small particle, which is quite small and therefore the surface of the particle interact with the liquid crystalline molecules (Fig. 5D). When the isotropic phase loses the thermal energy to liquid crystalline phase, the sharp NMR signal was changed to a broad signal

characteristic of the pure liquid crystalline phase. This enable observation of the microwave-induced isotropic phase, which can be thus distinguished from the liquid crystalline phase. The non-equilibrium local heating state stationary appeared due to heating by the absorption of microwave energy in the small isotropic phase particle. The dissipation rate of heat to the bulk of the liquid crystalline phase is balanced with the heating rate by microwave irradiation. When the power of the microwave heating was increased, the small isotropic phase particles grew into a bulk isotropic state (Fig. 5E) until the entire samples became isotropic phase (Fig. 5F). On the other hand, when the temperature was increased with thermal heating (TH) without microwave irradiation (top panel of Fig. 5), the isotropic phase appeared at 46 °C, which is slightly higher than the liquid crystalline-isotropic phase transition temperature (Tc = 45 °C) as an equilibrium state with liquid crystalline phase as shown in Fig. 5B (see also Fig. 3D). Non-equilibrium local heating phenomena have been reported for a liquid-solid mixed state [17], where solid particles absorbed microwave and acted as a heat source. In this experiment, a non-equilibrium local heating state was stationarily observed as an isotropic phase in the majority of liquid crystalline phase. It was also stressed that the phase transition was directly generated by microwave irradiation. It is likely that the high temperature of non-equilibrium locally heated domain of solvent may cause the acceleration of a chemical reaction rate as observed in the local heating effects of organic solvents.

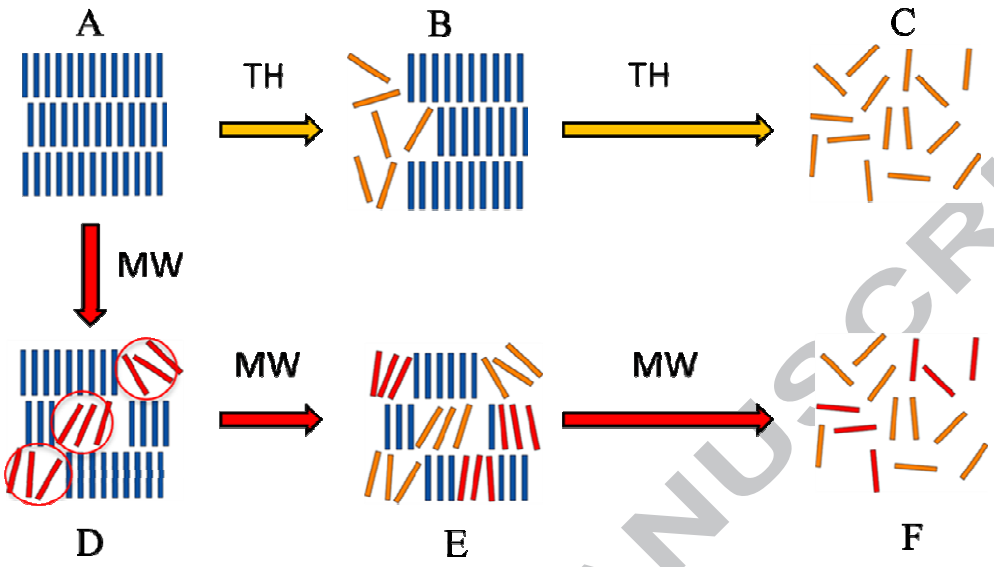

Fig. 5. Schematic diagram thermally (TH: A→B→C) and microwave (MW: A→D→E→F) heating processes for the liquid crystalline state (A). Under microwave irradiation (MW), a small fraction of the liquid crystalline domain transformed to the isotropic phase (D). This isotropic phase domain increases the temperature to much higher than that of the liquid crystalline phase because the dielectric loss of the isotropic phase is larger than that of liquid crystalline phase. This state is considered to be a non equilibrium local heating state. In contrast, under thermally heated (TH), a large fraction of the isotropic phases appeared at a temperature slightly higher than Tc (B), and the temperature of the isotropic phase is the same as that of the liquid crystalline state

High temperature microwave heating of isotropic phase of PCH3

Temperature was set at 50 °C, and much higher microwave power was applied to isotropic phase of PCH3. Fig. 6 shows that the individual proton signals were significantly shifted to a higher field with increase of microwave power and individual protons have different amount of chemical shifts. In addition, the line widths became broader with microwave irradiation at higher power (right panel of Fig. 6B, C and D). It is observed that the chemical shift dependence with temperature is very small in diamagnetic compounds as compared to that in paramagnetic compounds. Therefore, this significant chemical shifts suggest that the isotropic phase of PCH3 increased to quit high temperature under high power microwave irradiation. The temperature of PCH3 under CW microwave irradiation at 195 W for 10 min was estimated to be 210 – 290 °C. Moreover, the temperature distribution is estimated to be around 82 °C at 195 W from the linewidths of the ^{1}H NMR signals under microwave irradiation condition.

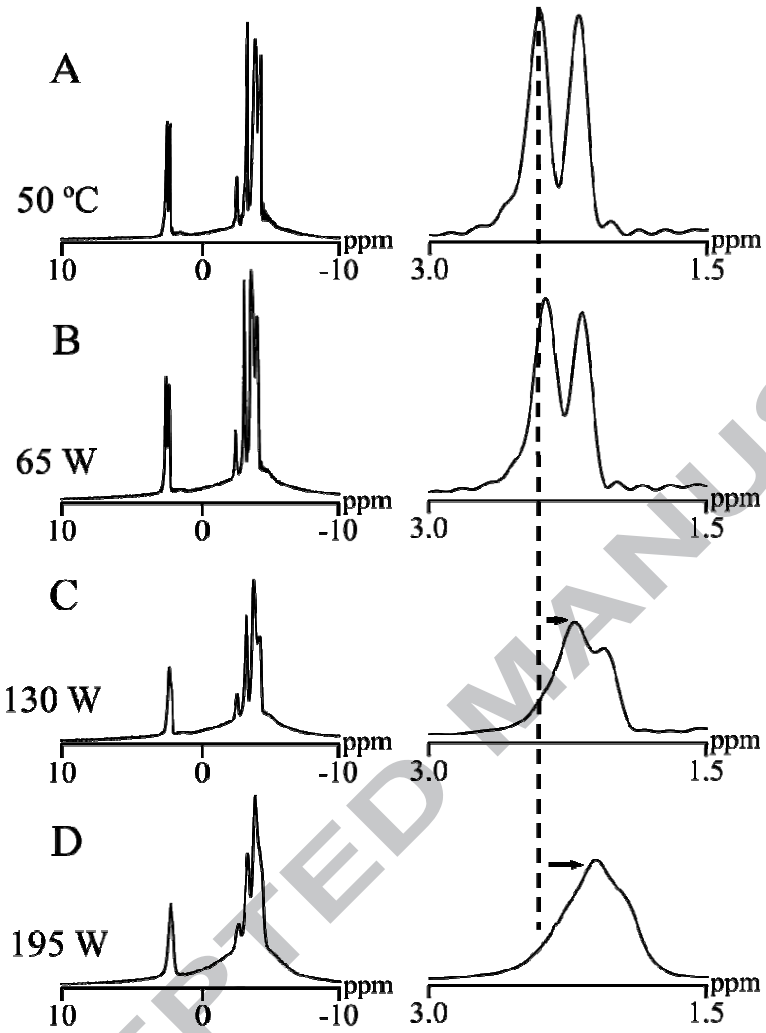

Fig. 6. ^{1}H NMR spectra of PCH3 at (A) 50 °C and under CW microwave irradiation for 10 min of (B) 65 , (C) 130 , and (D) 195 W by setting the gas flow temperature at 50 °C of the NMR spectrometer. Individual proton signals shifted to higher fields as higher microwave powers (right panel of B, C and D) were applied.

The extent of chemical shift is related to the temperature [24,25]; therefore, the chemical shifts of individual protons were experimentally measured as a function of temperature for the isotropic phase of PCH3 system as shown in Fig. 7. When the temperature was increased by 30 °C, an up-field shifts of only 0.06 and 0.03 ppm were observed for aromatic and aliphatic protons, respectively. The chemical shift values changed linearly with respect to the temperatures, which enabled the effective temperature of the isotropic phase of PCH3 under microwave irradiation to be evaluated. In addition, different slopes of chemical shift values vs. temperatures were observed for individual protons; therefore, it is possible to directly measure the temperature of samples according to the chemical shifts of protons as a type of thermal signature, even under microwave irradiation.

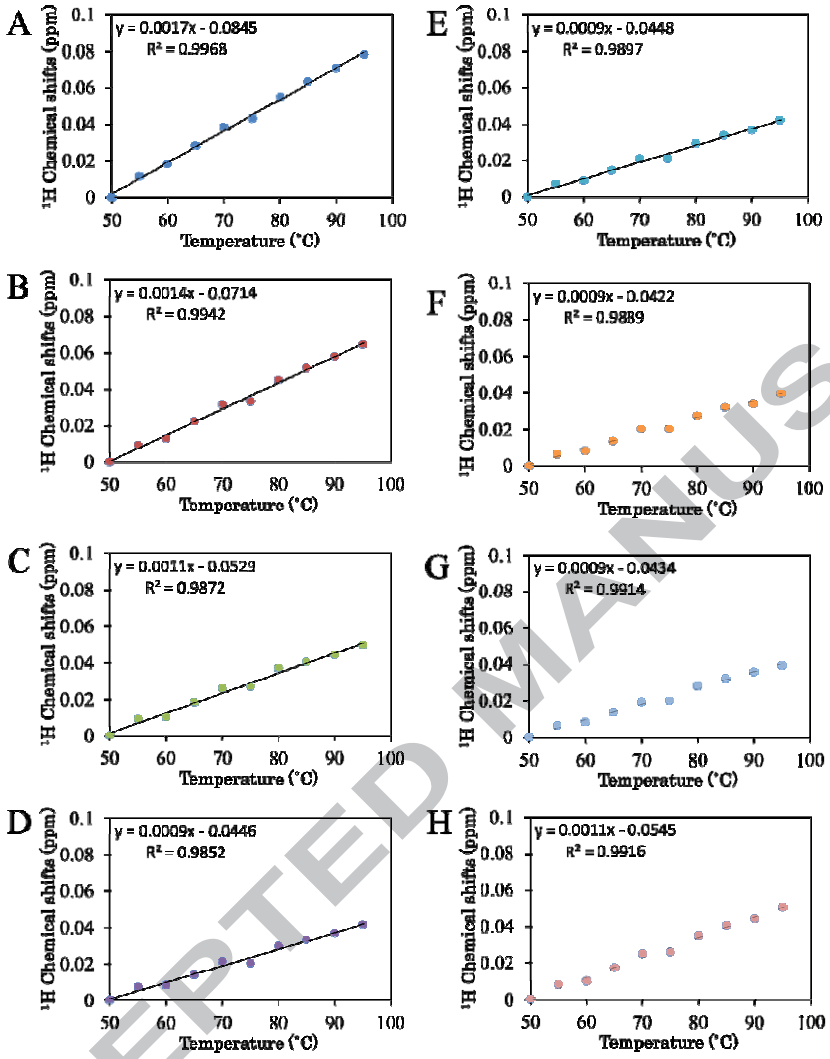

Fig. 7. Plots of ^{1}H chemical shifts vs. temperature for individual protons of PCH3. Chemical shifts for (A) 3', 5' (or 2', 6'), (B) 2', 6' (or 3', 5'), (C) 1, (D) 3, 5, (E) 2, 6, (F) α, β, (G) 4, and (H) γprotons were measured at the range of 50 - 95 °C.

Fig. 8 shows time course for the temperature of isotropic phase PCH3 samples under microwave irradiation at various power. When microwaves were irradiated continuously at 65 W, the temperature increased from 50 to 80 °C within 2 min and the same temperature was then maintained after 2 min. Under microwave irradiation at 130 W, the temperature increased from 50 to 190 °C and became constant within 5 min. Microwave irradiation at 195 W resulted in a temperature increase from 50 to 210 - 250 °C within 2 min. At 195 W, the temperature distributions of the sample appeared as a line broadening (see Fig. 6). Moreover, the temperature distribution of individual protons was observed under microwave irradiation as shown in Fig. 8C. These results indicate that individual protons have different temperatures according to the chemical shifts. Because the temperatures were obtained by extrapolation of the chemical shifts at lower temperatures and there might be deviation from the linearity observed at low temperature. Further experiments are necessary to verify the accuracy of temperatures in the sample under microwave heating.

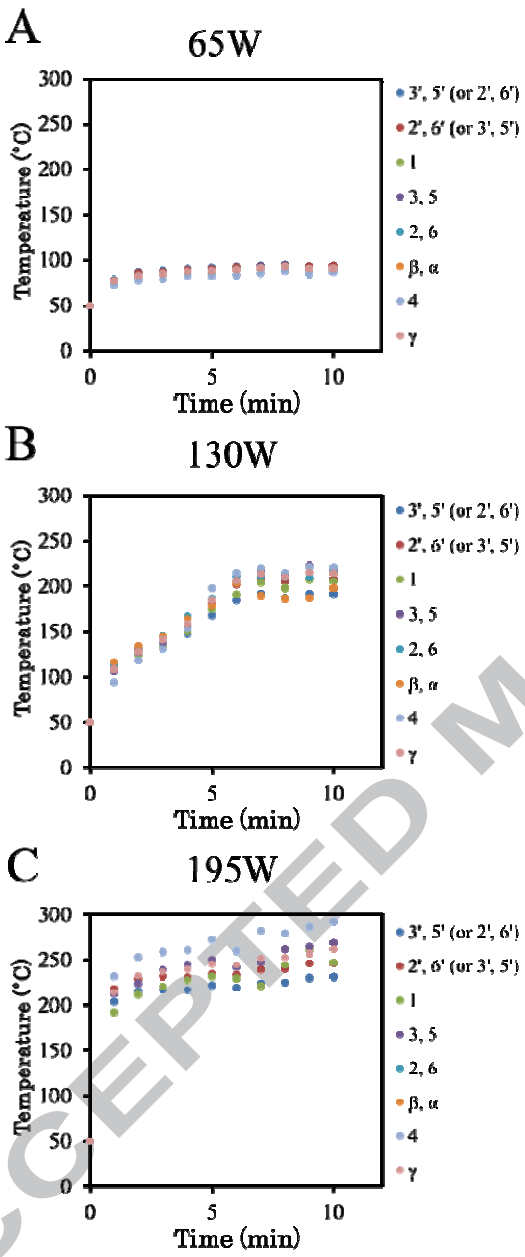

Fig. 8. Plots of temperature against microwave irradiation time at the power of (A) 65, (B) 130 and (C) 195 W. Initially, the gas flow temperatures were set at 50 °C. Each temperatures were evaluated using the slopes of chemical shifts vs. temperatures shown in Fig. 7.

Temperature measurements according to chemical shifts

It is difficult to determine the temperatures of the samples under microwave irradiation, because the temperature of the bulk state does not always reflect the temperature of microwave heating samples due to the effect of local heating. The temperature dependent chemical shifts for individual ^{1}H NMR signals is a good indicator of the sample temperature and can estimate the temperatures of individual molecules or individual group of the molecules under microwave irradiation. Different temperatures were observed for individual protons as far as chemical shifts were concerned as temperature indicator; therefore, the individual protons in the molecules show slightly different effective temperatures.

It is important to point out that microwave can increase the temperature of a sample with a large electric dipole moment in a short time and significantly high temperature can be achieved during NMR measurements. It should be stressed that the NMR probe used here was not designed for high temperature experiments. Nevertheless, it is possible to perform the high temperature NMR experiment using microwave as a heat source. It is also possible to perform rapid temperature jump experiments using pulsed microwave irradiation. As an application of a rapid temperature jump experiments, liquid crystalline-isotropic phase correlated 2D NMR experiments were successfully performed [18-22]. It is noted that liquid crystalline samples are good for high temperature experiments because they have high microwave absorption efficiently and high boiling points.

Conclusion

An *in situ* microwave irradiation NMR spectrometer was developed and the *in situ* NMR signal acquisition under microwave heating was performed for liquid crystalline PCH3. The non-equilibrium local heating state was stationary and the temperature of the state was higher than the bulk liquid crystalline state, according to analysis of the temperature dependent linewidth of liquid crystalline samples. The non-equilibrium local heating state at high temperature may cause the significant acceleration of chemical reactions. It was also demonstrated that very high temperature can be rapidly achieved for the isotropic phase of liquid crystalline sample using the *in situ* microwave irradiation NMR spectrometer without the need for high temperature protection in the probe.

Acknowledgment

This work was supported by a Grant-in-Aid for Scientific Research on Priority Area (24121709) and Innovative area (26102514 and 26104513), and a Grant-in-aid for Scientific Research (C) (24570127) from the Ministry of Education, Culture, Sports, Science and Technology of Japan.

References

[1] R.Gedye, F. Smith, K. Westaway, H. All, L. Baldisers, L. Laberge, J. Rousell, The use of microwave ovens for rapid organic synthesis, Tetrahedron Lett., 27 (1986) 279-282.

[2] R.J. Giguere, T.L. Bray, S.M. Duncan, G. Majetich, Application of commercial microwave ovens to organic synthesis, Tetrahedron Lett., 29 (1986) 4945-4948.

[3] D. Adam,Out of the kitchen, Nature, 421 (2003) 571-572.

[4] L. Perreux, A. Loupy, A tentative rationalization of microwave effects in organic synthesis according to the reaction medium, and mechanistic considerations, Tetrahedron, 57(2001) 9199-9223

[5] D. Bogdal, M. Lukasiewicz, J. Pielichowski, A. Miciak, Sz. Bednarz, Microwave-assisted oxidation of alcohols using Magtrieve, Tetrahedron, 59 (2003) 649-653.

[6] C.O. Kappe, Controlled microwave heating in modern organic synthesis, Angew. Chem. Int. Ed., 43 (2004) 6250-6284.

[7] Y. Yoshimura, H. Shimizu, H. Hinou, S.-I. Nishimura, A novel glycosylation concept; microwave-assisted acetal-exchange type glycosylation from methyl glycosides as donors, Tetrahedron Lett., 46 (2005) 4701-4705.

[8] M.-C. Parker, T. Besson, S. Lamare, M. -D. Legoy, Microwave radiation can increase the rate of enzyme-catalysed reaction in organic media, Tetrahedron Lett., 46 (1996) 8383-8386.

[9] B.N. Pramanik, U. A. Mirza, Y.H. Ing, Y.–H. Liu, P.L. Bartner, P.C. Weber, A.K. Bose, Microwave-enhanced enzyme reaction for protein mapping by mass spectrometry: A new approach to protein digestion in minutes, Protein Sci., 11

(2002) 2676-2687.

[10] W. Huang, Y.–M. Xia, H. Gao, Y.–J. Fang, Y. Wang, Y. Fang, Enzymatic esterification between n-alcohol homologs and n-caprylic acid in non-aqueous medium under microwave irradiation, J. Mol. Catalysis B: Enzymatic, 35 (2005) 113-116.

[11] S.-S. Lin, C.-H. Wu, M.-C. Sun, C.-M. Sun, Y.-P. Ho, Microwave-assisted enzyme-catalyzed reactions in various solvent systems, J. Am. Soc. Mass Spectrom., 16 (2005) 581-588.

[12] D. Obermayer, B. Gutmann, C.O. Kappe, Microwave chemistry in silicon carbide reaction vials: Separating thermal from nonthermal effects, Angew. Chem. Int. Ed., 48 (2009) 8321-8324.

[13] C.O. Kappe, B. Pieber, D. Dallinger, Microwave effects in organic synthesis: Myth or reality? Angew. Chem. Int. Ed., 52 (2013) 1088-1094.

[14] S. Yamada, A. Takasu, S. Takayama, K. Kawamura, Microwave-assisted solution polycondensation of L-lactic acid using a Dean-Stark apparatus for a non-thermal microwave polymerization effect induced by the electric field, Polym. Chem., 5 (2014) 5283-5288.

[15]. M. Tanaka, M. Sato, Microwave heating of water, ice, and saline solution: Molecular dynamics study, J. Chem. Phys., 126 (2007) 034509.

[16] M. Kanno, K. Nakamura, E. Kanai, K. Hoki, H. Kono, M. Tanaka, Theoretical verification of nonthermal microwave effects on intermolecular reactions, J. Phys. Chem. A, 116 (2012) 2177-2183.

[17] Y. Tsukahara, A. Higashi, T. Yamauchi, T. Nakamura, M. Yasuda, A. Baba, Y. Wada, In situ observation of nonequilibrium local heating as an origin of spherical effect

of microwave on chemistry, J. Phys. Chem. C., 114 (2010) 8965-8970.

[18] A. Naito, M. Imanari, K. Akasaka, Separation of local magnetic field of individual protons in nematic phase by state-correlated 2D NMR spectroscopy, J. Magn. Reson., 92 (1991) 85-93.

[19] A. Naito, M. Ramamoorthy, Structural Studies of Liquid Crystalline Materials Using Solid State NMR Technique. Thermotropic Liquid Crystal: Recent Advances. Springer, (2007) 85-116.

[20] A. Naito, M. Imanari, K. Akasaka, State-correlated two-dimensional NMR spectroscopy: Separation of local dipolar fields of protons in nematic phase of 4'-methoxybenzylidene-4-acetoxyaniline, J. Chem. Phys., 105 (1996) 4502-4510.

[21] K. Akasaka, M. Kimura, A. Naito, H. Kawahara, M. Imanari, Local order, conformation, and interaction in nematic 4-(n-pentyloxy)-4'-cyanobiphenyl and its one-to-one mixture with 1-(4'-cyanophenyl)-4-propylcyclohexane. A study by state-correlated ^{1}H two-dimensional NMR spectroscopy, J. Phys. Chem., 99 (1995) 9523-9529.

[22] A. Naito, Y. Tasei, Separation of local fields of individual protons in nematic phase of 4'-ethoxybenzylidene-4-n-butylaniline by microwave heating 2D NMR spectroscopy, Materials Science and Technology (MS&T)(2010) 2886-2894.

[23] K. Akasaka, A. Naito, M. Imanari, Novel method for NMR spectral correlation between the native and the denatured states of a protein. Application to ribonuclease A, J. Am. Chem. Soc., 113 (1991) 4688-4680.

[24] M.V. Gomez, H.H.J. Verputten. A. Diaz-Ortiz, A. Moreno, A. de la Hoz, A.H. Velders, On-line monitoring of a microwave-assisted chemical reaction by nanolitre NMR-spectroscopy, Chem. Commun., 46 (2010) 4514-4516.

[25] A.L. Van Geet, Calibration of the methanol and glycol nuclear magnetic resonance thermometers with a static thermistor probe, Anal. Chem., 40 (1968) 2227-2229.

[26] A.L. Van Geet, Calibration of methanol nuclear magnetic resonance thermometer at low temperature, Anal. Chem.,42 (1970) 679-689.

[27] A. Bielecki, D.P. Burum, Temperature dependence of ^{207}Pb MAS spectra of solid lead nitrate. An accurate, sensitive thermometer for variable-temperature MAS, J. Magn. Reson, Ser. A, 116 (1995) 215-220.

[28] C.S. Zuo, K.R. Metz, Y. Sun, and A.D. Sherry, NMR temperature measurements using a paramagnetic lanthanide complex, J. Magn. Reson., 133 (1998) 55-60.

[29] R.C. West (Edt in Chief), CRC Handbook of Chemistry and Physics, 64 th Ed. CRC Press, Boca Raton, Florida, 1984, pp E50-E56.

[30] Dielectric loss values of ice (-13 °C), water (25 °C) and glass at 2.45 GHz are reported to be 0.0028, 12.3 and 0.050, respectively, in the book; T. Koshijima (Edt. In Chief), Monograph of microwave heating technique, NTS, Tokyo, 1994, pp 9, written in Japanese.

Graphical abstract

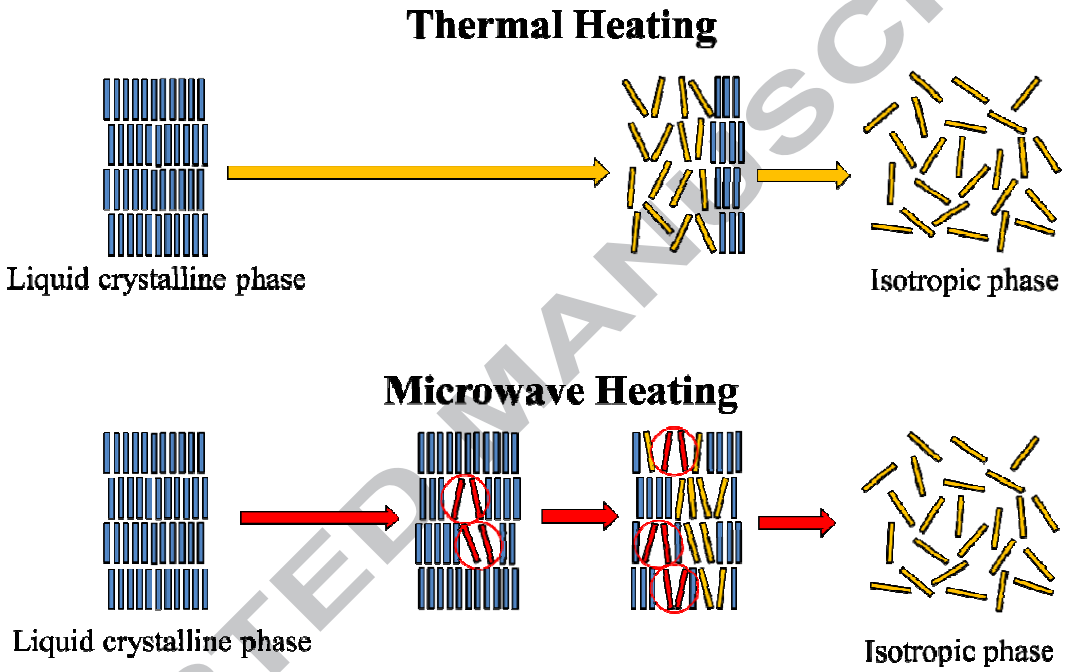

Research highlights

- *In situ* microwave irradiation NMR spectrometer was developed.
- ^{1}H NMR spectra of liquid crystal PCH3 under microwave irradiation were observed
- Non-equilibrium local heating state of PCH3 was observed as a isotropic phase
- Microwave heating generate very high temperature within a short time
- Temperature of PCH3 under microwave irradiation was estimated by chemical shifts

PCCP

PAPER

View Article Online
View Journal

Cite this: DOI: 10.1039/c5cp00476d

The microwave heating mechanism of *N*-(4-methoxybenzyliden)-4-butylaniline in liquid crystalline and isotropic phases as determined using *in situ* microwave irradiation NMR spectroscopy†

Yugo Tasei,[a] Fumikazu Tanigawa,[a] Izuru Kawamura,[a] Teruaki Fujito,[b] Motoyasu Sato[c] and Akira Naito*[a]

Received 26th January 2015,
Accepted 25th February 2015

DOI: 10.1039/c5cp00476d

www.rsc.org/pccp

Microwave heating effects are widely used in the acceleration of organic, polymerization and enzymatic reactions. These effects are primarily caused by the local heating induced by microwave irradiation. However, the detailed molecular mechanisms associated with microwave heating effects on the chemical reactions are not yet well understood. This study investigated the microwave heating effect of *N*-(4-methoxybenzylidene)-4-butylaniline (MBBA) in liquid crystalline and isotropic phases using *in situ* microwave irradiation nuclear magnetic resonance (NMR) spectroscopy, by obtaining ^{1}H NMR spectra of MBBA under microwave irradiation. When heated simply using the temperature control unit of the NMR instrument, the liquid crystalline MBBA was converted to the isotropic phase exactly at its phase transition temperature (T_c) of 41 °C. The application of microwave irradiation at 130 W for 90 s while maintaining the instrument temperature at 20 °C generated a small amount of isotropic phase within the bulk liquid crystal. The sample temperature of the liquid crystalline state obtained during microwave irradiation was estimated to be 35 °C by assessing the linewidths of the ^{1}H NMR spectrum. This partial transition to the isotropic phase can be attributed to a non-equilibrium local heating state induced by the microwave irradiation. The application of microwave at 195 W for 5 min to isotropic MBBA while maintaining an instrument temperature of 50 °C raised the sample temperature to 160 °C. In this study, the MBBA temperature during microwave irradiation was estimated by measuring the temperature dependent chemical shifts of individual protons in the sample, and the different protons were found to indicate significantly different temperatures in the molecule. These results suggest that microwave heating polarizes bonds in polar functional groups, and this effect may partly explain the attendant acceleration of organic reactions.

Introduction

Microwave heating is widely used to accelerate organic reactions,[1–11] to reduce polymerization times,[12–15] and to enhance the activity of enzymes.[16–18] The majority of the reaction acceleration obtained in this manner can be explained by the thermal effect of the microwaves.[19] However, nonthermal effects have also been identified and it has been reported that the thermal and nonthermal effects of microwaves can be separated.[20] The existence of nonthermal effects of microwave has recently been demonstrated by the observation that the rates of polymerization reactions are increased under electric fields but decreased under magnetic fields.[15] The microwave thermal effects are attributed to an increase in the solvent temperature due to dielectric loss.[4,5,7,21,22] The solvent molecule dipoles will align with an applied electric field and in the case of microwave irradiation, the applied field will oscillate. As the dipoles attempt to realign with this alternating electric field, heat energy is released by molecular friction and collision. Ions will also translate along the oscillating electric field, generating collisions or friction with other molecules in the sample matrix to produce additional thermal energy. However, the details of the molecular mechanisms associated with the microwave heating effect on chemical reaction rates have not yet been fully elucidated. One of the most important phenomena

[a] Graduate School of Engineering, Yokohama National University, 79-5 Tokiwadai, Hodogaya-ku, Yokohama 240-8501, Japan. E-mail: naito@ynu.ac.jp; Fax: +81-45-339-4251; Tel: +81-45-339-4232
[b] Probe Laboratory Inc., 1-7-17, Kawasaki, Haruma, Tokyo, 205-0021, Japan
[c] Faculty of Engineering, Chubu University, 200 Matsumoto-cho, Kasugai 457-8501, Japan

† Electronic supplementary information (ESI) available: Fig. S1–S3. See DOI: 10.1039/c5cp00476d

associated with microwave irradiation is non-equilibrium localized heating, defined as the generation of isolated regions with much higher temperatures than the bulk solution. This has been reported to occur in liquid–solid[23] systems in response to microwave irradiation, such as in the case of dimethyl sulfoxide (DMSO) molecules in contact with Co particles under microwave irradiation.

In the present study, an *in situ* microwave irradiation solid state NMR spectrometer was developed with the aim of characterizing microwave heating mechanisms. The technique of microwave irradiation liquid state NMR spectrometer was first envisioned by Naito *et al.*[24,25] and was used to obtain state-correlated two-dimensional (2D) NMR spectra. This allowed high resolution observation of ^{1}H dipolar patterns in ^{1}H NMR spectra in the liquid state rather than the liquid crystalline state. Using this method, the local dipolar interactions of individual protons in the liquid crystalline state can be examined *via* high resolution resonance in the isotropic phase[26–28] and the resulting data may also be used to obtain state-correlated two dimensional NMR spectra of proteins in both native and denatured states.[29] During the microwave irradiation process, electron dipole moments are excited, leading to heating of the sample. This differs from the excitation of electron spin magnetic moments, as occurs in electron spin resonance (ESR) and dynamic nuclear polarization (DNP) experiments.

Liquid crystalline samples are known to absorb microwaves with high efficiency, since they necessarily contain polar functional groups. It is therefore expected that microwave heating phenomena will be more readily observed in liquid crystals. Thus, an *in situ* microwave irradiation solid state NMR spectrometer set-up was designed specifically to obtain NMR signals during microwave irradiation. This system isolated the effects of the radio waves applied to obtain the NMR detection from the microwaves employed to generate local heating. This spectroscopic technique thus allowed clear NMR signals to be obtained while simultaneously applying microwave irradiation.

In the present study, microwave heating effects were characterized using a sample of liquid crystal *N*-(4-methoxybenzylidene)-4-butylaniline (MBBA). This compound was chosen, since liquid crystalline samples exhibit both highly efficient microwave heating and high boiling points. It was necessary to accurately measure the temperature of the sample during microwave irradiation and in this work, the variation in the ^{1}H chemical shifts was employed as an indicator of temperature. In the case of diamagnetic nuclei, it has been reported that the temperature dependence of chemical shift values is typically linear in nature,[30–34] and we therefore assessed the temperature of the MBBA sample based on the temperature dependent-chemical shifts of the protons in the MBBA molecule.

Materials and methods

A sample of *N*-(4-methoxybenzyliden)-4-butylaniline (MBBA) was purchased from the Tokyo Chemical Industry Co., Ltd. and used without further purification. The liquid crystal to isotropic phase transition temperature (T_c) of this compound is reported to occur at 41 °C.[35]

The temperature of a sample within an NMR spectrometer is normally regulated by the set point of the temperature control unit integrated into the instrument. In the present work, however, it was important to directly measure the temperature of the sample itself, since microwave heating was expected to increase the sample temperature and cause this temperature to depart from the setting of the instrument. It can be physically challenging to accurately measure the actual temperature of NMR samples under microwave irradiation due to the wide special variations in temperature throughout the bulk of the sample. For these reasons, the temperature-dependent chemical shift values of the sample were instead used as a temperature indicator. The difference in the chemical shifts, $\Delta\delta$, of the CH_3 and OH protons of methanol or glycol is commonly used for the purposes of temperature calibration in NMR spectrometers.[30,31] In the case of methanol, the relation between $\Delta\delta$ and temperature is not completely linear over a wide temperature range, and so a quadratic relationship is instead applied, with an associated error of 0.6 K. Over a narrow temperature range, however, the plot of $\Delta\delta$ as a function of temperature can be fit by a straight line with a minimal associated temperature error. In the case of glycol, the data can be perfectly fit by a straight line over a wide temperature range.[30] The ^{31}P chemical shift dependence of a paramagnetic lanthanide complex on temperature has also been shown to generate a straight line over a narrow temperature range,[32] although the chemical shift dependence of nuclei on paramagnetic electrons typically exhibits an inverse relationship with temperature. Variation of the chemical shifts of water protons in a bicelle sample *vs.* temperatures shows a linear relationship in the temperature range of 10 to 60 °C.[33] In solid state NMR studies, the variation in ^{207}Pb chemical shifts with temperature has exhibited a linear relationship over the temperature range of −130 to +150 °C.[34] Based on these previous reports, the variation in the ^{1}H chemical shift values of individual protons of the MBBA sample was assessed with regard to their variation with temperature. The resulting plots of chemical shifts as a function of temperature obtained from microwave irradiation were subsequently evaluated by assuming that the relationships between these chemical shifts and temperature were approximately linear.

The instrument used in this work consisted of a Chemagnetics solid state NMR spectrometer (CMX infinity 400) equipped with a microwave generator (IDX, Tokyo Electronics Co., Ltd.) capable of transmitting 1.3 kW pulsed or continuous microwave at a frequency of 2.45 GHz. This apparatus allowed us to obtain NMR signals without interference while simultaneously applying microwave irradiation. A 3 mm wide flat copper ribbon was used to form the capacitor of the resonance circuit, and was wound coaxially inside the radio wave circuit to reduce arcing and to increase isolation during microwave irradiation (see Fig. S1, ESI†). The microwave resonance circuit was tuned to 2.45 GHz and the radio wave was set to 398 MHz using a sweep generator. Microwaves were transmitted from the microwave generator to the vicinity of the magnet through the waveguide,

which served a coaxial cable and finally the microwaves were guided to the resonance circuit at the probe head. The microwave pulses were controlled by the gating pulses produced by the pulse programmer of the NMR spectrometer. The sample was initially cooled to obtain the liquid crystalline phase using the temperature control unit of the spectrometer. Samples were packed in an inner glass tube to insulate them from thermal contact with the outer glass tube.

Results

Microwave heating of liquid crystalline MBBA

Fig. 1A gives the molecular structure of MBBA. Fig. 1B shows the ^{1}H NMR spectra of MBBA in the liquid crystalline state at 35 °C, which is 6 °C below its phase transition temperature (T_c) of 41 °C. A broad ^{1}H NMR spectrum with a 20 kHz linewidth was obtained in the liquid crystalline sample due to ^{1}H–^{1}H dipolar couplings. Since MBBA molecules are aligned to the magnetic field in the liquid crystalline phase, residual ^{1}H–^{1}H dipolar interactions cause a number of transitions with various dipolar interactions and this generates the observed line broadening. These dipolar interactions can provide information concerning the order parameters of liquid crystals. A high resolution ^{1}H NMR spectrum of MBBA in the isotropic phase was also obtained at 45 °C, in which numerous proton signals were resolved and assigned to the various protons in the molecule,[36] as shown in Fig. 1C.

In subsequent trials, the MBBA temperature was increased from 20.0 °C, which is 20.5 °C below T_c, to 40.5 °C which was experimentally determined T_c using the spectrometer's temperature control unit. As shown in Fig. 2A, the ^{1}H NMR signal of the liquid crystalline phase appeared alone at 35 °C. At 40.0 °C, the liquid crystalline phase had partly transitioned to the isotropic phase (Fig. S2, ESI†). It was observed that the temperature of liquid crystal and isotropic phases was nearly the same. It was also evident that the signals obtained at this temperature were broader than those of the fully isotropic phase, which may be attributed to the interaction of the isotropic and liquid crystalline phases. This phase transition was completed at 40.5 °C (Fig. 2B, Fig. S2F, ESI†), which indicates that liquid crystal and isotropic phases coexisted near the phase transition temperature.

The instrument temperature was then set at 20 °C, (20.5 °C below T_c), followed by continuous wave (CW) microwave irradiation. The application of 130 W for 90 s generated weak isotropic phase signals (representing approximately 2% of the bulk sample)

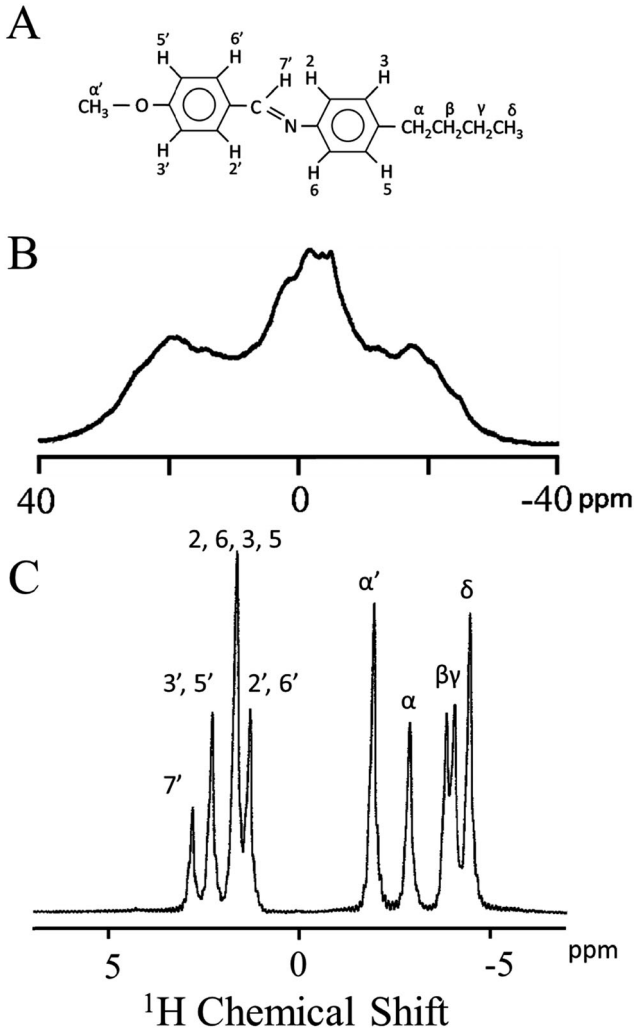

Fig. 1 (A) Molecular structure of *N*-(4-methoxybenzyliden)-4-butylaniline (MBBA). ^{1}H NMR spectra of MBBA at (B) 35 °C in the liquid crystalline phase and (C) 45 °C in the isotropic phase, together with signal assignments of the individual protons.[36]

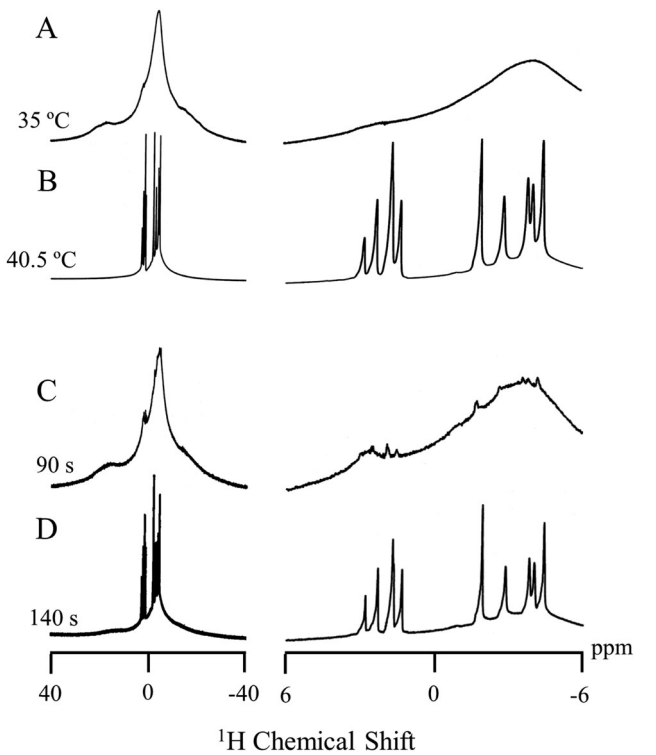

Fig. 2 ^{1}H NMR spectra (left) and expanded spectra (right) of MBBA at (A) 35 and (B) 40.5 °C and setting the temperature at 20 °C under 130 W CW microwave irradiation for (C) 90 and (D) 140 s.

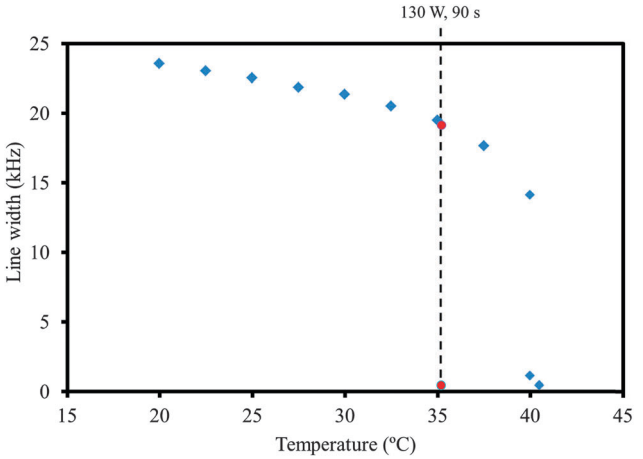

Fig. 3 Plot of the line widths of ^{1}H NMR spectra of MBBA at various temperatures as regulated by the instrument temperature control unit (blue square). The red square indicates the temperature (35 °C) of MBBA in the liquid crystalline state following microwave irradiation at 130 W for 90 s, in which a small amount of isotropic phase appeared within the liquid crystalline bulk.

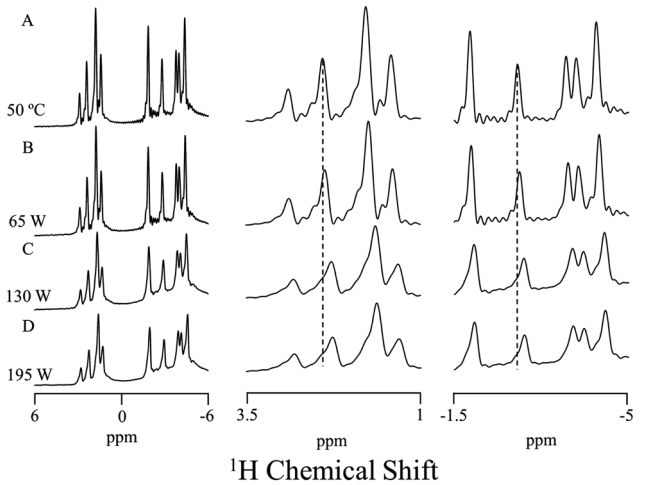

Fig. 4 ^{1}H NMR spectra (left) and expanded spectra (middle and right) of MBBA in the isotropic phase at (A) 50 °C and under CW microwave irradiation of (B) 65, (C) 130 and (D) 196 W for 10 min while regulating the instrument temperature at 50 °C.

among the liquid crystalline phase signals (Fig. 2C and also see Fig. S3A, ESI†). Based on the temperature dependence of the linewidths, the temperature of the liquid crystalline phase was estimated to be 35 °C by assessing the linewidths of the NMR signals (Fig. 3). Normally, such signals would not be expected until the temperature of the sample is close to its isotropic phase transition temperature of 40.5 °C as seen in the setting of a temperature control unit. The linewidth of the isotropic phase generated under these conditions was slightly narrower than that of the isotropic phase obtained by heating at 40.0 °C *via* the temperature control unit (Fig. 2C and Fig. S2E, ESI†). This result indicates that microwave irradiation generated localized heating in the sample to form regions of the higher temperature isotropic phase.

Typically, the temperature of locally heated regions obtained from microwave irradiation has been difficult to detect experimentally. Using *in situ* microwave irradiation NMR, however, the temperature of the sample was successfully determined, since the temperature of the liquid crystal MBBA was correlated with the NMR linewidths, as shown in Fig. 3. As noted, microwave irradiation generated a small fraction of the isotropic phase in the bulk liquid crystal at 35 °C, even though this is 5.5 °C lower than the phase transition temperature of 40.5 °C, suggesting a non-equilibrium localized heating within the sample.

Microwave heating of isotropic MBBA

In these trials, the instrument temperature was set at 50 °C and various power settings (65, 130 and 195 W) were used to irradiate the MBBA in the isotropic phase. As shown in Fig. 4, the individual proton signals were shifted to higher fields with the application of a greater amount of power for 10 min and different protons exhibited different degrees of chemical shifts. It is also evident that the linewidths were broadened by irradiation with higher power, although the chemical shift dependence on temperature is typically very small in diamagnetic compounds. These results indicate that the temperature of the MBBA sample was increased significantly and that the spatial temperature distribution was also very pronounced during microwave irradiation.

It is well known that the chemical shift values of a sample are affected by its temperature.[30–34] In the case of diamagnetic nuclei, the variation in chemical shift values with temperature is approximately linear. Therefore, the chemical shift values of individual protons were determined as a function of temperature for MBBA in the isotropic phase, as shown in Fig. 5. The chemical shift values did not vary greatly with temperature, when the temperature was increased by 30 °C, for example, a higher field shift of only 0.06 ppm was observed for the aromatic protons. Interestingly, the chemical shifts of different protons also had very different the temperature variation. However, the chemical shift did exhibit a linear change as a function of temperature for each different proton and thus it was possible to estimate the effective temperature of MBBA in the isotropic phase as induced by the microwave irradiation.

Fig. 6 presents the MBBA sample temperature increase in response to CW microwave irradiation. Applying 65 W of CW microwave irradiation increased the temperature from 50 to 70 °C within 2 min based on the majority of proton data, after which the temperature plateaued. However, there were significant variations in the apparent temperatures; the 7′ and α′ protons indicated 110 and 80 °C, respectively. When 130 W was applied, the temperature was increased to 140 °C according to the majority of the proton data, although values of 210 and 330 °C were indicated by the α′ and 7′ protons, respectively, and 8 min was required to obtain a stable temperature. The temperature of 7′ and α′ protons more significantly deviated from the others. Temperature increased by 15 °C during microwave irradiation at 130 W for 90 s in the liquid crystalline

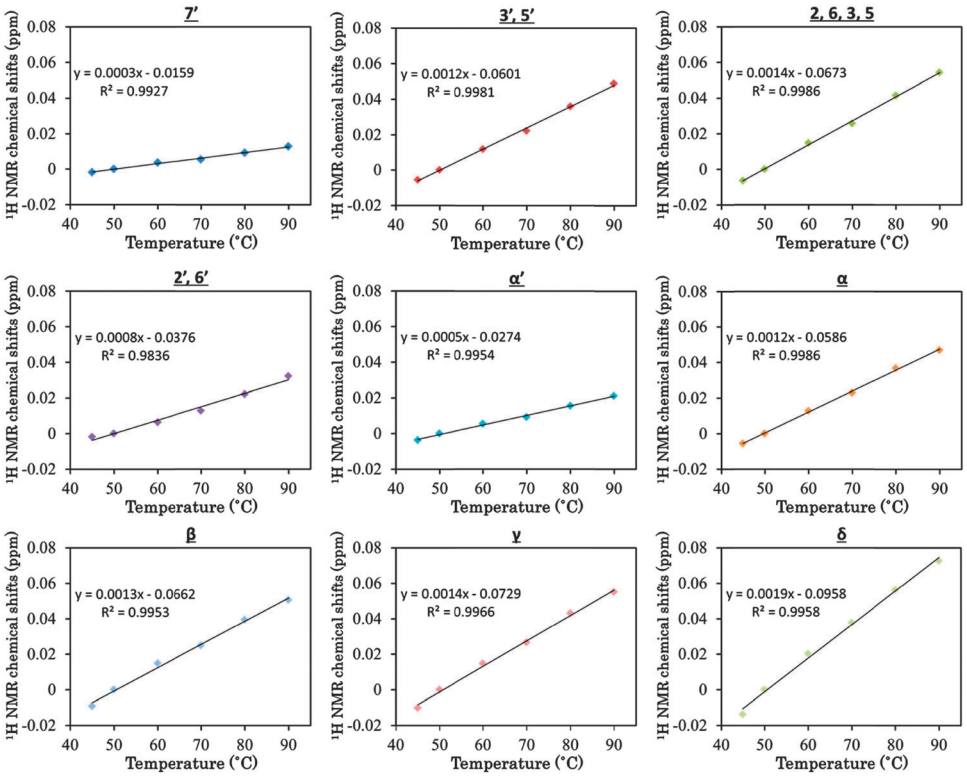

Fig. 5 Plots of ^{1}H chemical shift values of MBBA for individual protons against temperatures regulated by the instrument's temperature control system.

phase (Fig. 3). On the other hand, temperature increased by 20 °C during microwave irradiation at 65 W for 1 min (Fig. 7) in the isotropic phase. Thus, the temperature increase of the isotropic phase was larger than that of the liquid crystalline phase, and hence the isotropic phase more efficiently absorbs microwave than the liquid crystalline phase. Applying 195 W increased the temperature to 160 °C within 5 min, although again the α′ and 7′ protons were discrepant, indicating 220 and 350 °C, respectively. Thus, at this microwave power level, large temperature variations were evident among protons in the same molecule, indicating that individual protons within the same molecule experienced different temperatures.

As noted, it is difficult to determine the temperature of samples during microwave irradiation, because the bulk temperature measured using a thermometer is not always an accurate representation due to significant variation in temperature throughout the sample. This work found that the analysis of chemical shifts can determine the temperatures of individual moieties within the sample molecules.

Fig. 7A makes it evident that the 7′ and α′ protons evidently experienced much higher temperature than those of other protons in the same molecule. As shown in Fig. 7B, however, the temperature indicated by protons other than 7′ and α′ were all very similar and hence they are considered to represent the temperature of the bulk isotropic state. Thus, the temperature at a power of 65 W could be determined accurately, since the chemical shift values were within the range of experimentally determined values using the temperature controlled unit of the instrument.

Discussion

Mechanism of microwave heating effects on liquid crystalline MBBA

The microwave-induced local heating phenomena observed in the liquid crystalline MBBA can be explained as shown schematically in Fig. 8A–D. Here, heating the liquid crystalline phase, initially below its phase transition temperature, by microwave irradiation (indicated by "MW") to a temperature near the T_c, generates a small amount of the isotropic phase inside the sample (Fig. 8B). Because the dielectric loss of the isotropic phase is expected to be higher than that of the liquid crystalline phase, the isotropic phase is heated more efficiently by microwave irradiation, inducing a relatively high temperature in the isotropic phase region. This phenomenon can be considered as a kind of non-equilibrium localized heating state. These isotropic phases form small particles and the surfaces of these particles interact with the surrounding liquid crystal to generate different linewidths compared to those produced by the bulk isotropic phase. As this isotropic phase loses thermal energy to the liquid crystalline phase, the sharp signals of the isotropic phase transition back to the broad signals of the liquid crystalline phase. This allows us to distinguish the microwave-induced isotropic phase from the liquid crystalline phase. This non-equilibrium heating state can be maintained over long time spans because the rate at which heat is obtained by the small isotropic phase particles by absorbing microwave energy balanced the rate at which heat is dissipated to the bulk liquid crystalline phase. At higher power levels, the bulk

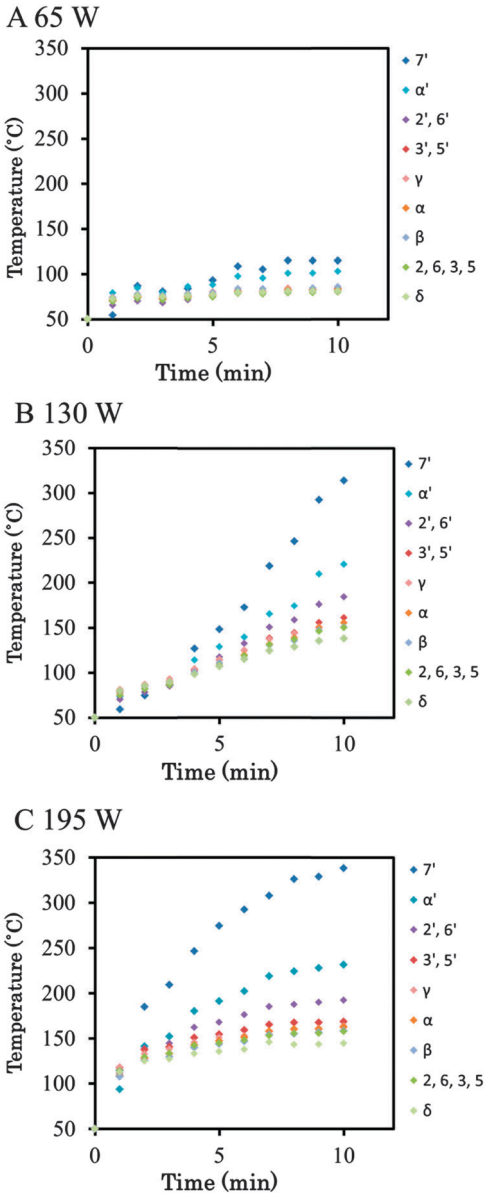

Fig. 6 Plots of temperatures against microwave irradiation time at microwave powers of (A) 65, (B) 130 and (C) 195 W. Temperatures were determined using the slopes obtained for the individual protons.

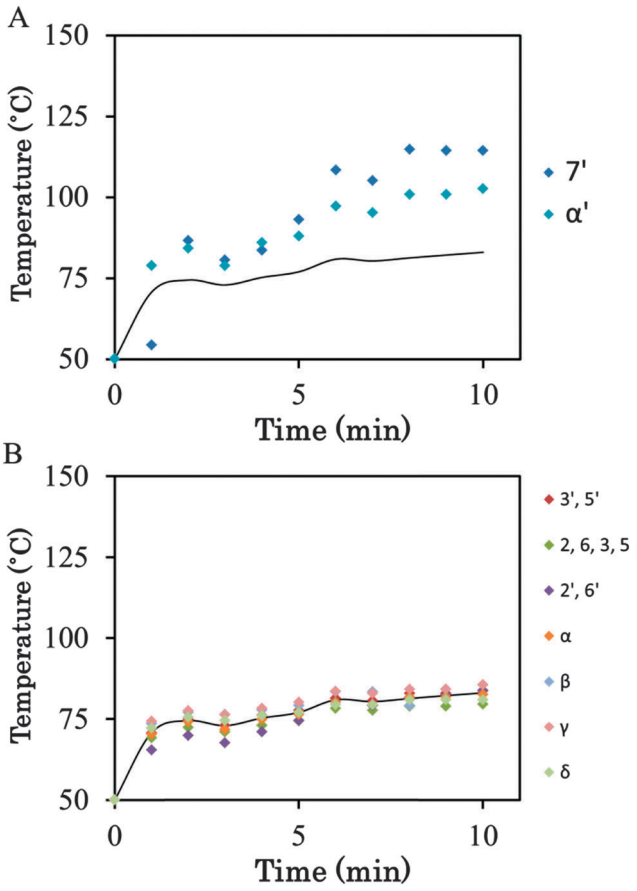

Fig. 7 Plots of temperatures against microwave irradiation times under microwave irradiation at 65 W for (A) the 7′ and α′ protons (blue symbols) and (B) the remainder of the protons. The black line in both plots indicates the average temperature of the remainder of the protons.

isotropic phase appears (Fig. 8C) and, eventually, the entire sample transitions to the isotropic phase (Fig. 8D). Conversely, increasing the temperature solely by thermal heating (TH) without microwave irradiation (Fig. 8E–G) causes the isotropic phase to appear at the surface of the sample (Fig. 8F). There, when a temperature nearly equal to the phase transition temperature is applied, an equilibrium state is achieved in which the temperature of the isotropic phase is the same as that of the liquid crystalline phase.

Similar non-equilibrium local heating phenomena under microwave irradiation have been reported for liquid–solid[23] mixtures. In the present study, the microwave irradiation of MBBA generated a non-equilibrium localized heating state that could be maintained for long time spans, in which an isotopic phase was present within the neat liquid crystalline state, solely as the result of the microwave irradiation.

Mechanism of microwave heating effects on isotropic phase MBBA

It is of interest to consider the reason why the 7′ and α′ protons of the MBBA molecules showed significantly different chemical shifts from the other protons. Since the chemical shifts had a linear relation with temperature, the 7′ and α′ protons also indicated significantly higher temperatures than the other protons, suggesting that these individual protons might actually have experienced different temperatures.

It is not, however, ruled out the possibility that the slopes of the chemical shifts of these two protons as a function of temperature deviate from linearity at high temperatures, thus generating exceptionally large chemical shifts in the higher temperature range.

However, another theory may be advanced by considering that both protons are associated with the polar bonds of the H–C═N– and CH_3–O– functional groups. Irradiation of the MBBA sample produces strong electric field that may interact with these polar groups to generate dielectric polarization which reduces the entropy term of the system. This reduction of the entropy term

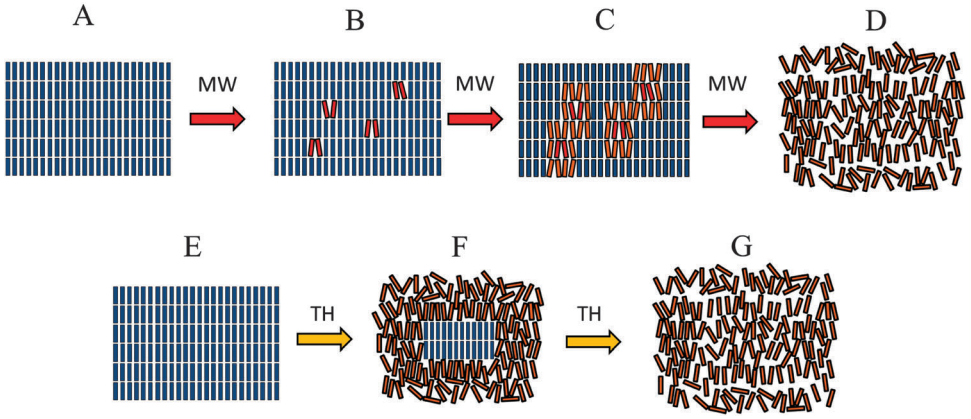

Fig. 8 Schematic diagrams showing the proposed (A–D) microwave (MW) and (E–G) thermal heating (TH) processes within the liquid crystalline state. During microwave irradiation, a small fraction of the liquid crystalline domain changes to the isotropic phase (image B). The rate of temperature increase in this isotropic phase domain is higher than in the liquid crystalline phase because the dielectric loss of the isotropic phase is larger than in the liquid crystalline phase. This may be considered to represent a non-equilibrium localized heating state. In contrast, thermal heating transitions a small fraction of the liquid crystalline state to the isotropic phase at the surface of the sample (image F). When applying thermal heating using the instrument's temperature control unit, the temperature of the isotropic phase is the same as that of the liquid crystalline state.

gives additional energy to the system which has gained thermal energy arising from the molecular friction to rise the temperature. Consequently, the electron density experienced by the 7′ and α′ protons increases slightly, producing higher field chemical shift changes during microwave irradiation. It should be pointed out that microwave energy at 2.45 GHz is far from affecting any change in the electron density through excitation of the electronic state. This energy of the entropy term causes deviation from the linear temperature increase by thermal energy. This energy increase of the polar group may in turn affect the rates of various chemical reactions. This kind of temperature increase of the particular protons bonded to the polar group may be discussed as a distinctive microwave effect as mentioned as thermal and non-thermal microwave effects.[5,37]

It is important to note that this study has shown that microwaves can increase the temperatures of samples with large dipole moments in a short span of time and can achieve significantly elevated temperatures during the measurement of NMR signals. Therefore, microwaves have potential as a heating source in NMR spectrometers. This effect could also be used for rapid temperature rise experiments such as have been performed using a liquid crystalline isotropic phase with correlated 2D NMR spectroscopy.[24–28]

The *in situ* microwave irradiation NMR spectroscopy makes it possible to observe organic reaction[1–7] and protein denaturation[29] pathways under microwave irradiation together with the structural information. These observations provide the information on the thermal and non-thermal microwave effects on the organic reaction in the atomic resolution, although it is controversial to distinguish them.[5,37] Furthermore, applications of the microwave rapid temperature jump experiments enabled us to perform a state correlated 2D NMR spectroscopy which provides ^{1}H–^{1}H dipolar interaction with the resolution of the isotropic phase[24–28] and hence allowed us to apply the technique to more complicated liquid crystalline samples as demonstrated using advanced 2D separated local field NMR.[38,39]

Conclusion

An *in situ* microwave irradiation NMR spectrometry technique was developed in which spectra were acquired simultaneously with microwave heating of liquid crystalline samples of MBBA. Analysis of the temperature dependence of the linewidths demonstrated that non-equilibrium localized heating of the sample generated regions of the isotropic state in which the temperature was higher than that of the bulk liquid crystal. These non-equilibrium localized zones may cause significant acceleration of chemical reactions. It was also shown that significantly elevated temperatures can be rapidly achieved using *in situ* microwave irradiation in conjunction with NMR spectroscopy. Finally, the temperatures indicated by the 7′ and α′ protons of the MBBA molecules were significantly higher than those of the other protons. These protons are bonded to polar functional groups, and hence it is possible to propose that microwave irradiation induced increased electron polarization in the associated bonds. This polarization would result in changes in the chemical shifts and may partly explain the mechanism by which organic reactions are accelerated through the distinctive microwave effects.

Acknowledgements

This work was supported by Grants-in-Aid for Scientific Research on a Priority Area (24121709) and an Innovative Area (26102514 and 26104513), and a Grant-in-aid for Scientific Research (C) (24570127) from the Ministry of Education, Culture, Sports, Science and Technology of Japan.

Notes and references

1 R. Gedye, F. Smith, K. Westaway, H. All, L. Baldisers, L. Laberge and J. Rousell, *Tetrahedron Lett.*, 1986, **27**, 279–282.
2 R. J. Giguere, T. L. Bray, S. M. Duncan and G. Majetcih, *Tetrahedron Lett.*, 1986, **27**, 4945–4948.

3 D. Adam, *Nature*, 2003, **421**, 571–572.
4 L. Perreux and A. Loupy, *Tetrahedron*, 2001, **57**, 9199–9223.
5 P. Lidström, J. Tiemey, B. Nathey and J. Westman, *Tetrahedron*, 2001, **57**, 9235–9283.
6 D. Bogdal, M. Lukasiewicz, J. Pielichowski, A. Miciak and Sz. Bednarz, *Tetrahedron*, 2003, **59**, 649–653.
7 C. O. Kappe, *Angew. Chem., Int. Ed.*, 2004, **43**, 6250–6284.
8 Y. Yoshimura, H. Shimizu, H. Hinou and S.-I. Nishimura, *Tetrahedron Lett.*, 2005, **46**, 4701–4705.
9 M. C. Parker, T. Besson, S. Lamare and M. D. Legoy, *Tetrahedron Lett.*, 1996, **46**, 8383–8386.
10 H. Shimizu, Y. Yoshimura, H. Hinou and S.-I. Hishimura, *Tetrahedron*, 2008, **64**, 10091–10096.
11 C. O. Kappe, B. Pieber and D. Dallinger, *Angew. Chem., Int. Ed.*, 2013, **52**, 1088–1094.
12 R. Hoogenboom, F. Wiesbroch, H. Huang, M. A. M. Leenen, H. M. L. Thijs, S. F. G. M. van Nispen, M. van der Loop, C.-A. Fustin, A. M. Jonas, J.-F. Goby and U. S. Schubert, *Macromolecules*, 2006, **39**, 4719–4725.
13 T. Iwamura, K. Ashizawa and M. Sakaguchi, *Macromolecules*, 2009, **42**, 5001–5006.
14 Y. Kajiwara, A. Nagai and Y. Chujo, *Polym. J.*, 2009, **41**, 1080–1084.
15 S. Yamada, A. Takasu, S. Takayama and K. Kawamura, *Polym. Chem.*, 2014, **5**, 5283–5288.
16 B. N. Pramanik, U. A. Mirza, Y. H. Ing, Y.-H. Liu, P. L. Bartner, P. C. Weber and A. K. Bose, *Protein Sci.*, 2002, **11**, 2676–2687.
17 W. Huang, Y.-M. Xia, H. Gao, Y.-J. Fang, Y. Wang and Y. Fang, *J. Mol. Catal.*, 2005, **35**, 115–116.
18 S.-S. Lin, C.-H. Wu, M.-C. Sun and Y.-P. Ho, *J. Am. Soc. Mass Spectrom.*, 2005, **16**, 581–588.
19 M. A. Herrero, J. M. Kremsner and C. O. Kappe, *J. Org. Chem.*, 2008, **73**, 36–49.
20 D. Obermayer, B. Gutmann and O. Kappe, *Angew. Chem., Int. Ed.*, 2009, **48**, 8321–8324.
21 M. Tanaka and M. Sato, *J. Chem. Phys.*, 2007, **126**, 034509.
22 M. Kanno, K. Nakamura, E. Kanai, K. Hoki, H. Kono and M. Tanaka, *J. Phys. Chem. A*, 2012, **116**, 2177–2183.
23 Y. Tsukahara, A. Higashi, T. Yamauchi, T. Nakamura, M. Yasuda, A. Baba and Y. Wada, *J. Phys. Chem. C*, 2010, **114**, 8965–8970.
24 A. Naito, M. Imanari and K. Akasaka, *J. Magn. Reson.*, 1991, **92**, 85–93.
25 A. Naito and A. Ramamoorthy, *Structural Studies of Liquid Crystalline Materials Using a Solid State NMR Technique. Thermotropic Liquid Crystal: Recent Advances*, Springer, 2007, pp. 85–116.
26 A. Naito, M. Imanari and K. Akasaka, *J. Chem. Phys.*, 1996, **105**, 4502–4510.
27 K. Akasaka, M. Kimura, A. Naito, H. Kawahara and M. Imanari, *J. Phys. Chem.*, 1995, **99**, 9523–9529.
28 A. Naito and Y. Tasei, *Mater. Sci. Technol.*, 2010, 2886–2894.
29 K. Akasaka, A. Naito and M. Imanari, *J. Am. Chem. Soc.*, 1991, **113**, 4688–4689.
30 A. L. Van Geet, *Anal. Chem.*, 1968, **40**, 2227–2229.
31 A. L. Van Geet, *Anal. Chem.*, 1970, **42**, 679–680.
32 C. S. Zuo, K. R. Metz, Y. Sun and A. D. Sherry, *J. Magn. Reson.*, 1998, **133**, 53–60.
33 S. V. Dvinskikh, K. Yamamoto, U. H. N. Dürr and A. Ramamoorthy, *J. Magn. Reson.*, 2007, **184**, 228–235.
34 A. Bielecki and D. P. Burum, *J. Magn. Reson., Ser. A*, 1995, **116**, 215–220.
35 H. Kelker and B. Scheurle, *Angew. Chem., Int. Ed. Engl.*, 1969, **8**, 884–885.
36 J. S. Prasad, *J. Chem. Phys.*, 1976, **65**, 941–944.
37 A. de la Hoz, Á. Diaz-Ortiz and A. Moreno, *Chem. Soc. Rev.*, 2005, **34**, 164–178.
38 T. Narasimhaswamy, D.-K. Lee, K. Yamamoto, N. Somanathan and A. Ramamoorthy, *J. Am. Chem. Soc.*, 2005, **127**, 6958–6959.
39 K. Nishimura and A. Naito, *Chem. Phys. Lett.*, 2006, **419**, 120–124.

Separation of Local Fields of Individual Protons in Nematic Phase of 4'-Ethoxybenzylidene-4-n-Butylaniline by Microwave Heating 2D NMR Spectroscopy

A. Naito 1 and Y. Tasei 1

1, Graduate School of Engineering, Yokohama 240-8501, Japan

Keywords: Liquid crystal, Nematic phase, Microwave heating, State correlated 2D NMR

Abstract

A nematic-isotropic phase-correlated 2D NMR spectra were successfully obtained in 4'-ethoxybenzylidene-4-n-buthylaniline (EBBA). The transition from nematic to isotropic phase was realized within 10 ms using a microwave pulse of 2.45 GHz in the transition period. Local dipolar fields of 11 magnetically different protons in EBBA in the nematic phase were separately observed in the F1 dimension of a 2D NMR experiment by means of well-resolved signals in the isotropic phase. The spectrum of the methyl protons of the ethoxy group clearly showed a triplet pattern, whereas those of the aromatic, methylene, and methane protons showed doublet patterns. Spin diffusion caused mixing of the spin states and gave mixed patterns in the 2D NMR spectrum in the F1 dimension. Inspection of the amplitude of the mixing pattern gave information on spin diffusion pathways in EBBA in the nematic phase.

Introduction

Microscopic orders of liquid crystalline samples have been studied successfully using quadrupole couplings in the ^{2}H NMR spectra of ^{2}H-labeled samples [1,2]. In principle, ^{1}H dipolar couplings can be also used for a similar purpose. A direct analysis of a proton spectrum of a liquid crystalline sample, however, has been difficult, because the strongly coupled dipolar spin network causes splitting of individual proton resonances into complex multiplicities of resonance lines, resulting in a highly overlapped one-dimensional NMR spectrum. A successful analysis has usually been performed only after a reduction of the number of protons and a simplification of spin network by partial deuteration [3]. For separating ^{13}C-^{1}H dipolar couplings of individual carbon nuclei in a liquid crystal, a two-dimensional NMR spectroscopy has been a powerful means [4]. In this approach, correlation between the ^{13}C NMR spectrum with heteronuclear decoupling and that with homonuclear decoupling in the liquid crystalline state is observed. This technique was further modified by combining an off magic angle spinning and a separated local dipolar field (SLF/VAS) [5,6] and by switching off magic angle spinning to magic angle spinning [7] to obtain scaled ^{13}C-^{1}H dipolar interactions in various liquid crystalline samples with excellent resolution. PISEMA experiments can separat local dipolar interaction into chemical shift interactions with high resolution and provide microscopic order of liquid crystals [8-11].

State-correlated 2D NMR (SC-2D NMR) spectroscopy [12, 13] has been developed as an alternative approach to elucidate microscopic order of liquid crystalline samples [14-16], to give correlation between native and denatured states of proteins [17], and to reveal correlation between the solid and liquid state of camphor using a CO_2 laser as a heat source [18]. This technique turned out to be useful to observe ^{1}H dipolar patterns of ^{1}H NMR spectra with high resolution. In this technique, local dipolar interaction of individual protons in the liquid crystalline state can be obtained via resonances in the isotropic phase [14-16]. A phase transition from a nematic to an isotropic phase is completed rapidly within the spin-lattice relaxation times of ^{1}H nuclei by applying a pulsed microwave. By this method, homonuclear dipolar interactions for individual protons can be separately observed without applying a multiple pulse technique. Thus it is not necessary to consider scaling factors depending on the pulse sequences, and hence provide a detailed information on microscopic order parameters. In particular, recent technical improvement in the microwave temperature jump probe has realized a transition in even less than 10 ms [15,16], and enable us to obtain simpler dipolar patterns.

In this work, an SC-2D NMR experiment between the nematic phase and the isotropic phase of liquid crystalline samples of 4'-ethoxybenzylidene-4-n-butylaniline (EBBA) is described, in which well separated dipolar patterns for individual protons are observed as cross sectional spectra. Besides, this technique can also provide spin diffusion pathways among proton spin networks. This information provides a detailed insight into the microscopic order of liquid crystalline materials.

State-Correlated 2D NMR Spectroscopy

Microwave heating NMR spectrometer

The microwave pulse is applied through a microwave circuit built into a JEOL high resolution ^{1}H NMR probe for liquids (Figure 1).

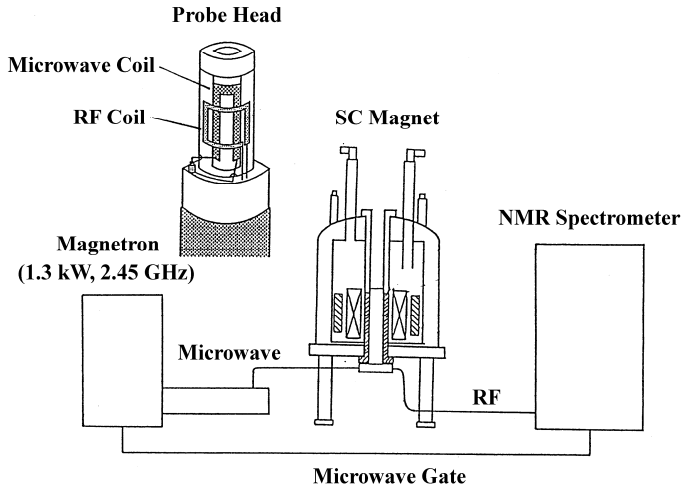

Figure 1 Block diagram of the microwave heating NMR spectrometer equipped with a microwave transmitter. Microwave and radiowave coils in the probe head are also shown.

A flat copper ribbon, 3 mm in width, is used for the microwave coil, which is wound inside the radio wave coil coaxially to reduce arching during the microwave irradiation (Figure 1). The microwave circuit is tuned properly to 2.45 GHz by using a sweep generator. NMR spectra were recorded at 399.8 MHz on a JEOL GX 400 pulse FT NMR spectrometer, equipped with a pulsed microwave transmitter (IDX, Tokyo Electric Co. Ltd.) capable of transmitting 1.3 kW pulsed microwave at a frequency of 2.45 GHz. After the temperature jump, the temperature of the sample was cooled down to that of nematic phase with a help of a JEOL gas flow temperature controller in order to repeat the pulse sequence of Figure 2.

State correlated 2D NMR experiments

The pulse sequence used in the state-correlated two dimensional (SC-2D) NMR spectroscopy is practically the same for the radio frequency part as that of 2D exchange or NOE experiment (Figure 2). The first 90^0 pulse creates the transverse magnetization. During the evolution period, the temperature of the sample is kept to maintain the nematic phase so that the ^1H spins show precession frequency under strong dipolar interactions between proton nuclei in the nematic phase. At time t_1, the second 90^0 pulse is applied to align the magnetization vector along the z axis. During the transition period, a pulsed microwave is applied for a short time to raise temperature, during which the nematic phase is transformed into the isotropic phase. Any remaining transverse magnetization is expected to diphase within a couple of milliseconds during the transition period under strong dipolar interactions of the nematic phase. To study the spin diffusion processes, mixing time, τ_m, is inserted in the beginning of the transition period. After the third 90^0 pulse, free induction decay is acquired for t_2 time in the detection period during which the system experienced magnetic interactions in the isotropic phase. Free induction decay signals recorded as functions of t_1 and t_2 are double Fourier-transformed to generate the correlated 2D NMR spectrum between the nematic and isotropic phases.

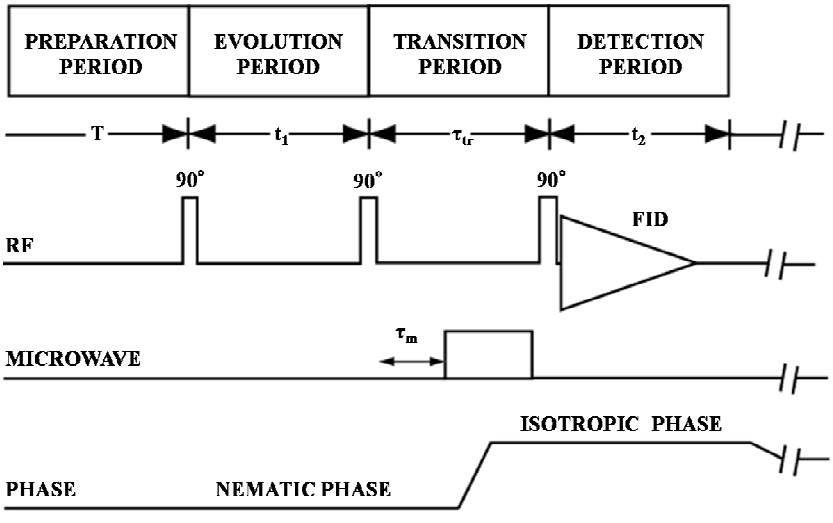

Figure 2 Pulse sequence for the state-correlated 2D NMR (SC-2D NMR) experiments. A mixing time τ_m is inserted into the beginning of a transition period to examine the spin diffusion properties.

Results and Discussion

Microwave heating of EBBA

Figure 3(top) shows a ^{1}H NMR spectrum of EBBA in the isotropic phase above 82 ^{o}C. By inspecting the multiplet patterns of individual signals and comparing them with the results of reported work. Assignments of the resonance lines to individual protons could be easily performed in the isotropic phase. Figure 3(bottom) shows the ^{1}H NMR spectrum of EBBA at 78 ^{o}C in the nematic phase. Resonance lines in the spectrum are quite broad and overlapped so that the feature of each proton signal cannot be detected.

A temperature-jump experiments of EBBA was performed using the microwave heating pulse sequence. The microwave pulse was applied for 10 ms, followed by a series of radiofrequency detection pulses. The results clearly demonstrates that the transition from the nematic phase to the isotropic phase is completed within 10 ms after starting the microwave irradiation, well within the spin-lattice relaxation time. The microwave pulse was applied for 10 ms, followed by a series of radiofrequency detection pulses. It was estimated that the isotropic phase returned to the nematic phase at 78 ^{o}C after 80 s. Therefore, the recycling time for the SC-2D NMR experiments were chosen to be 120 s.

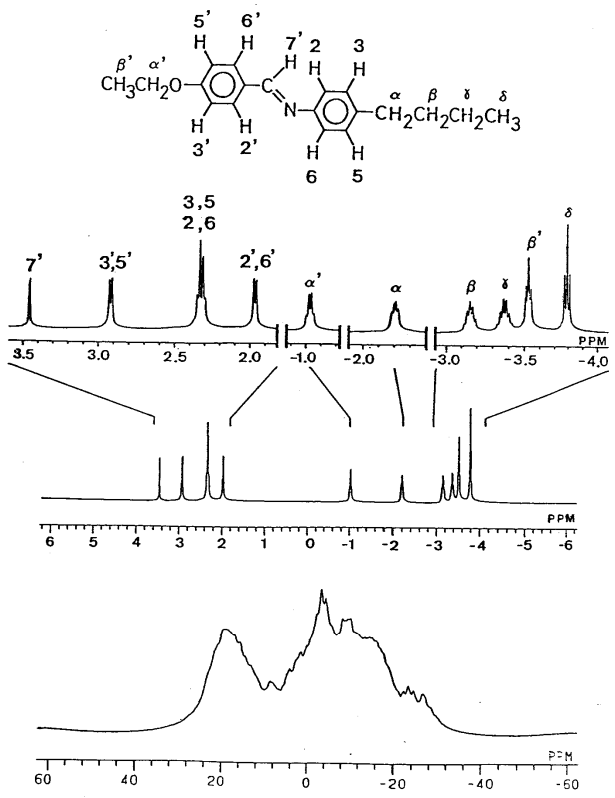

Figure 3 ^{1}H NMR spectra of EBBA in the isotropic phase at 82 ^{o}C (top) and in the nematic phase at 78 ^{o}C (bottom).The expansion of the top spectrum is shown above the spectrum of isotropic phase with signal assignments.

For successful SC-2D NMR experiments, a rapid transition from the nematic to the isotropic phase within the spin-lattice time is essential. Spin-lattice relxation times of the protons were measured in both phase, namely the isotropic phase at 82 ^{o}C and the nematic phase at 78^{o}C The T_1 values were commonly 1.4 s in the nematic phase and ranged between 0.9 and 1.9 s in the isotropic phase.

SC-2D NMR spectra of EBBA

Figure 4 (left column) shows the contour plot of the SC-2D NMR spectrum of 4'-ethoxybenzylidene-4-n-butylanilin (EBBA) between the nematic and isotropic phases, that was carried out using the pulse sequence of Figure 2. This figure clearly demonstrates that the SC-2D NMR experiment was successful in the liquid crystal sample of EBBA. It is recognized that the dipolar spectra of individual protons are separated in the F1 dimension with resolution in the F2 dimension, namely with resolution in the isotropic phase.

Figure 4 (right column) also shows cross sections of individual types of protons along the F1 direction as a stacked plot. The local dipolar fields of nine types of protons were resolved, but those of 2,6 and 3,5 protons, whose chemical-shift differences are too small even in the isotropic phase, overlapped. It is recognized that the local dipolar fields for the methyl protons of the ethoxy group (β' protons) contain a triplet pattern with 1:2:1 intensity ratio and a splitting of 9.6 kHz characteristic of a triangle network of the protons as discussed for APAPA [16] Besides, each triplet lines were further splitted into small couplings due to the couplings from the α' protons. On the other hand, the δ methyl protons show a singlet pattern indicating that the splitting constant is very small. The aromatic protons in the phenyl group (3,5/3',5' and 2,6/2',6' protons) are considered to give mainly doublet patterns with splittings of 12.8 kHz, as were reported previously using deuteration of the alkyl group [3]. The main features of the spectra of the methylene and methyl protons in the alkyl group (α, β, γ, and δ protons) reflect the mobility of the groups. Namely the most mobile δ methyl group shows a singlet pattern while the linewidth increases as the protons are close to the core group with splittings ranging from 8 to 15 kHz corresponding to the increasing order from δ to α protons. The splittings of the doublets for methylene protons were observed for a proton which is a little larger than those of the aromatic protons. Doublet patterns for the methylene protons have not been reported so far. It is of interest to note that the methane proton (7' proton) shows a mixture of doublet and singlet patterns and the singlet pattern should be from the 7' proton.

Although a triplet and singlet patterns were clearly observed for the β' and δ methyl protons, respectively, in the cross sections of the SC-2D NMR spectrum as shown in Figure 5 (τ_m = 0 ms), doublet patterns of the other protons mixed to the line-shapes of both the β' and δ protons at τ_m = 200 ms (Figure 5). This fact indicates that the spin states of the methyl protons and those of other protons exchange with each other by mutual dipolar interactions. Phenomenologically, this is similar to the appearance of the cross peak in a 2D exchange or 2D NOE spectrum. This phenomenon is expected to be efficient in the nematic phase since the intramolecular dipolar interactions are relatively strong. Because the intermolecular dipolar interactions are averaged out more effectively than the intramolecular ones due to the rapid intermolecular rearrangement, the mixing rate between intermolecular protons should be slower than that between intramolecular protons particularly in nematic phase. Therefore, this mixing of

the spectra should represent pathways of intramolecular rather than of intermolecular spin diffusion. Actually, Figure 5 clearly show that mixing among aromatic protons is the most efficient and that between methyl protons and methylene protons is less efficient. Particularly, the triplet pattern of the methyl protons of the ethoxy group is clear, because they are fairly isolated from the aromatic and butyl protons within the molecule. On the other hand, δ proton mixed rapidly with the other protons to grow doublet character. In contrast, β' protons still remain the triplet characters, leading that ethoxy group is more isolated from the aromatic protons. When τ_m is set to 600 ms, most of the protons show now same line-shapes with each other to indicate that it is long enough to establish equilibrium among all protons within the molecule of EBBA in the nematic phase.

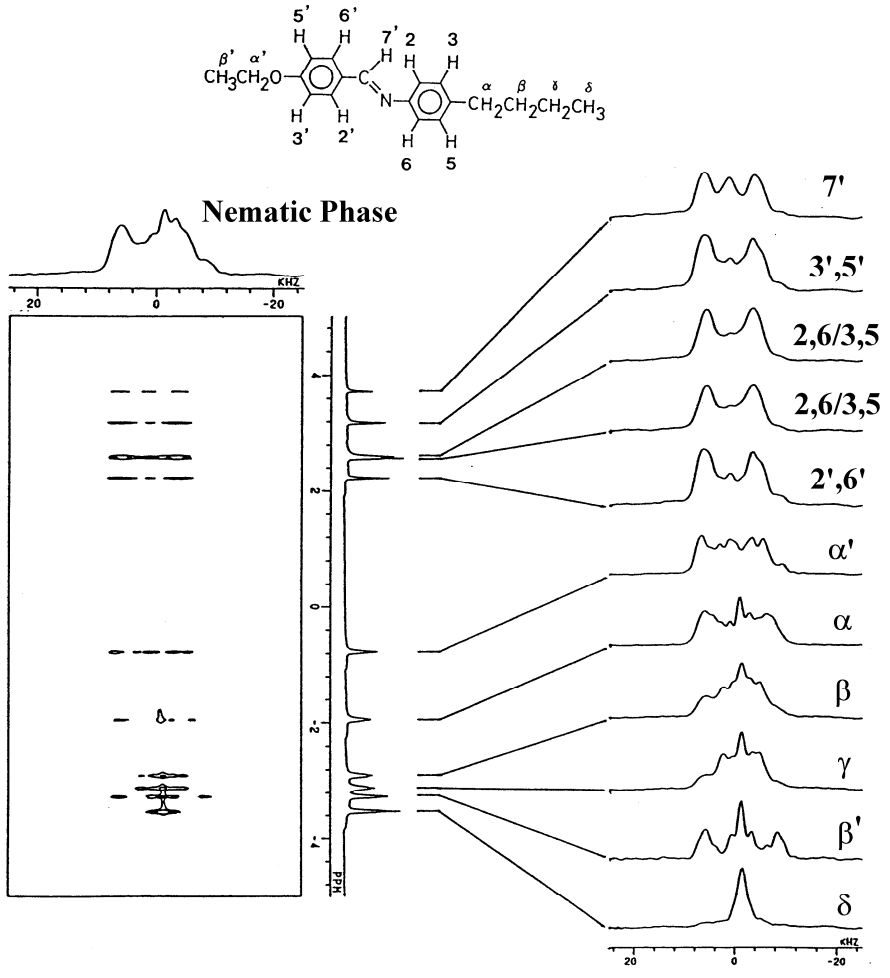

Figure 4 A nematic isotropic phase correlated 2D NMR spectrum (SC-2D NMR) of EBBA with cross sectional pattern by applying a microwave pulse of 10 ms.

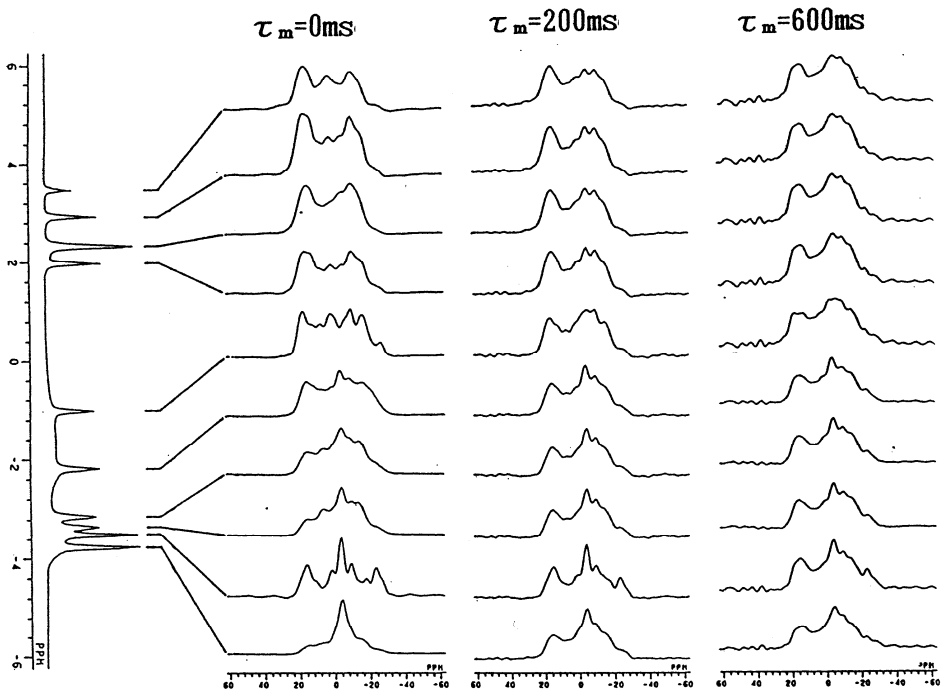

Figure 5 Dependence of the cross sectional patterns on the mixing time τ_m of 0, 200, 600 ms in the SC-2D NMR spectrum of EBBA.

Conclusions

SC-2D NMR spectroscopy allows elucidation of local-order parameters without the need for deuteration and therefore is readily applicable to a wide range of liquid crystalline samples. Second, specific ^{2}H labeling is not necessary for assignments of the cross sectional spectra, since SC-2D NMR allows their automatic assignments through cross peaks to the signals in the isotropic phase which are readily assignable by the conventional liquid state 2D method. Third, information on local conformation, as exemplified above by the torsion angle of the two phenyl rings, could be obtained through the analysis if fine structures of the cross sectional spectra are appeared. Finally, cross relaxation and spin diffusion can be a unique means to elucidate dynamics intramolecular as well as intermolecular interactions in liquid-crystalline molecules. Although the temperature range of measurement for SC-2D NMR spectroscopy of liquid crystals is limited to those close to Tc, the method has those unique advantages over the conventional ^{2}H NMR spectroscopy.

Acknowledgments

This work was supported, in part, by a Grant-in-Aid for Scientific Research on Prioty Areas (21017002) from the Ministry of Culture, Sports, Science and Technology of Japan. Authors also thank to Prof. Akasaka of Kinki University for his helpful discussion..

References

[1] J.W. Emsley, G.R. Luckhurst, E.J. Parsona, and B.A. Timimi, Mol. Phys., Chain Orientation and the Re-Entrant Nematic Phase: A Deuterium N.M.R. Study of 4-n-Hexyloxy-d_{13}, 4-n-Octyl d_{17}-4'-Cyano Biphenyl and Their Re-Entrant Mixture, *Mol. Phys*. Vol 56, 1985, p 767-774

[2] C.J.R. Counsell, J.W. Emsley, G.R. Luckhurst, and H.S. Sachdev, Orientation Order in the 4-n-Alkoxy-4'-Cyanobiphenyl: A Comparison between Experiment and Theory, *Mol. Phy. 63, 1988, p 33-47*

[3] J .S. Prasad, Orientational Order Parameters and Conformation of Nematic p-Ethoxybenzyliden-p-n-Butylaniline*, J. Chem. Phys*. Vol 65, 1976, p 941-944.

[4] A. Hohener, L. Muller, and R.R. Ernst, Dipole-Coupled Carbon-13 Spectra, a Source of Structural Information on Liquid Crystals, *Mol. Phys*. Vol 38, 1979, 909-922.

[5] B.M. Fung, J. Afzal, T.L. Foss, and M.H. Chan, Nematic Ordering of 4-n-Alkyl-4'-Cyanobiphenyls Studied by Carbon-13 NMR with Off-Magic Angle Spinning, *J. Chem. Phys*, Vol 85, 1986, 4808-4814.

[6] C.B. Frech, B.M. Fung, and M. Schadt, Orientational Ordering of 4-Substituted Phenylcyclohexanes Studied by Carbon-13 Two-Dimensional N.M.R., Liq. Cryst., Vol 3, 1988, p 713-722.

[7] M. Hong, K. Schmidt-Rohr, and A. Pines, NMR Measurement of Signs and Magnitudes of C-H Dipolar Couplings in Lecitin, *J. Am. Chem. Soc*., Vol 117, 1995, p 3310-3311.

[8] D.K. Lee, T. Narasimhaswamy, and A. Ramamoothy, PITANSEMA, a Low-Power PISEMA Solid-State NMR Experiment, *Chem. Phys. Lett.*, Vol 399, 2004, 359-362

[9] K. Nishimura and A. Naito, Dramatic Reduction of the RF Power for Attenuation of Sample Heating in 2D-Separated Local Field Solid-State NMR Spectroscopy, *Chem. Phys. Lett*., Vol 402, 245, 2005, p 245-250.

[10] T. Narasimhaswamy, D.K. Lee, K. Yamamoto, N. Somanathan, and A. Ramamoothy, A 2D Solid-State NMR Experiment to Resolve Overlapped Aromatic Resonances of Thiophene-Based Nematogens, *J. Am. Chem. Soc*., Vol 127, 2005, 6958-6959

[11] K. Nishimura and A. Naito, Remarkable Reduction of RF Power by ATANSEMA and DATANSEMA Separated Local Field in Solid-State NMR Spectroscopy, *Chem. Phys. Lett*., Vol 419, 2006, p 120-124

[12] A. Naito, H. Nakatani, M. Imanari, and K. Akasaka, State-Correlated Two-Dimensional NMR Spectroscopy, *J. Magn. Reson.*, Vol 87, 1990, p 429-432

[13] A. Naito and A. Ramamoorthy, Atomic Resolution Structural Studies of Liquid Crystalline Materials Using Solid State NMR Technique. Thermotropic Liquid Crystals: Recent Advances, Springer, 2007, p85-116

[14] A. Naito, M. Imanari, and K. Akasaka, Separation of Local Magnetic Fields of Individual Protons in Nematic Phase by State-Correlated 2D NMR Spectroscopy, *J. Magn. Reson*., Vol 92, 1991, p 85-93

[15] K. Akasaka, M. Kimura, A. Naito, H. Kawahara, and M. Imanari, Local Order, Conformation, and Interaction in Nematic 4-(n-Pentyloxy)-4'-Cyanobiphenyl and Its One-to-One Mixture with 1-(4'-Cyanophenyl)-4-Propylcyclohexane. A Study by State-Correlated ^{1}H Two-Dimensional NMR Spectroscopy, *J. Phys. Chem*., Vol 99, 1995, p 9523-9529.

[16] A. Naito, M. Imanari, and K. Akasaka, State-Correlated Two-Dimensional NMR Spectroscopy: Separation of Local Dipolar Fields of Protons in Nematric Phase of 4'-Methoxybenzylidene-4-Acetoxyaniline, *J. Chem. Phys.*, Vol 105, 1996, p 4502-4510

[17] K. Akasaka, A. Naito, and M Imanari, Novel Method for NMR Spectral Correlation between the Netive and the Denatured States of a Protein. Application to Ribonuclease A. *J. Am. Chem. Soc*., Vol 113, 1991, p 4688-4689

[18] D.B. Ferguson, T.R. Kramiete, and J.F. How, Two-Dimensional Correlation of Solid State and Liquid State NMR Using a Laser Temperature Jump, *Chem. Phys. Lett*., Vol 229, 1994, p 71-74